ARISTOTLE UNIVERSITY OF THESSALONIKI
FACULTY OF ENGINEERING
CHEMICAL ENGINEERING DEPARTMENT

DIVISION OF ANALYSIS, DESIGN AND CONTROL
OF CHEMICAL PLANTS AND PROCESSES

Modeling, simulation, and optimization of milk heat treatment processes under fouling conditions

Diploma Thesis

Eleni Nikolaidou
(Reg. Number: 5309)

Supervisor: Prof. Michael Georgiadis

Thessaloniki
November 2023

Abstract

One of the most important issues in the food industry is fouling during heat treatments. The formation of undesired layers of deposits in the heat exchanger surface affects energy efficiency, operation runtimes and maintenance costs. Fouling is extremely detrimental for dairy products and can be physicochemical or microbial. Several studies have been published in recent years to investigate mitigation strategies for this industrial problem which incurs high costs and safety issues in the dairy industry. Despite these numerous publications, there is still scope for improvement of prediction techniques through mechanistic modeling in an attempt to derive optimal operating policies of dairy plants under fouling conditions.

This thesis presents a mathematical model that describes protein fouling and bacterial contamination of milk due to the adherence, growth, and release of bacteria in thermal processing equipment. For shell and tube heat exchangers three different configurations are studied while for plate heat exchangers two different arrangements. Then, advanced dynamic optimization strategies are employed for the three different shell and tube heat exchanger configurations aiming at minimizing the total cleaning cost due to fouling. The optimization procedure results in the optimal length and diameter of the heat exchanger as well as in the optimal operating policies.

Simulation results indicate that plate heat exchangers are less prone to fouling compared with shell and tube heat exchangers due to their lower surface temperature and to their higher turbulence. The arrangement of plate heat exchanger with six channels per pass with total one pass results in lower fouling than the other with one channel per pass with total six passes due to the lower heating load. It is demonstrated that an increased initial native protein concentration as well as a decreased Reynolds number results in higher deposits. Hence, higher Reynolds number is preferred for fouling mitigations. Furthermore, considering all the cost factors related to the milk heat treatment for all the configurations, an optimal heat exchanger size is determined by considering the trade-offs between operating and capital costs. The value of the objective function of the optimized configuration of counter-current operations seems to have the most significant improvement (52.8%) compared to other configurations. Counter-current operation runs for shorter heating time because this configuration enables maximum heat recovery that favors fouling

and presents lower deposit thickness and lower bacterial wall coverage compared to the other two configurations.

Εκτενής Περίληψη

Ένα από τα σημαντικότερα ζητήματα στη βιομηχανία τροφίμων είναι οι επικαθήσεις κατά τη διάρκεια της θερμικής επεξεργασίας. Η πιο συχνή διεργασία θερμικής επεξεργασίας είναι η παστερίωση. Ο σχηματισμός ανεπιθύμητων επικαθήσεων στην επιφάνεια των εναλλακτών θερμότητας επηρεάζει την ενεργειακή τους απόδοση, τον χρόνο λειτουργίας τους και το κόστος συντήρησής τους. Οι επικαθήσεις μπορεί να είναι φυσικοχημικές ή μικροβιακές και είναι εξαιρετικά επιζήμιες για τα γαλακτοκομικά προϊόντα. Η β-Λακτοσφαιρίνη (β-Lg) και η α-Λακταλβουμίνη (α-La) είναι οι δύο βασικές πρωτεΐνες ορού γάλακτος που επηρεάζουν τις επικαθήσεις. Η β-Lg ωστόσο έχει βρεθεί ότι σχετίζεται περισσότερο με τις επικαθήσεις καθώς είναι θερμικά ασταθέστερη. Με τη θέρμανση του γάλακτος η φυσική πρωτεΐνη (native protein, β-Lg) πρώτα μετουσιώνεται (denaturated protein), και στη συνέχεια τα μετουσιωμένα μόριά της αντιδρούν με παρόμοιους ή άλλους τύπους μορίων πρωτεΐνης (π.χ. καζεΐνη, α-La) και σχηματίζουν συσσωματώματα (aggregated protein). Το βακτήριο που εντοπίζεται κυρίως στους εναλλάκτες θερμότητας στη γαλακτοβιομηχανία είναι ο *Streptococcus Thermophilus*. Η αύξηση της συγκέντρωσής του οφείλεται σε μεγάλο βαθμό στην ανάπτυξη του κατά τη θέρμανση. Αρκετές μελέτες έχουν δημοσιευθεί τα τελευταία χρόνια προκειμένου να διερευνηθούν στρατηγικές μείωσης των επικαθήσεων, οι οποίες οδηγούν σε υψηλό κόστος και θέτουν ζητήματα ασφάλειας στην παραγωγή γαλακτοκομικών προϊόντων. Παρά τις πολυάριθμες αυτές δημοσιεύσεις, υπάρχει ακόμα περιθώριο βελτίωσης των τεχνικών πρόβλεψης μέσω μηχανιστικής μοντελοποίησης, η οποία μπορεί να χρησιμοποιηθεί για την κατανόηση των φαινομένων και την τελική βελτιστοποίηση της παραγωγικής διαδικασίας.

Στόχος της παρούσας διπλωματικής εργασίας είναι η ανάπτυξη ενός μαθηματικού μοντέλου που περιγράφει τόσο τις πρωτεϊνικές επικαθήσεις όσο και τη βακτηριακή μόλυνση του γάλακτος λόγω της προσκόλλησης, της ανάπτυξης και της απελευθέρωσης βακτηρίων στους εναλλάκτες θερμότητας. Το μαθηματικό μοντέλο είναι ικανό να προβλέψει την αντίσταση στη μεταφορά θερμότητας με την πάροδο του χρόνου λόγω των επικαθήσεων και της μικροβιακής μόλυνσης και μπορεί να αποτελέσει ένα χρήσιμο εργαλείο για τη γαλακτοβιομηχανία αρχικά για

τη βελτιστοποίηση της λειτουργίας των εναλλακτών θερμότητας και στη συνέχεια ολόκληρης της παραγωγικής διαδικασίας.

Το μαθηματικό μοντέλο επιλύεται στο gPROMS™. Για τους εναλλάκτες θερμότητας κελύφους – αυλών μελετώνται τρεις διαφορετικές διατάξεις: θέρμανση του γάλακτος με ατμό στους 374K, θέρμανση του γάλακτος με θερμό νερό στους 385K που βρίσκεται σε ομορροή με το γάλα και θέρμανση του γάλακτος με θερμό νερό στους 385K που βρίσκεται σε αντιρροή με το γάλα. Για τους πλακοειδείς εναλλάκτες θερμότητας μελετώνται δύο διαφορετικές διατάξεις. Η πρώτη διάταξη έχει ένα κανάλι ανά πέρασμα και συνολικά έξι περάσματα ενώ η δεύτερη διάταξη έχει έξι κανάλια ανά πέρασμα και συνολικά ένα μόνο πέρασμα.

Τα αποτελέσματα της παρούσας διπλωματικής εργασίας δείχνουν ότι οι πλακοειδείς εναλλάκτες θερμότητας έχουν λιγότερες επικαθήσεις σε σύγκριση με τους εναλλάκτες θερμότητας κελύφους – αυλών λόγω της χαμηλότερης επιφανειακής τους θερμοκρασίας και του υψηλότερου τυρβώδους τους. Η διάταξη του πλακοειδή εναλλάκτη θερμότητας με έξι κανάλια ανά πέρασμα και συνολικά ένα μόνο πέρασμα έχει ως αποτέλεσμα λιγότερες επικαθήσεις σε σύγκριση με την άλλη διάταξη με ένα κανάλι ανά πέρασμα και συνολικά έξι περάσματα λόγω του χαμηλότερου θερμικού φορτίου. Και στις δύο διατάξεις η μάζα των επικαθήσεων αυξάνεται με την πάροδο του χρόνου σε κάθε πλάκα αλλά είναι διαφορετική ακόμη και μεταξύ των πλακών που ορίζουν το ίδιο κανάλι λόγω του διαφορετικού θερμοκρασιακού προφίλ της κάθε πλάκας.

Οι επικαθήσεις αυξάνονται κατά μήκος του εναλλάκτη καθώς αυξάνεται και η συγκέντρωση της συσσωματωμένης (aggregated) πρωτεΐνης λόγω της αύξησης της θερμοκρασίας. Ο ολικός συντελεστής μεταφοράς θερμότητας από την άλλη μειώνεται με την πάροδο του χρόνου λόγω των επικαθήσεων. Η αυξημένη αρχική συγκέντρωση της φυσικής πρωτεΐνης καθώς και ο μειωμένος αριθμός Reynolds οδηγούν σε υψηλότερες επικαθήσεις. Ως εκ τούτου, ο υψηλότερος αριθμός Reynolds προτιμάται για τον περιορισμό των επικαθήσεων, πρωτεϊνικών και βακτηριακών.

Με τη χρήση του εργαλείου gOPT βελτιστοποιούνται οι τρεις διαφορετικές διατάξεις των εναλλακτών κελύφους – αυλών με στόχο την ελαχιστοποίηση του συνολικού κόστους καθαρισμού λόγω των επικαθήσεων. Η βελτιστοποίηση έχει ως αποτέλεσμα την εύρεση του βέλτιστου μήκους και της βέλτιστης διαμέτρου του εναλλάκτη καθώς επίσης και την εύρεση της βέλτιστης λειτουργίας του. Το βέλτιστο μέγεθος εναλλάκτη θερμότητας, λαμβάνοντας υπόψη όλους τους

παράγοντες κόστους που σχετίζονται με τη θερμική επεξεργασία του γάλακτος, επιτυγχάνει μια ισορροπία μεταξύ του λειτουργικού κόστους και του παγίου κόστους. Παρατηρείται ότι ο αριθμός των διαστημάτων ελέγχου επηρεάζει την τιμή της αντικειμενικής συνάρτησης, καθώς όσο αυξάνεται ο αριθμός τους η αντικειμενική συνάρτηση βελτιώνεται. Η μεγαλύτερη βελτίωση της αντικειμενικής συνάρτησης (14%) παρατηρείται για 12 διαστήματα ελέγχου.

Για όλες τις διατάξεις των εναλλακτών θερμότητας κελύφους – αυλών η βέλτιστη διάμετρος είναι σχετικά χαμηλή και κοντά στο κατώτερο όριο ενώ το βέλτιστο μήκος είναι σχετικά υψηλό προκειμένου να επιτρέπεται η σταδιακή θέρμανση του γάλακτος και να περιορίζονται οι επικαθήσεις. Η τιμή της αντικειμενικής συνάρτησης κόστους της βελτιστοποιημένης διάταξης αντιρροής παρουσιάζει τη σημαντικότερη βελτίωση (52.8%) σε σύγκριση με τις άλλες δύο διατάξεις. Η περίπτωση της αντιρροής οδηγεί σε μικρότερο χρόνο λειτουργίας, επειδή αυτή η διάταξη επιτρέπει τη μέγιστη ανάκτηση θερμότητας που ευνοεί τις επικαθήσεις ενώ παρουσιάζει χαμηλότερο πάχος επικαθήσεων και χαμηλότερη βακτηριακή κάλυψη τοιχώματος σε σύγκριση με τις άλλες δύο διατάξεις.

Acknowledgements

First of all, I would like to thank my supervisor Professor Michael Georgiadis for his support and guidance in this thesis and in my academic life as well. In addition, I am really grateful for the perfect collaboration we had throughout this period as well as for the important knowledge he provided me and professionalism and consistency he taught me.

I would also like to express my thankfulness to Lefteris Charakleias, applications engineer at Siemens Process Systems Engineering (SPSE) for his guidance throughout this project. His experience in the field of process modeling and optimization helped me to overcome any obstacles that arose and to acquire important knowledge in this field.

Many thanks to all my friends for their support and for the beautiful moments we experienced during the last five years.

Last but not least, I would like to express my sincerest gratitude to my family for their love, support, encouragement and belief through all these years.

Table of Contents

List of Tables

List of Figures

Nomenclature

A	Constant
A_j	Heat transfer area of channel *j*, m^2
Area	Cross-sectional area of the tube, m^2
Area2	Heat transfer area, m^2
AvRe	Average Reynolds number
Av_vel	Average velocity after fouling, m/s
A_x	Channel cross-section area, m^2
A_{xp}	Plate cross-section area, m^2
Bi	Biot number
$\overline{Bi}$	Average Biot
Bi_p	Biot number in plate *p*
c	Bacterial bulk concentration, cfu/m^3
$\overline{c}$	Average bacterial bulk concentration, cfu/m^3
C_A	Bulk aggregated protein concentration, kg/m^3
C_A^*	Aggregated protein concentration in thermal boundary layer, kg/m^3
$C_{A,in}$	Inlet bulk aggregated protein concentration, kg/m^3
$C_{A,in}^*$	Inlet aggregated protein concentration in thermal boundary layer, kg/m^3
C_{Aj}	Bulk aggregated protein concentration in channel *j*, kg/m^3
C_{Ap}^*	Layer aggregated protein concentration in plate *p*, kg/m^3
CC	Total annual operating cost, $/year
$C_{cleaning}$	Total cost of cleaning operation, $/cycle

C_D	Bulk denaturated protein concentration, kg/m^3
C_D^*	Denaturated protein concentration in thermal boundary layer, kg/m^3
$C_{D,in}$	Inlet bulk denaturated protein concentration, kg/m^3
$C_{D,in}^*$	Inlet denaturated protein concentration in thermal boundary layer, kg/m^3
C_{Dj}	Bulk denaturated protein concentration in channel *j*, kg/m^3
C_{Dp}^*	Layer denaturated protein concentration in plate *p*, kg/m^3
C_{HE}	Heat exchanger operating cost, $/year
c_{in}	Inlet bacterial bulk concentration, cfu/m^3
c_j	Bacterial bulk concentration in channel *j*, cfu/m^3
C_{losses}	Cost of production losses, $/cycle
C_N	Bulk native protein concentration, kg/m^3
C_N^*	Native protein concentration in thermal boundary layer, kg/m^3
$C_{N,in}$	Inlet bulk native protein concentration, kg/m^3
$C_{N,in}^*$	Inlet native protein concentration in thermal boundary layer, kg/m^3
C_{Nj}	Bulk native protein concentration in channel *j*, kg/m^3
C_{Np}^*	Layer native protein concentration in plate *p*, kg/m^3
CO_{ef}	Cost of effluent disposal after the cleaning operation, $/cycle
CO_{NaOH}	Cost of NaOH for the cleaning operation, $/cycle
CO_{steam}	Cost of steam for the cleaning operation, $/cycle
CO_{water}	Cost of water for cleaning operation, $/cycle
Cp_f	Milk specific heat capacity, J/kg/K
Cp_j	Fluid specific heat capacity, J/kg/K
Cp_p	Plate specific heat capacity, J/kg/K

Cp_w	Heating medium specific heat capacity, J/kg/K
Crossarea	Cross-sectional area of the tube after fouling, m^2
C_{steam2}	Cost of steam for the heating operation, $/cycle
D_A	Aggregated protein diffusion coefficient, m^2/s
d_A	Particle diameter of aggregated protein, m
D_D	Denaturated protein diffusion coefficient, m^2/s
d_D	Particle diameter of denaturated protein, m
D_e	Equivalent diameter, m
Diam	Tube diameter, m
D_N	Native protein diffusion coefficient, m^2/s
d_N	Particle diameter of native protein, m
E_a	Activation energy of bacteria destruction, J/mol
E_D	Activation energy for denaturated protein, J/mol
e_j	Gap between plates, m
E_N	Activation energy for native protein, J/mol
f	Friction factor
fi	Fanning friction factor
h	Local heat transfer coefficient, $W/m^2/K$
h_{cold}	Local heat transfer coefficient in the cold side, $W/m^2/K$
h_{hot}	Local heat transfer coefficient in the hot side, $W/m^2/K$
k_a	Adhesion rate constant, m/s
k_{de}	Destruction rate constant, 1/s
k_{D0}	Pre-exponential factor for denaturated protein, $m^3/kg/s$

k_{de0}	Pre-exponential factor of bacteria destruction, 1/s
k_{mA}	Aggregated protein mass transfer coefficient, m/s
k_{mD}	Denaturated protein mass transfer coefficient, m/s
k_{mN}	Native protein mass transfer coefficient, m/s
k_{N0}	Pre-exponential factor for native protein, 1/s
k_r	Release constant, m^2/cfu
k_w	Mass transfer coefficient to the deposit, m/s
L	Tube length, m
Mass	Deposit mass, kg/m^2
$\overline{mass}$	Average deposit mass, kg/m^2
mass_vel	Mass velocity, kg/s/m^2
$Mass_p$	Deposit mass, kg/m^2
mean_n_{wp}	Average bacterial wall coverage over one plate, cfu/m^2
m_{steam}	Steam mass flowrate for the heating operation, kg/s
N_{AV}	Avogadro constant, 1/mol
NCL	Number of heating and cleaning cycles per year
Nu	Nusselt number
n_w	Bacterial wall coverage, cfu/m^2
$\overline{n_w}$	Average bacterial wall coverage between two plates, cfu/m^2
$n_{w,in}$	Initial bacterial wall coverage, cfu/m^2
n_{wp}	Bacterial wall coverage in plate p, cfu/m^2
p_j	Thickness of plate *j*, m
Pr	Prandtl number

R	Ideal gas constant, J/K/mol
Re	Reynolds number
release_b	Bacterial release constant
$\overline{\text{release\_b}}$	Average bacterial release constant
Sc	Schmidt number
Sh	Sherwood number
S_{net}	Net profit from milk sale, $/kg
t_{clean}	Cleaning time, h
T_f	Milk temperature, K
T_f^{in}	Inlet milk temperature, K
T_f^{out}	Outlet milk temperature, K
t_{heat}	Heating time, h
T_i	Interface temperature, K
T_j	Temperature of milk or utility in channel *j*, K
T_{max}	Maximum temperature for Ratkowsky equation, K
T_{min}	Minimum temperature for Ratkowsky equation, K
T_{pj}	Temperature of plate p adjacent to channel *j*, K
T_s	Heating medium temperature, K
T_s^{in}	Inlet heating medium temperature, K
T_s^{out}	Outlet heating medium temperature, K
tube_diam	Tube diameter after fouling, m
$\overline{\text{tube\_diam}}$	Average tube diameter after fouling, m

T_w	Wall temperature, K
u	Milk velocity, m/s
U	Overall heat transfer coefficient, $W/m^2/K$
U^*	Friction velocity, m/s
u^+	Dimensionless velocity
U_0	Overall heat transfer coefficient under clean conditions, $W/m^2/K$
u_{aver}	Average velocity, m/s
U_j	Overall heat transfer coefficient in channel *j*, $W/m^2/K$
u_s	Heating medium velocity, m/s
u_z	Average fluid velocity, m/s
V_A	Aggregated protein molecular volume, m^3
V_D	Denaturated protein molecular volume, m^3
V_N	Native protein molecular volume, m^3
w_f	Milk mass flowrate, kg/s
w_s	Heating medium mass flowrate, kg/s
x_d	Deposit thickness, m
$\overline{x_d}$	Average deposit thickness, m
y	Laminar boundary layer, m
y^+	Dimensionless distance

Greek Letters

α_0	Ratkowsky constant, $1/h^{0.5}/K$
α_1	Ratkowsky constant, 1/K

β	Deposition rate constant, m^2/kg
βi	Correction factor due to friction
δ	Laminar boundary layer, m
ΔP	Pressure drop, Pa
$\overline{\Delta P}$	Average pressure drop, Pa
δ_T	Thermal boundary layer, m
ε_{fic}	Fictious efficiency
λ_d	Deposit thermal conductivity, W/m/K
λ_f	Milk thermal conductivity, W/m/K
λ_{steam}	Steam thermal conductivity, W/m/K
μ_f	Milk viscosity, kg/m/s
μ_T	Bacterial growth rate, 1/h
μ_{Tj}	Bacterial growth rate in channel *j*, 1/h
μ_{Tp}	Bacterial growth rate in plate *p*, 1/h
ρ_d	Deposit density, kg/m^3
ρ_f	Milk density, kg/m^3
ρ_j	Fluid density in channel *j*, kg/m^3
ρ_w	Heating medium density, kg/m^3
τ_w	Wall shear stress, Pa
φ	Milk volumetric flowrate, m^3/s
Φ_i	Correction factor for non-isothermal flow

Chapter 1

Introduction

1.1 Introduction to fouling

In the food industry many thermal treatments are employed such as pasteurization and ultra-high temperature (UHT) processing to assure product hygienic safety and long shelf life. In the dairy industry thermal processing is an energy-intensive process because every product is heated at least once (de Jong, 1997). In the dairy industry the most common heat treatment process is pasteurization. During milk heating in a heat exchanger, due to its instability, an undesirable deposit of milk solids is formed on the heat exchanger surface. This process of deposit formation is called fouling.

Although this deposit is not sufficient to affect milk composition significantly, it results in hydraulic and thermal performance degradation and created the need for cleaning operations. Fouling of heat exchangers by dairy liquids is a major problem in the dairy industry. The costs of temporarily halting a process and cleaning are very high. Fouling causes undesirable effects such as decreasing in heat-transfer coefficient, increasing in pressure drop and hence a decrease in pumping efficiency, loss of product remaining on the heated wall and contamination of the processed product by loosened deposits (Müller-Steinhagen, 1993; Toyoda et al., 1994).

Apart from protein fouling, biofouling or microbial fouling is also an important issue in the dairy industry. Adherence and growth of microorganisms on heat exchanger surfaces is a significant source of bacterial contamination of dairy products that can lead to spoilage and defects in final product. The pasteurizers operate for a limited time due to the growth of thermoresistant streptococci. The streptococci isolated from milk is mainly *Streptococcus thermophilus* (Bouman et al., 1982; M. Te Giffel et al., 2002).

The increase in bacterial levels of the product during processing is partially due to their growth within the product. A significant factor is also the release of bacteria that have developed on the equipment's surfaces (Bouman et al., 1982; Te Giffel, 1997). Microbial adhesion to surfaces

is regulated by a complex interplay of Van der Waals forces, electrostatic interactions, hydrodynamic conditions, interactions between cells and the potential production of antiadhesive biosurfactants by the bacteria (Austin & Bergeron, 1995; Mozes et al., 1987; Zottola & Sasahara, 1994).

Fouling in the dairy industry is a severe problem compared with other industries. For instance, in the petrochemical industry, heat exchangers may be cleaned only once a year, but in the dairy industry it is common practice to clean them every 5-10 hours (Georgiadis et al., 1998a). According to Georgiadis et al. (1998a) in the dairy industry the cost due to the interruption in production can be dominant compared with the cost due to reduction in performance efficiency. Along with the cost, quality issues are equally important, and in fact many times a shutdown is required due to concerns about product quality/contamination instead of the performance of a heat exchanger. Hence, the need for cleaning gives rise to extra processing costs in terms of capital, energy, maintenance, and production losses (Sandu & Singh, 1991).

In recent years, an attempt to model fouling and microbial fouling has been made so as to simulate the fouling conditions and optimize dairy equipment design and operation (Jun & Puri, 2005).

1.2 Literature Review

1.2.1 Protein Fouling

Milk fouling has been studied for many years. β-Lactoglobulin (β-Lg) and α-lactalbumin (α-La) are the two major whey proteins which affects fouling, but the dominant protein in heat-induced fouling is only β-Lg. The key role of proteins and especially β-Lg in fouling has been recognized in many studies. It has high heat sensitivity and hence figures prominently in the fouling process (Gotham et al., 2007; Lalande & Tissier, 1985; Lyster, 1970). Although the exact mechanisms and reactions between different milk components are not yet fully understood, a relationship between the denaturation of native β-Lg and fouling of heat exchangers has been established (Dalgleish, 1990). Upon heating of milk, the native proteins (β-Lg) first denature (unfold) and expose the core containing reactive sulphydryl groups. The denatured or unfolded protein molecules then react

with similar or other types of protein molecules such as casein and α-La and form aggregates (Jeurnink et al., 1996).

Nowadays, there is extensive literature and many authors have modelled milk fouling both in tubular and in plate heat exchangers. The contribution of Fryer et al. (1996); Georgiadis et al. (1998a); Lalande et al. (1989); Sandu C. & Lund D. (1985) around milk fouling is significant.

Lalande & Tissier (1985) were the first who investigated the effect of β-Lg denaturation in milk fouling and they demonstrated that heat denaturation of this protein governs the milk deposit formation on the heat transfer area.

Building upon this foundation de Jong et al. (1992) applied the kinetics of the β-Lg reaction to analyze fouling in plate heat exchangers. Their research revealed that the amount of deposit could be linked to the rates of protein reactions.

In their initial studies Fryer & Slater (1985) developed a fouling model using a dimensionless number, known as the Biot number (Bi) and a straightforward reaction scheme. This model effectively predicted the typical fouling behavior according to which fouling builds up to an asymptotic level. However, it should be noted that milk fouling may not always exhibit this asymptotic behavior, as later pointed out by the same authors (Paterson & Fryer, 1988). On the other hand, one limitation of this model is its inability to capture the effect of critical parameters like milk composition. The protein reaction scheme is not taken into account and fouling is controlled by reaction at interface layer while also mass transfer operations are omitted.

Paterson & Fryer (1988) conducted a noteworthy analysis concerning the chemical reactions governing fouling. They demonstrated, applying principles from reaction engineering, that milk fouling is a result of chemical reaction(s) occurring throughout the region of the fluid where the temperature is sufficiently high to significant reaction rates. This finding implies that there is no need to assume that the rate controlling step in reaction fouling is the surface reaction. It also implies that bulk reactions could play a substantial role, along with the mass transfer from the bulk region to the hot sublayer.

Building upon this analysis Belmar-Beiny et al. (1993) investigated the impact of Reynolds number and fluid temperature on whey protein fouling. Their research indicated a significant increase in fouling as the fluid temperature rises. They considered two possible mechanisms: (i)

fouling is mass transfer controlled and (ii) fouling is reaction controlled. De Jong et al. (1992) observed that the fouling process was reaction controlled and was not limited by mass transfer.

Delplace et al. (1994) investigated milk fouling within various plate heat exchanger flow arrangements. To predict the dry mass of deposits in each channel, they developed an empirical model that relies on the calculation of heat-induced denaturation of β-Lg protein. This model is based on steady state numerical simulations for temperature profiles prediction. In a related study, Delplace et al. (1995) studied fouling in plate heat exchangers with different plate geometries. Their findings indicated that herringbone plates were less susceptible to fouling compared to straight corrugation plates. Based on steady state temperature profiles and a simple protein kinetics approach, they proposed two empirical models for predicting deposit mass in each channel.

Fryer et al. (1996) developed a statistical model for fouling of a plate heat exchanger. Through a statistically designed series of experiments, they examined and quantified the importance of various factors, including β-Lg reaction rate, on fouling within an ultra-high temperature process. Toyoda et al. (1996) presented a comprehensive fouling model which takes account of mass transfer between bulk and layer.

Sandu (1989) developed a detailed physico-mathematical model where fouling kinetics and dynamics were defined based on experimental results. Sandu & Lund (1985) developed a general model for fouling dynamics for the simple case of an inverse-solubility salt under the assumption that the deposition rate is entirely mass transfer controlled. While this model was extended under more assumptions for more complex fluid systems, it is worth noting that they did not provide simulation results as part of their work.

Until now, in most studies, fouling has been modelled with a simple representation of the heat exchangers hydrodynamics. However, it is known that there are strong interactions between the physicochemical, hydro-and thermodynamic fundamentals involved in fouling. For example, if mass transfer operations are important these are determined by the boundary layer thickness which depends on the fluid velocity. Consequently, it is crucial to take into account all the relevant transport phenomena occurring during milk heat treatment along with the fouling kinetics (Georgiadis et al., 1998a).

According to Fryer (1989) and Sandu & Lund (1985) there is imperative need for optimizing dairy plants suffering severe fouling problems. Accurate prediction analysis of fouling dynamics for a specific system with realistic and detailed models would pave the way for obtaining the optimal design and operating policies for industrial heat exchangers and for saving money.

Georgiadis et al. (1998a) pioneered studying milk fouling as a process affected by momentum, heat, and mass transfer phenomena using fundamental kinetic theories. They developed a detailed dynamic model of a tubular heat exchanger and a plate heat exchanger respectively integrating the fouling model of Toyoda et al. (1996) with a detailed dynamic heat exchanger model that takes into account in detail transport phenomena. The change of heat transfer due to fouling was described in terms of the dimensionless Biot number, related to a rate model for the deposition of aggregated protein. The simulation results were verified against available experimental data and current industrial techniques for fouling mitigation. The 2D model of plate heat exchangers of Georgiadis & Macchietto (2000) was taken up as a basis for further studies by several authors (Jun & Puri, 2005).

1.2.2 Biofouling

According to Flint et al. (2020) biofilms in the dairy industry is a research area with increasing interest the last 30 years as they can act as a source of contamination to product and other surfaces. Initial investigations into biofilms were primarily centered on identifying the bacterial species present, determining the locations within the plant where these bacteria adhered, examining the influence of surface physicochemical properties on microorganism attachment, and assessing the efficiency of cleaning and sanitization procedures in eliminating them. The contribution of Flint in biofouling is significant (Flint et al., 2001; Flint, Bremer, et al., 1997; Flint et al., 1999).

According to de Jong (2002) and Flint et al. (1999) thermoduric bacteria, such as *Streptococcus Thermophilus* are able to survive pasteurization and attach to the surface of heat exchangers acting like contaminants.

According to Yoo et al. (2006) the viability of *Bacillus Stearothermophilus* is enhanced by the presence of protein aggregated. Additionally, the metabolic activity of *Bacillus*

Stearothermophilus contributes to the acidity of milk and lactose solution. Consequently, this acidity reduces protein stability during processing and accelerates the aggregation of milk protein.

Lindsay & Flint (2009) review the concerns of thermophiles in milk powder related to spoilage caused by the production of acids and enzymes, as well as the sensory defects resulting from such spoilage. It also pointed out a significant knowledge gap concerning the structure and composition of biofilms formed by thermophilic bacteria. The same research group conducted comparative genomic research which revealed how *Geobacillus Stearothermophilus* has adapted to thrive in a dairy environment (Burgess et al., 2017).

According to Burgess et al. (2017) the most common group of microorganisms that form biofilms in the dairy industry is thermophilic bacilli and they are considered as an indicator of poor hygiene. These bacteria can thrive in specific areas such as the preheating and evaporation sections of milk powder plants, where temperature is conducive to their growth (Murphy et al., 1999; Scott et al., 2007). Burgess et al. (2017), also, studied the factors affecting spore formation of *Anoxybacillus Flavithermus*. These spores are of most concern in milk powder production since they are present in the evaporators. These spores are formed between 55 and 60^{o}C. Zhao et al. (2013) confirmed the results from Burgess et al. (2017) by showing that *Anoxybacillus Flavithermus* and *Geobacillus Stearothermophilus* prefer to grow in temperature ranges between 55 and 65^{o}C.

1.3 Project objectives

The aim of the diploma thesis is the development of a mathematical model that describes both protein fouling and bacterial contamination of milk due to the adherence, growth, and release of bacteria in thermal processing equipment after an extensive literature review. The developed approach is able to predict heat transfer resistance evolution due to fouling and microbial contamination and aid the dairy industry to improve the operating conditions. Moreover, different cases of simulations for shell and tube heat exchanges and plate heat exchanges have been studied using the process modeling environment gPROMS™ for process understanding. Finally, using the gOPT tool three different configurations of shell and tube heat exchangers are optimized, minimizing the total cleaning cost due to fouling. The accurate prediction of fouling dynamics and

contamination helps obtain optimal operating policies, desired product quality and design characteristics of industrial heat exchangers.

This thesis is divided into 6 chapters, the content of which is described as follows:

- **Chapter 2:** Presents the theoretical background for fouling, the heating equipment, and the cleaning process of heat exchangers.
- **Chapter 3:** Presents the fouling mathematical model of shell and tube heat exchangers along with the simulation results.
- **Chapter 4:** Presents the fouling mathematical model of plate heat exchangers along with the simulation results.
- **Chapter 5:** Uses the mathematical model of Chapter 3 and presents the optimization results of three different configurations of shell and tube heat exchangers.
- **Chapter 6:** Presents the main conclusions of this work and proposes actions for future work.

Chapter 2

Theoretical Background

2.1 Protein Fouling

Milk is a complicated biological fluid and contains a number of species. Its average composition is given in Table 2.1. Whey proteins constitute only about 4% of the milk solids, but they account for more than 50% of the fouling deposits in type A fouling. An important limitation of heating milk products is the deposition of proteins. Decreased heat transfer coefficient, increased pressure drops, product losses and increased cleaning costs and environmental load are the main drawbacks of fouling.

Table 2.1 Average composition of milk (Bansal & Chen, 2006)

Constituents	**Average concentration (%)**
Water	87
Total solids	13
• **Proteins**	3.4
○ **Casein**	2.6
○ **β-Lactoglobulin (β-Lg)**	0.32
○ **α-Lactalbumin (α-La)**	0.12
• **Lactose**	4.8
• **Minerals**	0.8
• **Fat**	3.9

Bovine β-Lg exists in milk as a dimer of two monomeric subunits non-covalently linked. Each monomer contains two disulphide bridges and one single thiol group which in the native state is buried in the interior of the molecule. In Figure 2.1 the native, unfolded and aggregated state of β-Lg is represented.

Figure 2.1 Schematic representation of the native, unfolded and aggregated state of β-Lg (Morr, 1985)

Milk fouling can be classified into 2 categories known as type A and type B depending on the intensity of heating (Burton, 1968).

- Type A (protein) fouling takes place at temperatures between 75°C and 110°C. The deposits are white, soft, and spongy (milk film), and their composition is 50-70% proteins, 30-40% minerals, and 4-8% fat.
- Type B (mineral) fouling takes place at temperatures above 110°C. The deposits are hard, compact, granular in structure, and gray in color (milk stone), and their composition is 70-80% minerals (mainly calcium phosphate), 15-20% proteins, and 4-8% fat.

The characteristics of mineral fouling differ significantly from those of protein fouling. The scarcity of modeling publications in the area of mineral fouling is attributed to the complexity of the underlying phenomena. In terms of pressure drop and thermal resistance, fouling related to mineral precipitation might have a comparatively minor impact on the process compared to protein fouling. This is likely due to the fact that protein fouling is much more voluminous than mineral precipitation (Visser & Jeurnink, 1997).

The composition of fouling at different processing temperature ranges is shown in Table 2.2.

Table 2.2 Classification of protein fouling (Hinton, 2003)

Classification	Temperature (^{o}C)	Process	Composition (%wt.)		
			Protein	Mineral	Fat
Type A	75-110	Pasteurization	50-70	30-50	4-8
Type B	>110	UHT treatment	15-20	70-80	4-8

2.1.1 Factors Affecting Milk Protein Fouling

Fouling depends on various parameters such as heat transfer method, hydraulic and thermal conditions, heat transfer surface characteristics, and type and quality of milk along with its processing history. These factors can be broadly classified into 4 major categories: milk composition, operating conditions in heat exchangers, type and characteristics of heat exchangers, presence of microorganisms.

- Milk composition: The composition of milk depends on its source and hence may not be possible to change. Increasing the protein concentration results in higher fouling (Changani et al., 1997; Toyoda et al., 1994). Additives may reduce fouling by enhancing the heat stability of milk but may be forbidden in many countries (Changani et al., 1997; Lyster, 1970; Skudder et al., 1981).
- Operating conditions in heat exchangers: Important operating parameters that can be varied in a heat exchanger are air content, velocity/turbulence, and temperature. The presence of air in milk enhances fouling only when the air bubbles are formed on the heat-transfer surface, which then act as nuclei for deposit formation (Burton, 1968). Fouling decreases with increasing turbulence (Belmar-Beiny et al., 1993; Santos et al., 2003). According to Changani et al. (1997) and Paterson & Fryer (1988), the thickness and subsequently the volume of laminar sublayer decrease with increasing velocity and as a result, the amount of deposit on the heat-transfer surface decreases. Temperature of milk in a heat exchanger is probably the single most important factor controlling fouling (Belmar-Beiny et al., 1993; Burton, 1968; Corredig & Dalgleish, 1996; Elofsson et al., 1996; Jeurnink et al., 1996; Santos et al., 2003; Toyoda et al., 1994). Increasing the temperature results in higher

fouling. It is worth mentioning that both the absolute temperature and temperature difference are important for fouling.

- Type and characteristics of heat exchangers: Plate heat exchangers are commonly used in the dairy industry because they offer advantages of superior heat-transfer performance, lower temperature gradient, higher turbulence, ease of maintenance, and compactness over tubular heat exchangers. However, plate heat exchangers are prone to fouling because of their narrow flow channels (Delplace et al., 1994) and contact points between adjacent plates (Belmar-Beiny et al., 1993). The surface characteristics are generally important only until the surface gets covered with the deposits. Stainless steel is the standard material used for surfaces that are in contact with milk. Factors that may affect fouling of a stainless-steel surface are presence of a chromium oxide or passive layer, surface charge, surface energy, surface microstructure (roughness and other irregularities), presence of active sites, residual materials from previous processing conditions, and type of stainless steel used (Jeurnink et al., 1996; Visser & Jeurnink, 1997).
- Presence of microorganisms: The formation of deposits promotes the adhesion of microorganisms to heat-transfer surface, resulting in biofouling. Furthermore, the deposits provide nutrients to microorganisms, ensuring their growth. Their inactivation is important for the products with longer shelf life. The presence of microorganisms in the process stream and/or deposit layer not only affects the product quality, but it also influences the fouling process as well (Flint, Bremer, et al., 1997; Flint et al., 1999; Yoo et al., 2006).

2.2 Biofouling

Biofouling is the attachment and growth of microorganisms on the heat transfer surface. Biofouling in heat exchangers, either by micro-organisms deposition or biofilm formation results in serious quality issues. According to Bott (1993) biofouling takes place through two different mechanisms:

- The micro-organisms accumulate directly on the heat transfer area.
- The micro-organisms attach to the deposit layer formed on the heat transfer area. With the supply of nutrients by the deposits micro-organisms multiply.

According to Flint, Bremer, et al. (1997); Flint et al. (1999); Yoo et al. (2006), the deposit layer of micro-organisms is able to influence the protein fouling process.

Biofouling can take place at any stage of the manufacturing process. In Table 2.3 are presented the zones in dairy industry where biofouling has been identified as causing issue (S. Flint et al., 2020).

Table 2.3 Biofilms in dairy manufacturing plant

Location	Typical microbes	Conditions favoring growth
Raw milk handling/transportation	*Pseudomonas*	Chilled temperatures
Membrane processing	*Klebsiella*	Water source
Plate heat exchangers	*Streptococci*/thermophiles	Large surface area at 30-65^{o}C
Separators	Mesophilic/thermophilic bacteria	Large surface area
Filler heads	*Bacillus cereus*	Milk
Environment	Listeria/Cronobacter	Moisture/ organic material
Evaporators	Thermophiles	High temperature/ milk fouling
Waste treatment	Gram-negative bacteria	Ambient temperature/ nutrients

2.2.1 Factors Affecting Biofilm Formation

The initial layer of material (protein, fat, salts) that deposits onto a clean surface, commonly referred as “conditioning layer” plays a significant role (al-Makhlafi et al., 1994; L. Barnes et al., barnes2001; L.-M. Barnes et al., 1999). The surface topography, the roughness, the charge, the hydrophobicity, and the cell surface proteins also affect biofouling (Boulangé-Petermann et al., 1997; Briandet et al., 2001; S. H. Flint, Brooks, et al., 1997; Lindsay et al., 2000).

Bacteria demonstrated a tendency to adhere more favorably to stainless steel and zinc substrates in comparison with other metals and glass substrates. Additionally, a higher number of bacteria adhered to stainless steel 316L than to 304L. The adherence of bacteria to surfaces with a range of surface roughness was observed to be predominantly unaffected by the substrate’s

topography (S. H. Flint, Bremer, et al., 1997). The attachment and survival of pathogenic bacteria is increased by the presence of other bacteria (Bremer et al., 2001).

2.3 Heating Equipment

In the dairy industry, there are two basic types of heat treatment equipment, called direct and indirect heating systems. Tubular and plate heat exchanger are indirect heating systems. The tubular heat exchangers are more robust than plate heat exchangers, but the specific heat-exchange area (area/m^3) is smaller than that of plate heat exchangers. For improvement of the heat-transfer coefficient natural turbulence as a result of a high Reynolds number is used (de Jong et al., 1992).

Plate Heat Exchangers (PHE) are extensively used in the food industry for thermal processes. They have excellent heat transfer performance enabling the design of more compact systems compared to conventional shell and tube heat exchangers. Apart from their easy maintenance and other advantages, PHEs constitute the first choice for numerous engineering applications involving liquid-liquid heat transfer duties. PHEs are widely used in the dairy, beverage, general food processing and pharmaceutical industries due to their ease of cleaning and their thermal control characteristics required for thermal sterilization and pasteurization purposes.

PHEs offer an ideal environment for biofilm growth due to their expansive surface area and the presence of temperature gradients appropriate for a wide variety of bacteria. Extensive research has been conducted on the growth of *Streptococcus Thermophilus* in plate heat exchangers because of its potential impact on milk quality (Bouman et al., 1982). The thermotolerant nature of *Streptococcus Thermophilus* allows some cells to survive the pasteurization process and inhabit the pasteurizer. Dairy product contamination often occurs as a result of the transfer of microorganisms from biofilms that form on the surfaces of milk processing plants.

However, PHEs used in milk thermal treatments are subject to rapid fouling and require frequent cleanings not only to recover their thermal and hydraulic performance but also for microbiological hygiene reasons.

2.4 Cleaning in Place – Optimization

Cleaning-in-place (CIP) systems are widely used in the food industry to ensure the hygienic safety of foods and to optimize plant performance. CIP systems require large quantities of clean water and caustic and/or acid solutions. 0.5-1.5 %wt. NaOH solutions are the most used chemical cleaning detergent on an industrial scale (Bylund, 1995). In the dairy industry milk fouling is so rapid that heat exchangers need to be cleaned daily to maintain production capability and efficiency and meet strict hygiene standards. The CIP operations are based on pre-determined heating-cleaning cycles. These cycles are developed empirically, as well as the equipment design and control policies and they neglect broad economic considerations leading to increased operating and capital costs.

The presence of fouling in heat exchangers represents extra capital, additional energy consumption, water, and labor costs to the industrial sector. According to Van Asselt et al. (2005), NIZO, a leading dairy and food research organization, has linked 80% of production expenses in the dairy industry to the impacts of fouling and cleaning. According to Georgiadis et al. (1998b) the cost of fouling includes:

- increased capital cost because of oversized or redundant equipment
- additional downtime costs for maintenance and repair
- costs for production losses
- costs for energy, water, and cleaning equipment
- increased energy (fuel) costs due to decreased heat transfer coefficient.

The appropriate size of the heat exchanger chosen for milk heat treatment should be determined by finding an economic balance between the capital cost of the equipment and the potential advantages derived from improved thermal efficiency and reduced cleaning costs.

Sandu C. & Lund D. (1985) examined the potential for optimal design and operation of heat exchangers, they underscored the strong correlation between the dynamics of fouling and the design and operation of heat exchangers utilized in pasteurization and they emphasized on quantifying and optimizing thus relationship.

In an effort to explore aspects of optimization problems, some authors examined the impact of different operating procedures on milk fouling. Yoon & Lund (1994) conducted an experimental comparison of two different operating procedures affecting the temperature profile under milk fouling. De Jong & Van Der Linden (1992) presented a mathematical model that defines the optimal operating conditions in heat treatment equipment for milk, drawing an analogy with a cascade of non-isothermal plug flow and isothermal tank reactors. However, this analysis did not address the challenge of defining an optimal control policy to maintain milk temperature close to its target value as this entire analysis relies on simulation rather than optimization schemes. Fryer & Slater (1985) used simplified models to simulate alternative strategies for controlling heat exchangers susceptible to fouling. While their work did not rely on an optimization procedure, valuable insights were gained regarding the effectiveness of different control strategies.

Chapter 3

Modeling and Simulation of Shell and Tube Heat Exchangers under Fouling

3.1 Mathematical Model

3.1.1 Description of Mathematical Model

The mathematical model used was originally proposed by Georgiadis et al. (1998a). This mathematical model has been validated by experimental data from Belmar-Beiny et al. (1993) and presents a good agreement with these data. The β-Lg reaction scheme used for the fouling model was first proposed by de Jong et al. (1992) and then adopted from Toyoda et al. (1996). This mass transfer reaction scheme is depicted in Figure 3.1 and is the most detailed in the literature. Heating milk above 65^{o}C, causes β-Lg to lose its thermal stability leading to a molecular denaturation process. This denaturation results in the exposure of reactive sulphydry (-SH) groups leading to irreversible polymerization and the formation of insoluble particles in aggregation (de Jong et al., 1992; Georgiadis et al., 1998a; Toyoda et al., 1994). For an effective study of fouling, it is essential to capture the interrelationship between the chemical reactions that lead to deposition and the fluid mechanics associated with the heat-transfer equipment taking into account the fluid velocity, the milk composition and temperature (Georgiadis & Macchietto, 2000).

The reaction scheme is described as follows:

- Proteins react in both the bulk and the thermal boundary layer in the milk. Native protein N is transformed to denaturated protein D, in a first-order reaction. The denaturated protein then reacts to give aggregated protein A in a second-order reaction.
- For every protein, there is mass transfer between the bulk and the thermal boundary layer.
- There is only a deposition of the aggregated protein on the wall. The deposition rate is proportional to the concentration of aggregated protein in thermal boundary layer.
- The resistance to heat transfer caused by fouling is proportional to the thickness of the deposit.

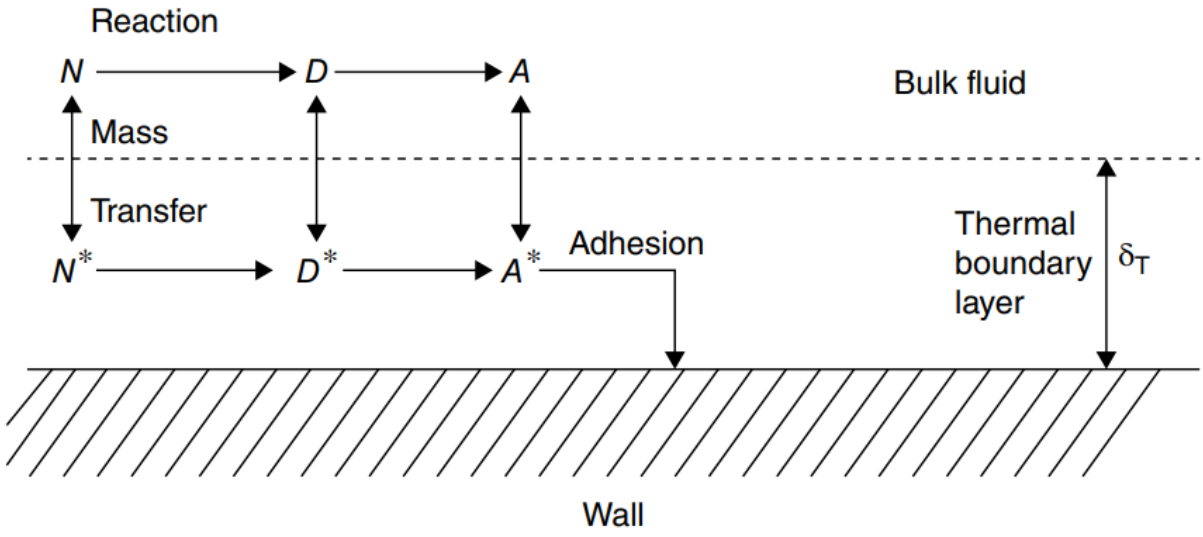

Figure 3.1 Protein reaction scheme (Georgiadis et al., 1998a)

The reaction rate constant follows the form of Arrhenius and is expressed by Equation (3.1).

$$k = k_0 \exp\left(-\frac{E}{RT}\right) \tag{3.1}$$

Where k_0 is the pre-exponential factor and E is the activation energy. The values of these parameters for the two reactions are taken from de Jong et al. (1992) and given in Table 3.1.

Table 3.1 Kinetic data for the reactions of β-lactoglobulin

Temperature Range (°C)	**E_N (kJ/mol)**	**k_{N0} (1/s)**	**E_D (kJ/mol)**	**k_{D0} (m^3/(kg·s)**
70-90	261	$3.37 \cdot 10^{37}$	312	$1.36 \cdot 10^{43}$
90-150	-	-	56	$1.83 \cdot 10^{6}$

The subscripts N and D refer to the first and second reaction respectively.

Although there is considerable research regarding mathematical modeling of biofilms, there is limited work on biofilm modeling in the dairy industry. The earliest and the only quantitative model to describe bacteria adherence, growth and release within process equipment was developed by de Jong (2002). However, this model has successfully been validated on an industrial scale only for plate heat exchangers (S. Flint et al., 2020). Since there is no other

available mathematical model for biofouling in dairy industry, the model of de Jong (2002) was adopted for biofouling during milk processing.

The transportation of bacteria to the surface and the adsorption reaction with the surface determine the number of bacteria adhered to a surface (Figure 3.2).

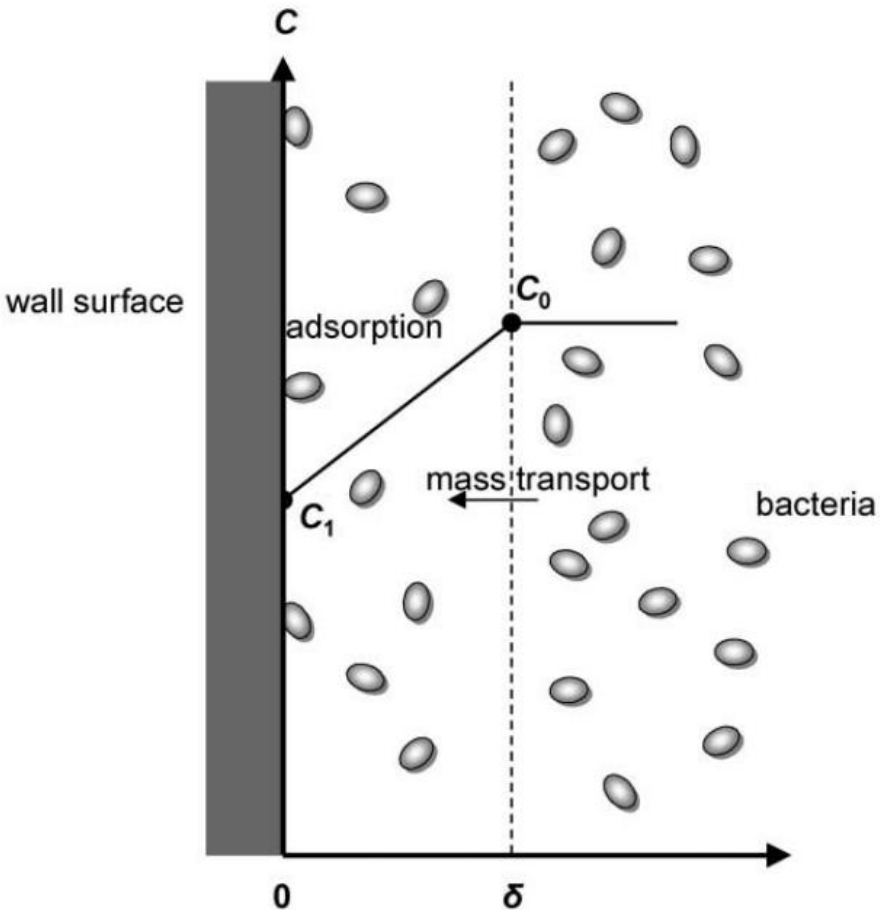

Figure 3.2 Schematic representation of the adherence of bacteria as a heterogenous adsorption reaction at solid surface (de Jong, 2002)

3.1.2 Modeling Framework

The mathematical model concerning protein fouling was based on that of Georgiadis et al. (1998a) and was simplified from a two-dimensional (axial and radial distribution) to one-dimensional (only axial) problem while the one concerning biofouling was based on that of de Jong (2002).

The model was developed based on the following assumptions:

- The radial dependency of velocity and proteins concentration is not taken into account.
- The milk temperature remains uniform radially both in the bulk and the thermal boundary layer meaning that the temperature does not vary across the tube's radius.
- The flow of the milk is plug with a uniform velocity while the velocity in the thermal boundary layer is considered unsignificant.
- The changes in milk's physical properties due to temperature variation were not considered and the physical properties assumed to be consistent with those of skimmed milk (McKetta, 1984) (Table 3.2). However, transport properties are calculated in detail.
- The overall heat transfer resistance is calculated by that on the tube side fluid (milk).
- The concentration and the temperature for proteins at the boundary layer are radially uniform.
- The adhesion of bacteria is a heterogeneous adsorption reaction of bacteria to a solid surface.
- The adhesion rate constant, k_a, is constant within the temperature range considered.
- The growth rate at the surface is equal to that of bacteria in the bulk.
- The bacteria release from the wall is related to the wall coverage by Equation (3.2). Equation (3.3) implies that at complete wall coverage all the grown bacteria at the bacteria – liquid interface is released to the bulk.

$$release\_\beta = 1 - Ae^{-k_r \cdot n_w} \tag{3.2}$$

$$A = 1 - \text{release}\_\beta \; at \; n_w = 0 \tag{3.3}$$

where k_r is a release constant equal to $6.1 \cdot 10^{-12}$ m^2/cfu and A is equal to 0.82 (de Jong, 2002).

The first and second assumption simplify the conservation laws which are described by partial differential equations that describe hydrodynamics, reactions and mass transfer between the bulk and the layer.

To align with the reaction scheme involving mass transfer between the bulk and the thermal boundary layer, the bulk is distinguished from the boundary layer based on the conversation laws. The velocity within the thermal boundary layer, although is small, it cannot be disregarded.

The model is developed considering a differential element in a circular tube, with r_0 the inner radius and L the length of the tube as is shown in Figure 3.3.

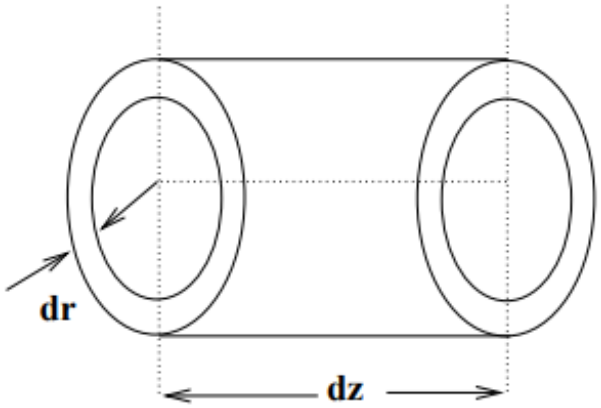

Figure 3.3 Differential element in a shell and tube heat exchanger

3.1.3 Material Balances for Proteins in the Bulk

The material balances for the native, denaturated and aggregated protein in the bulk are expressed by Equations (3.4), (3.5) and (3.6) respectively.

Native protein:

$$\frac{\partial C_N}{\partial t} + u\frac{\partial C_N}{\partial z} = -k_{N0}\exp\left(-\frac{E_N}{RT_f}\right)C_N + \frac{4}{diam}k_{mN}(C_N^* - C_N) \tag{3.4}$$

Denaturated protein:

$$\frac{\partial C_D}{\partial t} + u\frac{\partial C_D}{\partial z} = k_{N0}\exp\left(-\frac{E_N}{RT_f}\right)C_N - k_{D0}\exp\left(-\frac{E_D}{RT_f}\right)C_D^2 + \frac{4}{diam}k_{mD}(C_D^* - C_D) \tag{3.5}$$

Aggregated protein:

$$\frac{\partial C_A}{\partial t} + u\frac{\partial C_A}{\partial z} = k_{D0}\exp\left(-\frac{E_D}{RT_f}\right)C_D^2 + \frac{4}{diam}k_{mA}(C_A^* - C_A) \tag{3.6}$$

T_f is the milk temperature and is axial dependent. The surface reactions are assumed to take place at the interface temperature T_i, which is axial dependent so as to distinguish bulk and surface reaction rates.

3.1.4 Material Balances for Proteins in the Thermal Boundary Layer

The material balances for the native, denaturated and aggregated protein in the thermal boundary layer are expressed by Equations (3.7), (3.8) and (3.9) respectively.

Native protein

$$\frac{\partial C_N^*}{\partial t} = -k_{N0}\exp\left(-\frac{E_N}{RT_i}\right)C_N^* - \frac{k_{mN}}{\delta_T}(C_N^* - C_N) \tag{3.7}$$

Denaturated protein

$$\frac{\partial C_D^*}{\partial t} = k_{N0}\exp\left(-\frac{E_N}{RT_i}\right)C_N^* - k_{D0}\exp\left(-\frac{E_D}{RT_i}\right)C_D^{*2} - \frac{k_{mD}}{\delta_T}(C_D^* - C_D) \tag{3.8}$$

Aggregated protein

$$\frac{\partial C_A^*}{\partial t} = k_{D0}\exp\left(-\frac{E_D}{RT_i}\right)C_D^{*2} - \frac{1}{\delta_T}[k_{mA}(C_A^* - C_A) + k_w C_A^*] \tag{3.9}$$

The dimensionless Biot (*Bi*) number is used to express the change of heat transfer due to fouling and it is correlated with the deposition rate via constant β (Toyoda et al., 1994). The deposition rate is linked to the concentration of aggregated protein in the boundary layer with the mass transfer coefficient k_w. The correlation between Biot number and deposition rate is given by Equation (3.10).

$$\frac{\partial \mathrm{Bi}}{\partial \mathrm{t}} = \beta \mathrm{k_w} \mathrm{C_A^*} \tag{3.10}$$

The value of the mass-transfer coefficient to the deposit k_w, is given by Toyoda et al. (1996) and it is equal to 10^{-7} m/s while the value of constant β, is given by Georgiadis et al. (1998a) and it is equal to 58 m^2/kg.

3.1.5 Energy Balances

The energy balance on the milk side is given by Equation (3.11) while for the heating medium is given by Equation (3.12) for co-current and by Equation (3.13) for counter-current.

$$\rho_f \cdot \mathrm{Cp}_f \cdot \frac{\partial \mathrm{T_f}}{\partial \mathrm{t}} + \rho_f \cdot \mathrm{Cp}_f \cdot \mathrm{u} \cdot \frac{\partial \mathrm{T_f}}{\partial \mathrm{z}} = \mathrm{U} \cdot \frac{4}{\mathrm{diam}} \cdot (\mathrm{T_w} - \mathrm{T_f}) \tag{3.11}$$

For the shell side (utility) one option is the use of steam as heating fluid and another option is the use of hot water as heating fluid for counter current and co-current operation. In the case of steam usage, it is assumed that the inlet and the outlet steam temperature are equal (flow rate is high enough for the given thermal duty) providing its heat of condensation for the heating duties.

- Co-current operation with milk

$$\frac{\partial T_s}{\partial t} + u_s \frac{\partial T_s}{\partial z} = -\frac{1}{\rho_w Cp_w} \cdot U \cdot \frac{4}{diam} \cdot (T_s - T_f) \tag{3.12}$$

- Counter-current operation with milk

$$\frac{\partial T_s}{\partial t} - u_s \frac{\partial T_s}{\partial z} = -\frac{1}{\rho_w Cp_w} \cdot U \cdot \frac{4}{diam} \cdot (T_s - T_f) \tag{3.13}$$

3.1.6 Calculation of Transport Properties

The values of the variables of the thickness of the thermal boundary layer, δ_T, and the mass transfer coefficients k_{mN}, k_{mD}, k_{mA} that are included in the fouling model of the shell and tube heat exchanger are calculated by the following equations.

The thickness of the thermal boundary layer, δ_T, is related to that of the laminar boundary layer, δ, and is estimated by Equation (3.14).

$$\frac{\delta_T}{\delta} = Pr^{1/3} \tag{3.14}$$

where *Pr* is the dimensionless Prandl number given by Equation (3.15):

$$Pr = \frac{C_{pf} \cdot \mu_f}{\lambda_f} \tag{3.15}$$

The thermophysical properties of milk, water, and deposit are given in Table 3.2.

Table 3.2 Thermophysical properties of milk, deposit, and water

	Density, ρ (kg/m^3)	**Thermal Conductivity, λ (W/m/K)**	**Heat Capacity, C_p (J/kg/K)**	**Viscosity, μ (kg/m/s)**	**Source**
Milk	1030	0.59	3930	$1.5 \cdot 10^{-3}$	(McKetta, 1984)
Deposit	1030	0.50	1970	-	(Leclerq-Perlat & Lalande, 1991; Sharma & Macchietto, 2021)

Assuming laminar layer, δ, is equal to the thickness of the viscous sub-layer (Brodkey & Hershey, 2003) and building upon the fact that the flow of milk during heating is turbulent (Reynolds > 2100) it is easy to calculate laminar layer, δ, (using the dimensionless velocity, u^+, and the dimensionless distance, y^+).

$$u^+ = y^+ \tag{3.16}$$

$$u^+ = \frac{u}{U^*} \tag{3.17}$$

$$y^+ = \frac{y \cdot U^* \cdot \rho_f}{\mu_f} \tag{3.18}$$

U^* is the friction velocity and is given by Equation (3.19).

$$U^* = \sqrt{\frac{\tau_w}{\rho_f}} \tag{3.19}$$

By setting δ equal to y, since it is equal to the boundary layer thickness, and y^+ equal to 5 it is possible to calculate laminar layer, δ.

The wall shear stress can be calculated using the Equations (3.20) – (3.24).

$$f = 0.079 \cdot Re^{1/4} \tag{3.20}$$

$$f = \frac{\tau_w}{\frac{1}{2}\rho_f u_{aver}^2} \tag{3.21}$$

$$Re = \frac{diam \cdot u_{aver} \cdot \rho_f}{\mu_f} \tag{3.22}$$

$$u_{aver} = \frac{w_f}{\rho_f \cdot Area} \tag{3.23}$$

$$Area = \frac{\pi \cdot diam^2}{4} \tag{3.24}$$

The mass-transfer coefficients for the three proteins are related to the diffusion coefficients and given by Equation (3.25).

$$k_{mF} = \frac{D_F}{\delta}, \qquad F = N, D, A \tag{3.25}$$

The diffusion coefficients can be estimated by the Wilke-Chang equation (Perry & Green, 2019) and given by Equation (3.26):

$$D_F = 1.31 \cdot 10^{-17} \cdot \frac{T_i}{\mu V_F^{0.6}}, \qquad F = N, D, A \tag{3.26}$$

where V_F, is the molecular volume of the absorbed particles which is calculated by Equation (3.27).

$$V_F = N_{AV} \cdot \frac{1}{6} \cdot \pi \cdot d_i^3, \qquad F = N, D, A \tag{3.27}$$

The particle diameters are shown in Table 3.3.

Table 3.3 Values of particle diameters for the three proteins (Georgiadis et al., 1998a)

Native, d_N (m)	Denaturated, d_D (m)	Aggregated, d_A (m)
$7.5 \cdot 10^{-11}$	$7.5 \cdot 10^{-11}$	$4.2 \cdot 10^{-10}$

3.1.7 Quantifying Fouling

For fouling estimation some extra variables are used. Since the Biot number is a function of the tube distance *z* (it is determined by the aggregated protein concentration in the thermal boundary layer), an average Biot number can be defined over the tube by Equation (3.28).

$$\overline{Bi} = \frac{1}{L}\int_0^L Bi(z)dz \tag{3.28}$$

The deposit thickness, x_d, at each position *z* along the heat exchanger can be estimated using the Biot number by Equation (3.29).

$$x_d(z) = \frac{\lambda_d \cdot Bi(z)}{U_0} \tag{3.29}$$

An average deposit thickness is defined over the tube by Equation (3.30).

$$\overline{x_d} = \frac{1}{L}\int_0^L x_d(z)dz \tag{3.30}$$

The deposit mass at each position z along the heat exchanger is a function of Biot number and is defined by Equation (3.31).

$$Mass(z) = \frac{\lambda_d \cdot Bi(z) \cdot \rho_d}{U_0} \tag{3.31}$$

Similarly, the average deposit mass over the tube is defined by Equation (3.32).

$$\overline{mass} = \frac{1}{L}\int_0^L mass(z)dz \tag{3.32}$$

An alternative way for fouling estimation is by the “fictitious” efficiency of the heat exchanger given by Equation (3.33).

$$\varepsilon_{fic} = \frac{heat\ exchanged\ operation\ without\ control}{maximal\ heat\ exchanged} = \frac{T_f^{out}(t) - T_f^{in}}{T_f^{out}(0) - T_f^{in}}, \forall t \in (0, t_{heat}] \quad (3.33)$$

where $T_f^{out}(0)$ is the milk outlet temperature at steady state, $T_f^{out}(t)$ is the same temperature during the heating operation and t_{heat} is the total heating period.

The overall heat-transfer coefficient, *U*, and the interface temperature, T_i, are given by Equations (3.34) - (3.36) (Fryer & Slater, 1985).

$$U = \frac{U_0}{1 + Bi} \quad (3.34)$$

- Steam as heating fluid

$$T_i = \frac{T_w + Bi \cdot T_f}{1 + Bi} \quad (3.35)$$

- Hot water as heating fluid

$$T_i = \frac{T_s + Bi \cdot T_f}{1 + Bi} \quad (3.36)$$

3.1.8 Quantifying Pressure Drop

As fouling proceeds, the reduction in size of the flow channels results in an increase in pressure drop over the heat exchanger. Thus, a new tube diameter is calculated by Equation (3.37).

$$Tube\_diam(z) = diam - 2 \cdot x_d(z) \quad (3.37)$$

The average new tube diameter is estimated by Equation (3.38).

$$\overline{tube\_diam} = \frac{1}{L}\int_0^L Tube\_diam(z)dz \quad (3.38)$$

The pressure drop due to fouling is calculated by Equation (3.39) and the mean pressure drop by Equation (3.40) (Peters S. M. et al., 2006)

$$\Delta P(z) = \frac{2 \cdot \beta_i \cdot f_i \cdot mass\_vel^2 \cdot L}{\rho_f \cdot Tube\_diam(z) \cdot \Phi_i} \quad (3.39)$$

$$\overline{\Delta P} = \frac{1}{L}\int_0^L \Delta P(z)dz \quad (3.40)$$

where β_i is equal to 1.2, and Φ_i is equal to 1.05.

The variables used for the calculation of pressure drop are estimated by Equations (3.41) - (3.45).

$$f_i = \frac{0.046}{(AvRe)^{0.2}}, \qquad AvRe > 2100 \tag{3.41}$$

$$AvRe = \frac{\overline{tube\_diam} \cdot \text{av\_vel} \cdot \rho_f}{\mu_f} \tag{3.42}$$

$$\text{av\_vel} = \frac{w_f}{\rho_f \cdot \text{Cross}Area} \tag{3.43}$$

$$CrossArea = \frac{\pi \cdot \overline{tube\_diam}^2}{4} \tag{3.44}$$

$$\text{mass\_vel} = \frac{w_f}{\text{Cross}Area} \tag{3.45}$$

3.1.9 Growth and Inactivation of Bacteria

The bacterial growth is a function of temperature and is given by the modified expanded model of Ratkowsky, et al. (1983):

$$\mu_T = [a_0(T_f - T_{min})\left(1 - \exp\left(a_1(T_f - T_{max})\right)\right)]^2 \tag{3.46}$$

For temperatures lower than 13.4ºC and higher than 54.2ºC, Equation (3.46) is equal to zero ($\mu_T = 0$).

The values of the parameters of Equation (3.46) are presented in Table 3.4.

Table 3.4 Parameters of Ratkowsky equation (de Jong, 2002)

a_0 (1/h$^{0.5}$/K)	a_1 (1/K)	T_{min} (ºC)	T_{max} (ºC)
0.0671	0.143	13.4	54.2

The surface growth rate is assumed to be equal to the bulk growth rate (de Jong, 2002).

The destruction of bacteria is also a function of temperature, and it follows the Arrhenius expression:

$$k_{de} = k_{de0}\exp\left(-\frac{E_a}{RT_f}\right) \tag{3.47}$$

where k_{d0} is pre-exponential factor equal to $1.42 \cdot 10^{108}$ s^{-1} and E_a is the activation energy equal to 723.5 kJ/mol (de Jong et al., 2002).

3.1.10 Adherence, Growth, and Release in Equipment

Bacteria adhere to the surface and multiply. The model is described from two mass balances: one for the wall on which bacteria adhere and one for the milk which are expressed by Equation (3.48) and Equation (3.49) respectively.

$$Change\ in\ wall\ coverage\ with\ time = Produced\ at\ the\ surface - Released + Adhered$$

$$\frac{dn_w}{dt} = \mu_T n_w (1 - release\_\beta) + k_a c \tag{3.48}$$

$$Change\ in\ bulk\ conc\ with\ position = Released - Adhered + Produced\ in\ the\ bulk - Destroyed$$

$$\frac{dc}{dz} = \frac{\pi \cdot diam}{\varphi}(release\_\beta \mu_T n_w - k_a c) + \frac{\pi \cdot diam^2}{4\varphi}(\mu_T - k_{de})c \tag{3.49}$$

where k_a is the adhesion constant equal to $4.14 \cdot 10^{-8}$ m/s (de Jong et al., 2002).

The average bacterial bulk concentration is defined over the tube by Equation (3.50).

$$\bar{c} = \frac{1}{L}\int_0^L c(z)dz \tag{3.50}$$

3.1.11 Boundary Conditions

The values of the inlet protein concentrations (z = 0) and are the following (McKetta, 1984):

$$C_{N,in} = 3.8\ kg/m^3$$

$$C_{D,in} = 0.0\ kg/m^3$$

$$C_{A,in} = 0.0\ kg/m^3$$

The values of the inlet (z = 0) concentrations of the layer proteins are the following (McKetta, 1984):

$$C^*_{N,in} = 3.8\ kg/m^3$$

$$C^*_{D,in} = 0.0\ kg/m^3$$

$$C^*_{A,in} = 0.0\ kg/m^3$$

The inlet bulk concentration and the inlet wall coverage ($z = 0$) are respectively:

$$C_{in} = 10^9\ cfu/m^3$$

$$n_{w,in} = 10^5\ cfu/m^2$$

The boundary conditions for all heat-exchanger arrangements considered are the following:

$$T_f = 323\ K, \qquad z = 0$$

$$\frac{\partial Bi}{\partial z} = 0.0, \quad z = 0$$

The boundary conditions for the heating medium are the following:

- Co-current operation

$$T_s(z) = 385\ \mathrm{K}, \quad z = 0$$

- Counter-current operation

$$T_s(z) = 385\ K, \quad z = L$$

3.1.12 Initial Conditions

Assuming that before milk circulation, and thus prior to the onset fouling, the heat exchanger was running under steady state conditions with a non-fouling fluid on tube side. This assumption is supported by the practice of pre-heating and sterilizing pasteurizers using hot water before processing milk.

$$\frac{\partial T_f(z,t)}{\partial t} = 0.0, \qquad t = 0 \qquad \forall z \in (0, L]$$

$$\frac{\partial T_s(z,t)}{\partial t} = 0.0, \qquad t = 0 \qquad \forall z \in (0, L]$$

$$C_N(z,t) = C_D(z,t) = C_A(z,t) = 0.0, \quad t = 0 \qquad \forall z \in (0, L]$$

$$C_N^*(z,t) = C_D^*(z,t) = C_A^*(z,t) = 0.0, \qquad t = 0 \qquad \forall z \in (0, L]$$

$$Bi(z,t) = 0.0, \quad t = 0 \qquad \forall z \in (0, L]$$

$$n_w(z,t) = 0.0, \qquad t = 0 \qquad \forall z \in (0, L]$$

3.1.13 Heat Exchanger Details

In Table 3.5 are presented the operation details of heat exchanger used in simulation while in Table 3.6 the data of the heat exchangers characteristics. Three different cases were examined (Figure 3.4):

1. The heating medium is steam at 374 K.
2. The heating medium is hot water at 385 K in co-current flow with milk.
3. The heating medium is hot water at 385 K in counter-current flow with milk.

Table 3.5 Details of heat exchanger used in simulation

Case	Type of heat exchanger	Length (m)	Diameter (m)	T_f^{in} (K)	T_f^{out} (K)	T_s^{in} (K)
1	Steam, T_w = 374K	10	0.025	323	365.4	-
2	Hot water, co-current	10	0.025	323	365.4	385
3	Hot water, counter-current	10	0.025	323	365.4	385

Table 3.6 Heat exchanger data used in simulation

Milk flowrate, w_f (kg/s)	Hot water flowrate, w_s (kg/s)	u_s (m/s)
0.25	1.5	4.08

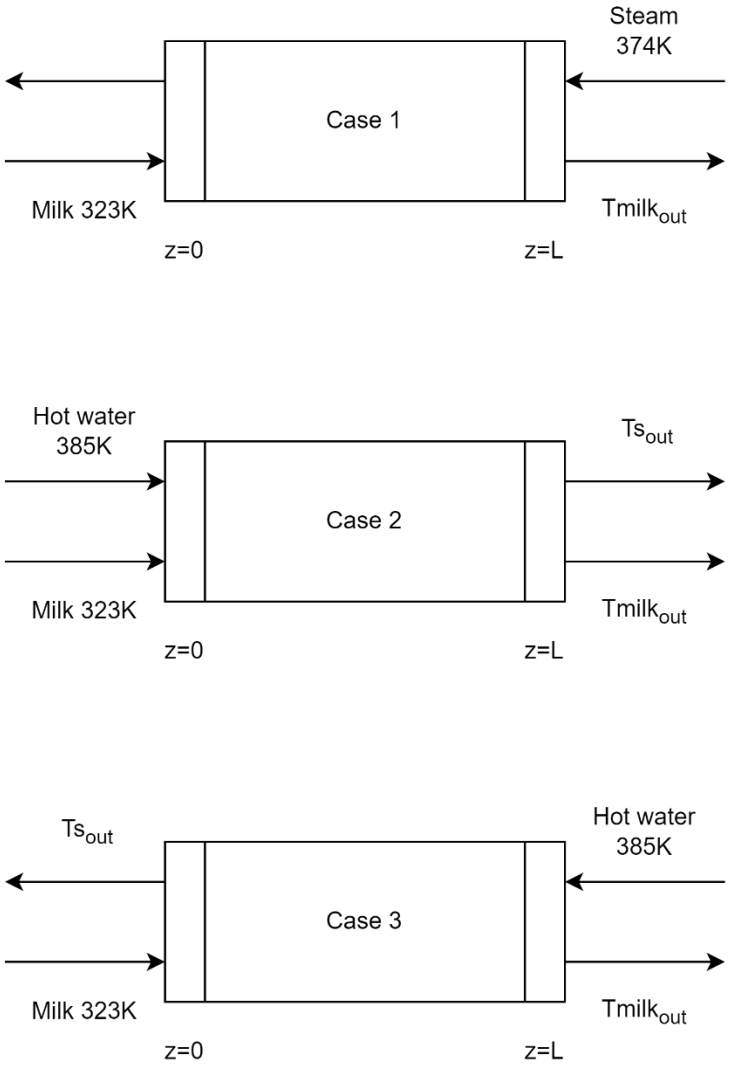

Figure 3.4 Shell and tube heat exchanger configurations

3.2 Simulation Results

The mathematical model of shell and tube heat exchangers was solved in gPROMS™ from Siemens Process System Enterprise. In all simulations the solver used for the solution of linear algebraic equations is MA48, for the solution of non-linear algebraic equations is BDNLSOL while for the solution of differential equations is DAEBDF. All the aforementioned solvers are the default solvers in gPROMS™ (Process Systems Enterprise Ltd, 2023).

The fouling behavior of three different heat exchanger configurations was investigated as described in Section 3.1.13. Simulation results are reported via the illustration of the main variables response.

The concentration of native protein in the thermal boundary layer decreases while denaturated protein initially increases and then decreases along the tube. On the other hand, the concentration of the aggregated protein is small until about 6 meters and then increases as is shown in Figure 3.5 for the case of constant wall temperature (T_w = 374K). Similar behavior is observed in the other two cases (co-current and counter-current operation).

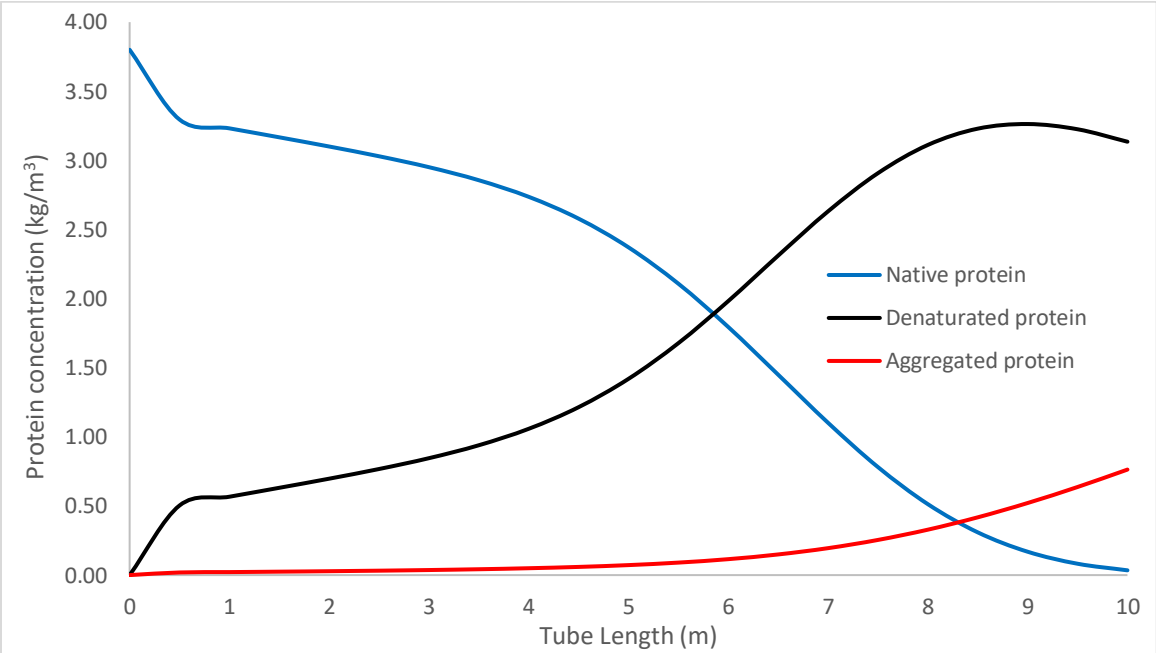

Figure 3.5 Thermal boundary layer protein concentration

In Figure 3.6 is shown the aggregated protein concentration in thermal boundary layer in different times. Since both the bulk and the interface temperature are decreased due to fouling the protein reaction rates are also decreased. Hence, the concentration of the aggregated protein is decreased both in the bulk and in the thermal boundary layer.

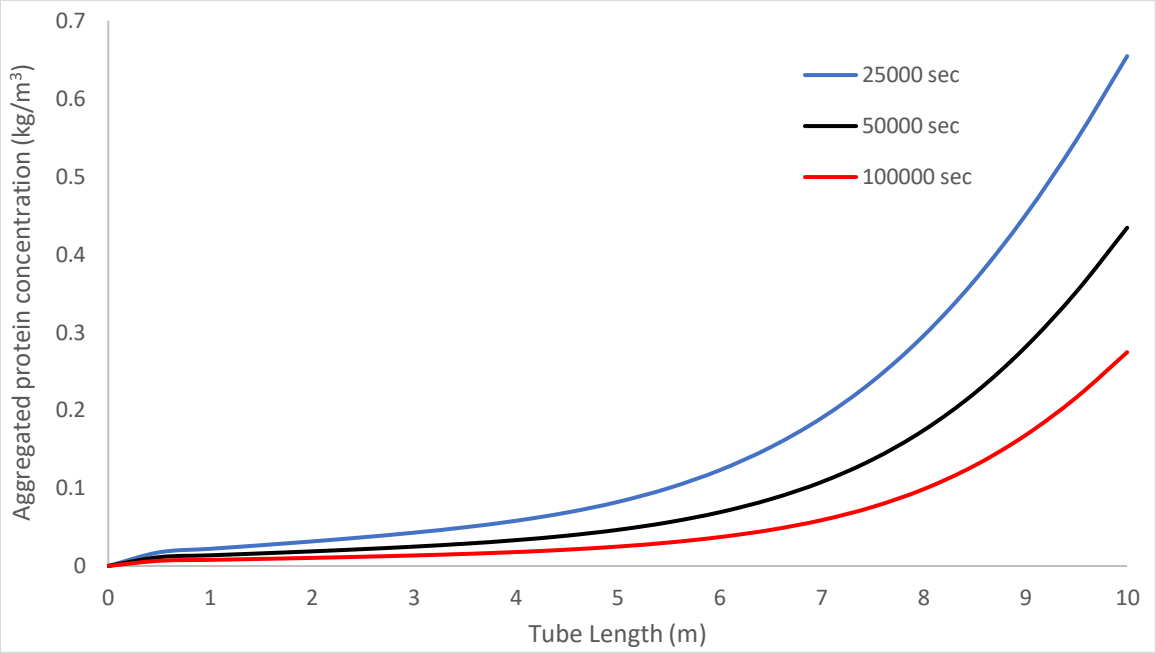

Figure 3.6 Aggregated protein concentration in thermal boundary layer in different times

As already mentioned, the Biot number expresses the resistance in heat transfer due to fouling and is related to concentration of aggregated protein in the thermal boundary layer (Equation (3.10)). Since the concentration of aggregated protein increases along the tube with respect to time, due to the increase of the bulk surface and interface temperature, the protein reaction rate increase and the Biot number also increases along the tube. In Figure 3.7 is shown the profile of Biot number at different times in the case of the constant wall temperature (T_w = 374K). Similar behavior is observed in the other two cases (co-current and counter-current operation).

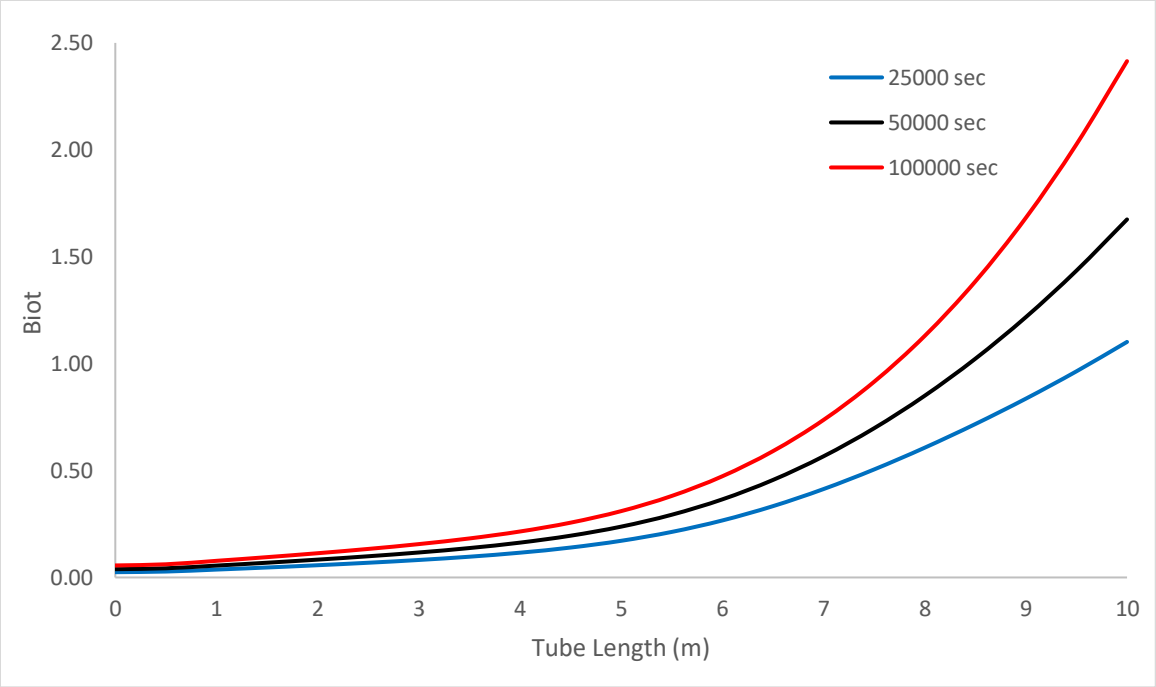

Figure 3.7 Biot number profile in different times for T_w = 374K

The deposit thickness and the deposit mass are proportional to the Biot number and therefore show a similar behavior to that of the Biot number. Therefore, both are increased along the tube as shown in Figure 3.8 and in Figure 3.9 respectively. It is observed that in the case of co-current operation, the increase in the deposit thickness and hence in the deposit mass is more intense compared to the case of constant wall temperature, T_w = 374K. In the case of counter-current operation, the deposit thickness is greater in relatively small tube lengths compared to the other two cases because this configuration enables maximum heat recovery, but after about 6 meters it seems that the case of co-current exhibits greater deposit thickness.

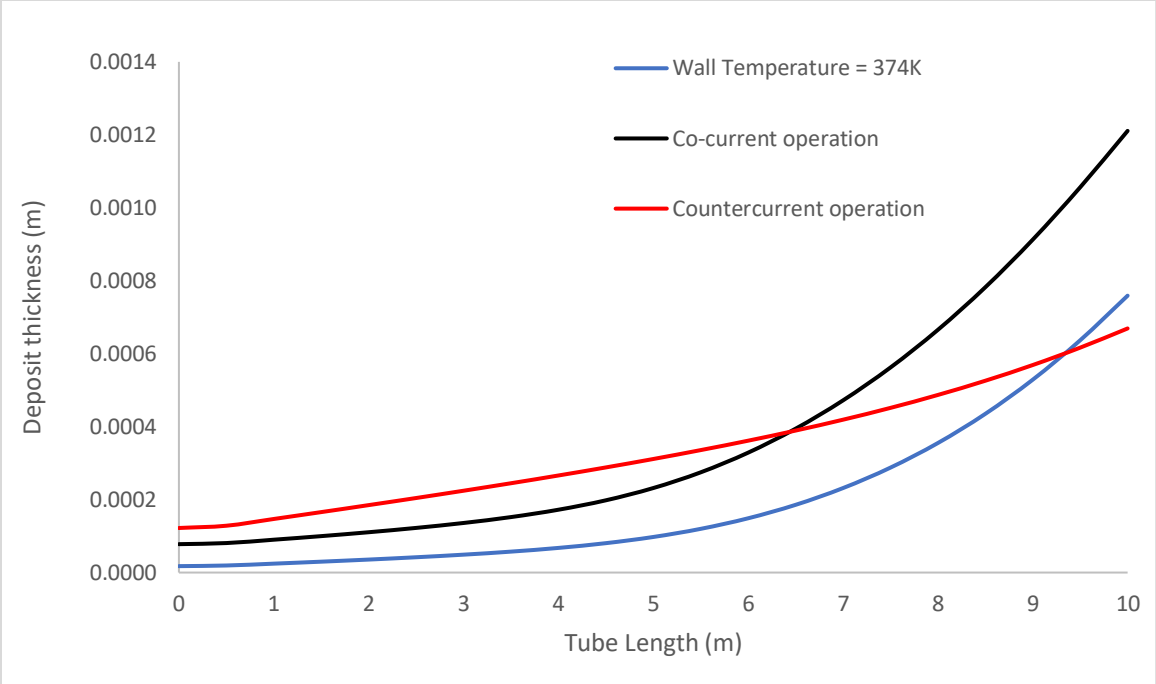

Figure 3.8 Deposit thickness profile for all cases at t = 100000 sec

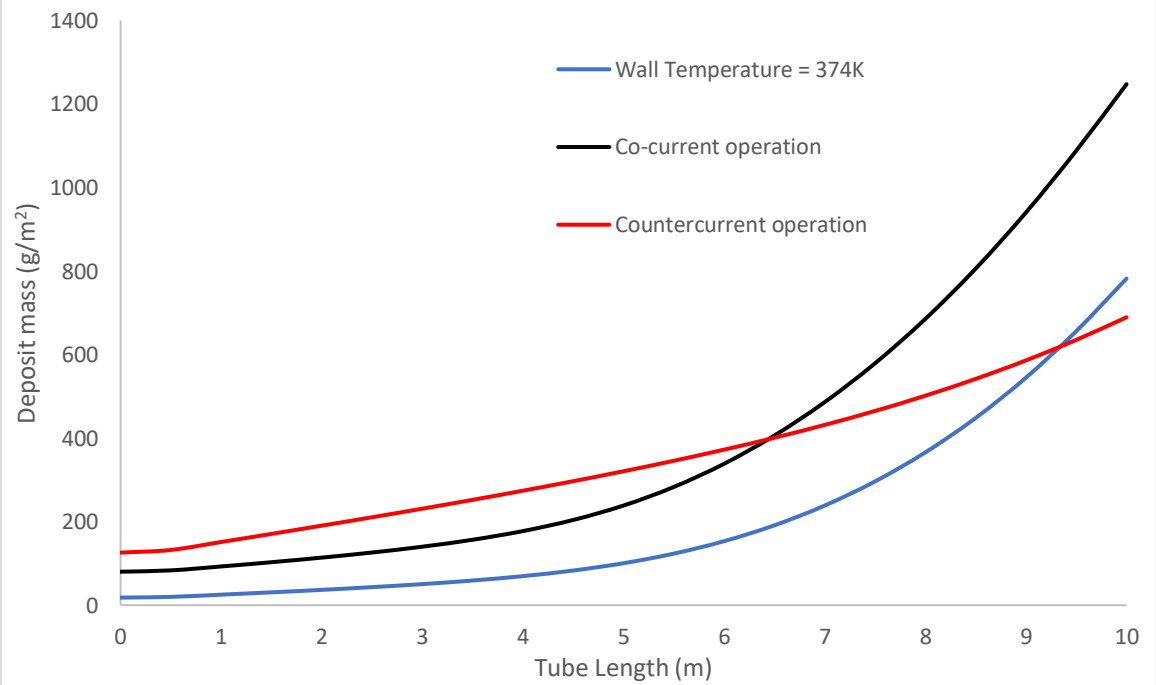

Figure 3.9 Deposit mass profile for all cases at t = 100000 sec

The overall heat transfer coefficient decreases with time as it is expected due to fouling. The profile of the overall heat transfer coefficient for the case of constant wall temperature (T_w = 374K) is shown in Figure 3.10. The value of the overall heat transfer coefficient under clean and fouling conditions for each case is presented in Table 3.7.

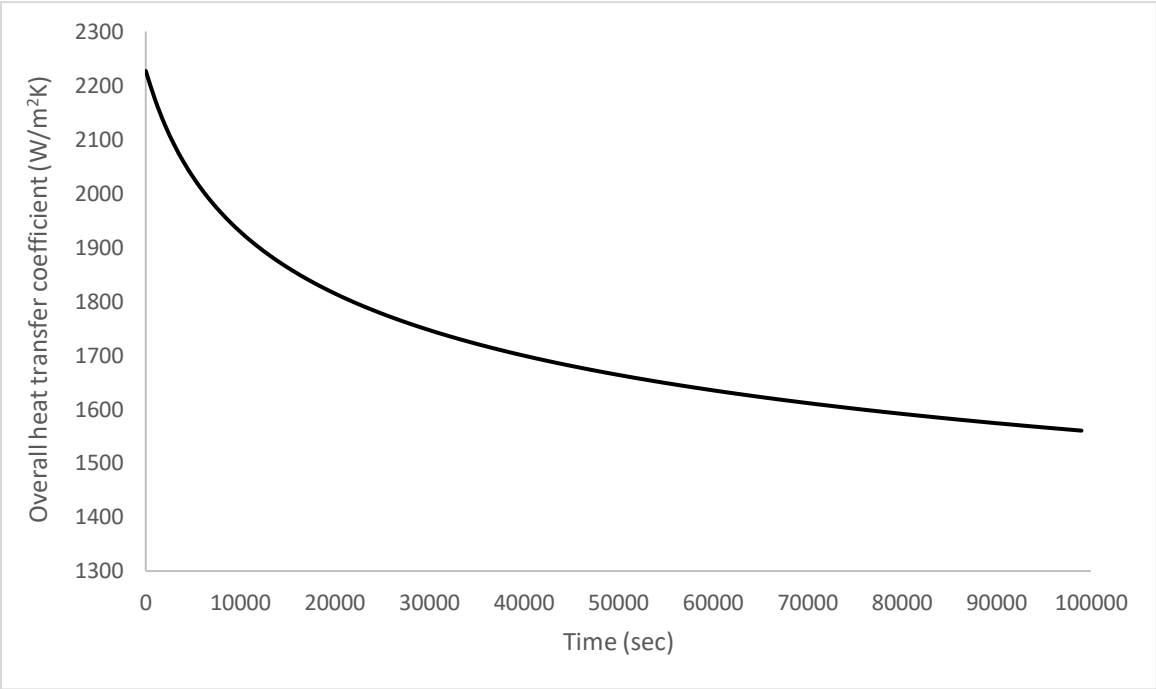

Figure 3.10 Overall heat transfer coefficient at L = 10 m.

Table 3.7 Overall heat transfer coefficient under clean and fouling conditions for all cases

Case	U_0 (W/m^{2}K)	U (W/m^{2}K)
1	2,227	1,559
2	2,471	1,282
3	1,196	781

Comparing the three cases concerning the milk outlet temperature, the case of the counter-current operation presents the most severe decrease as is shown in Figure 3.11. The decrease in milk outlet temperature also decreases the fouling rate.

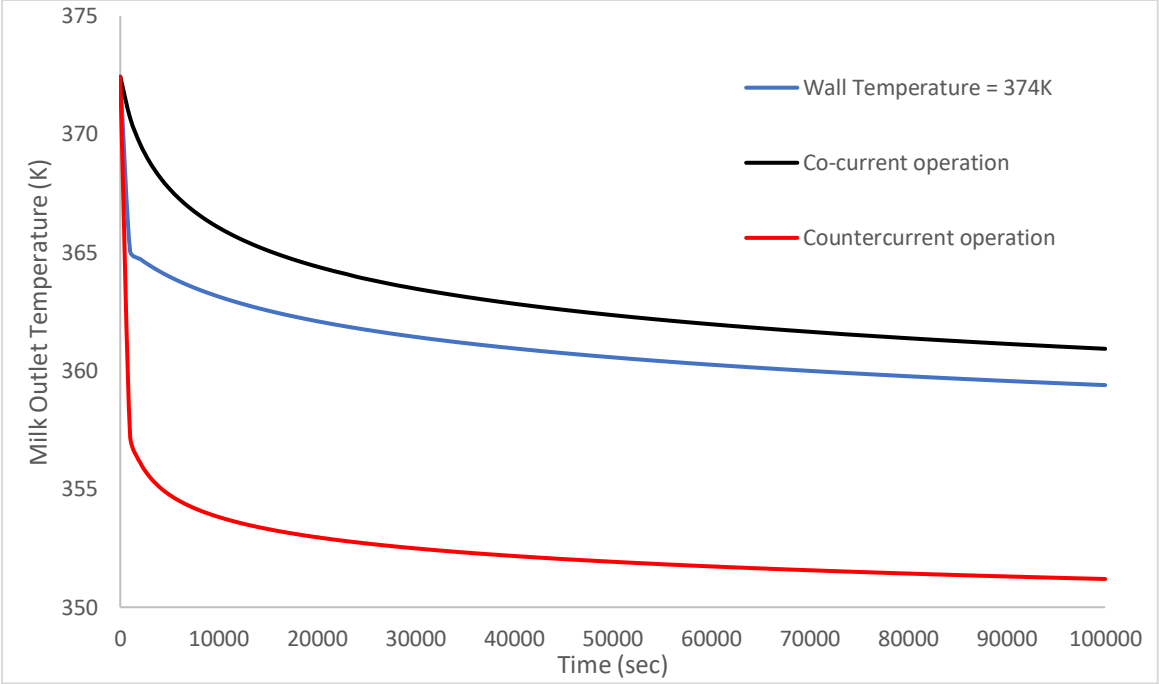

Figure 3.11 Milk outlet temperature for all cases at L = 10 m.

Comparing the three cases concerning the bacterial bulk concentration and the bacterial wall coverage, the case of the counter-current operation presents the most severe increase as it is shown in Figure 3.12 and in Figure 3.13 respectively. Moreover, it is observed that the bacterial bulk concentration and the bacterial wall coverage presents a similar behavior. The cases of constant wall temperature and co-current operation exhibit almost the same behavior and both of aforementioned variables present a small increase.

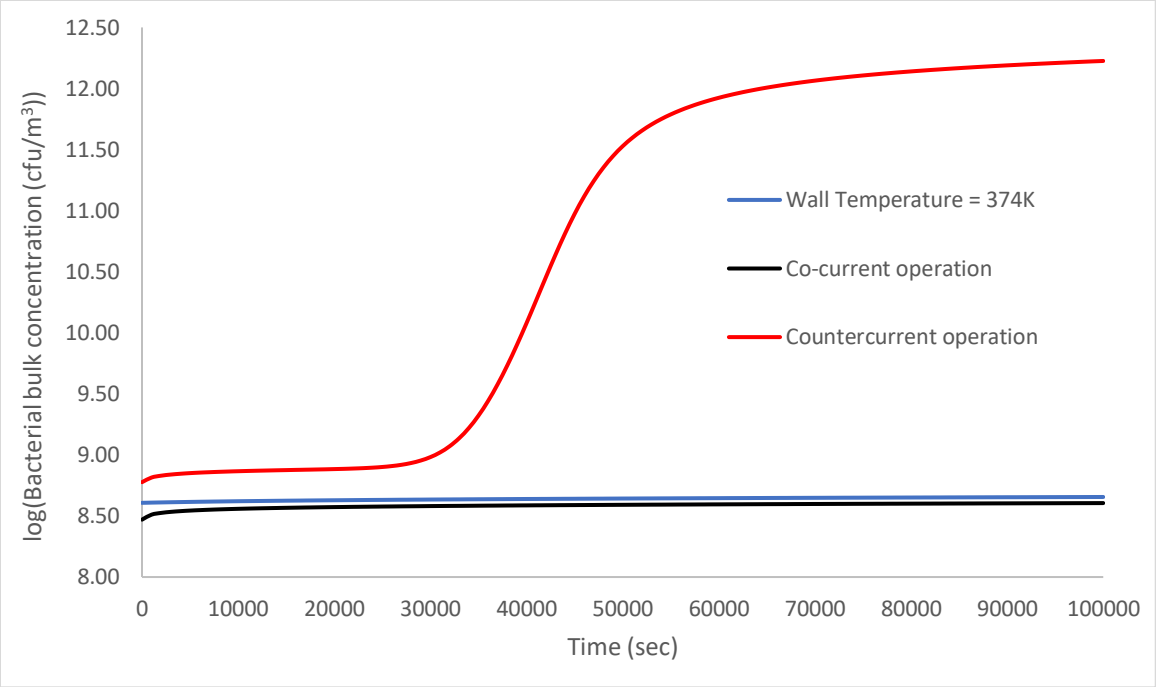

Figure 3.12 Bacterial bulk concentration for all cases

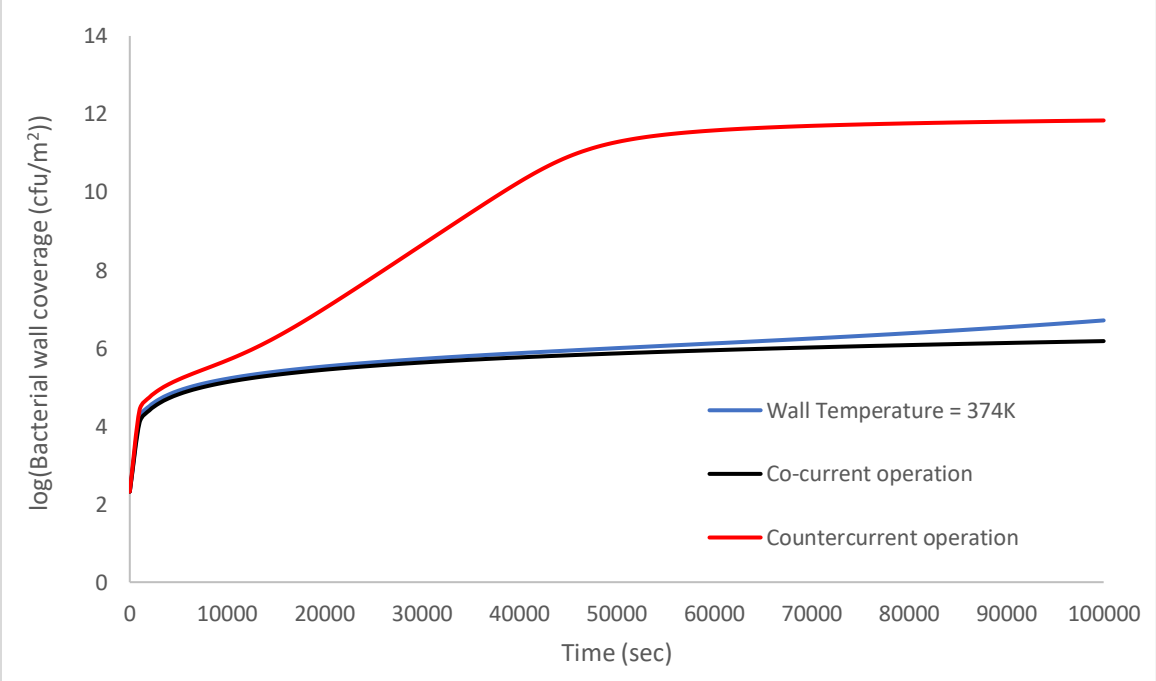

Figure 3.13 Bacterial wall coverage for all cases

3.3 Sensitivity analysis

In the mathematical model there are parameters including the initial protein and bacterial concentration with uncertainty. This uncertainty in the values of these parameters is due to the variation of milk composition and it affects fouling. All the results presented in this section is from the simulation of constant wall temperature case, but similar are the results from the other two cases.

The initial native protein concentration plays an important role in the milk outlet temperature as it is shown in Figure 3.14. An increase in the initial native protein concentration from 3.8 kg/m^3 to 5 kg/m^3 results in a 14K drop of milk temperature. On the other hand, the reduced (2.5 kg/m^3) initial native protein presents a smaller temperature drop compared to the base case (3.8 kg/m^3). Hence, the increased initial native protein concentration results in higher deposit mass as is shown in Figure 3.15.

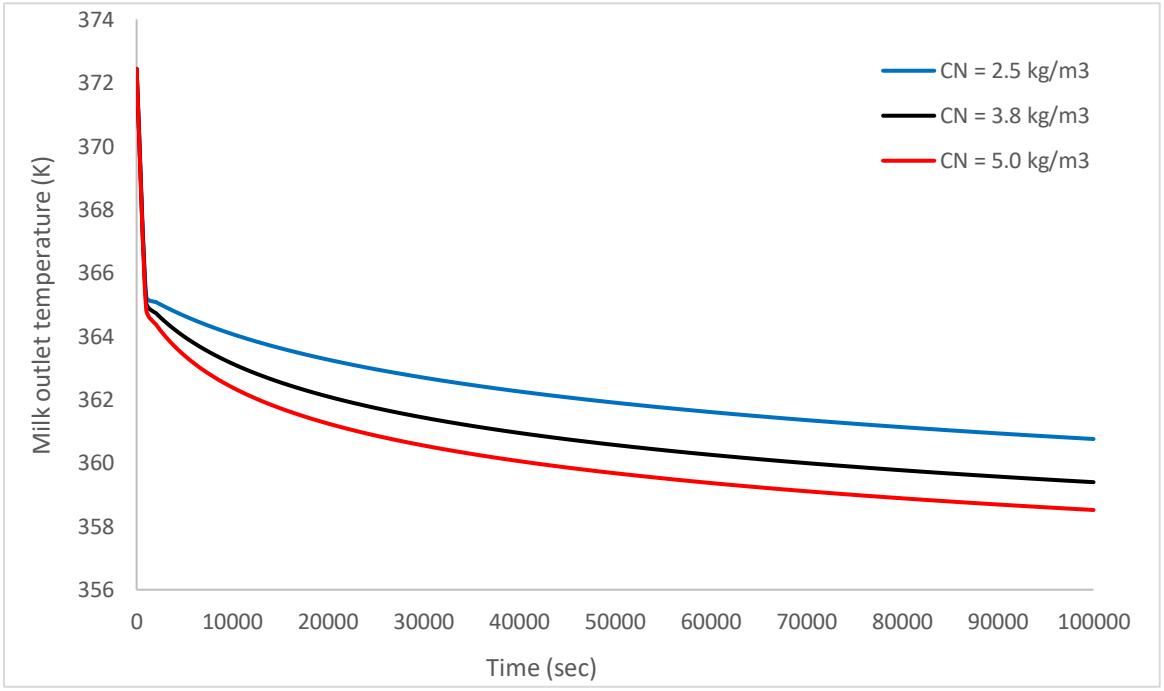

Figure 3.14 Effect of initial native protein concentration on milk outlet temperature

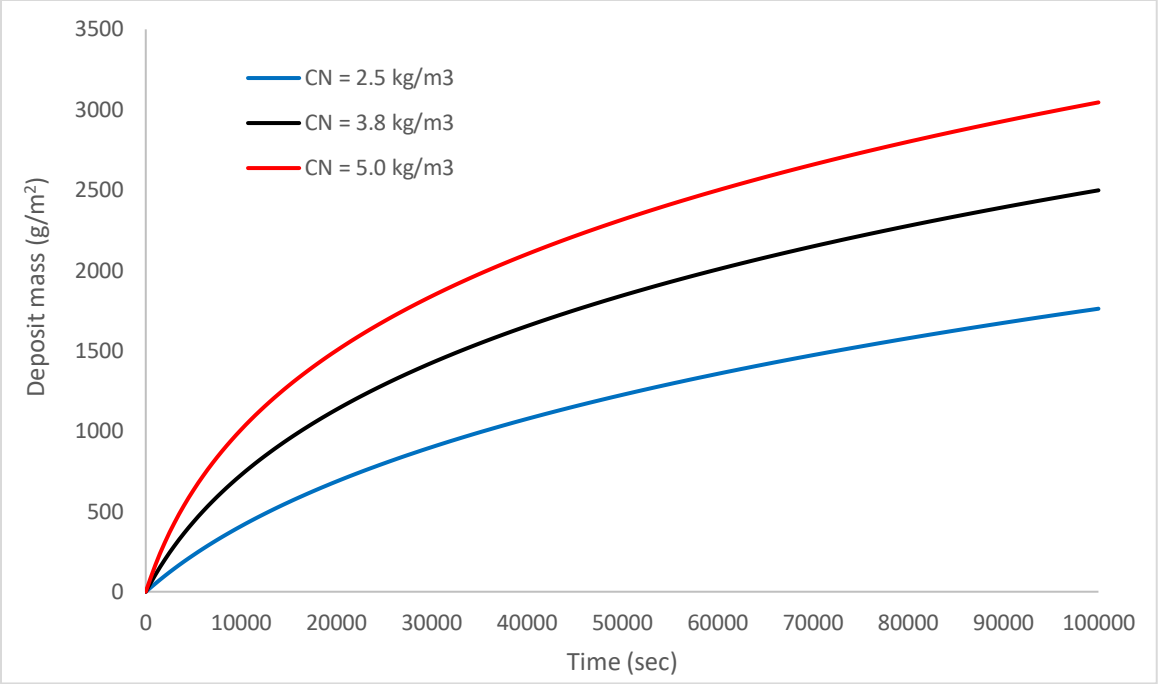

Figure 3.15 Effect of initial native protein concentration on deposit mass

The impact of milk flowrate and hence of Reynolds number on fouling is depicted in Figure 3.16 and in Figure 3.17. By doubling the milk flowrate, it is observed a significant mitigation of fouling. On the contrary, decreasing milk flowrate results in substantial increase in fouling. These results agree with the experimental work of Belmar-Beiny et al. (1993). Similar behavior exhibits bacterial wall coverage. When milk flowrate is reduced, significant increase in bacterial wall coverage is observed but when milk flowrate is doubled, the bacterial wall coverage is decreased but not significantly, as is shown in Figure 3.18.

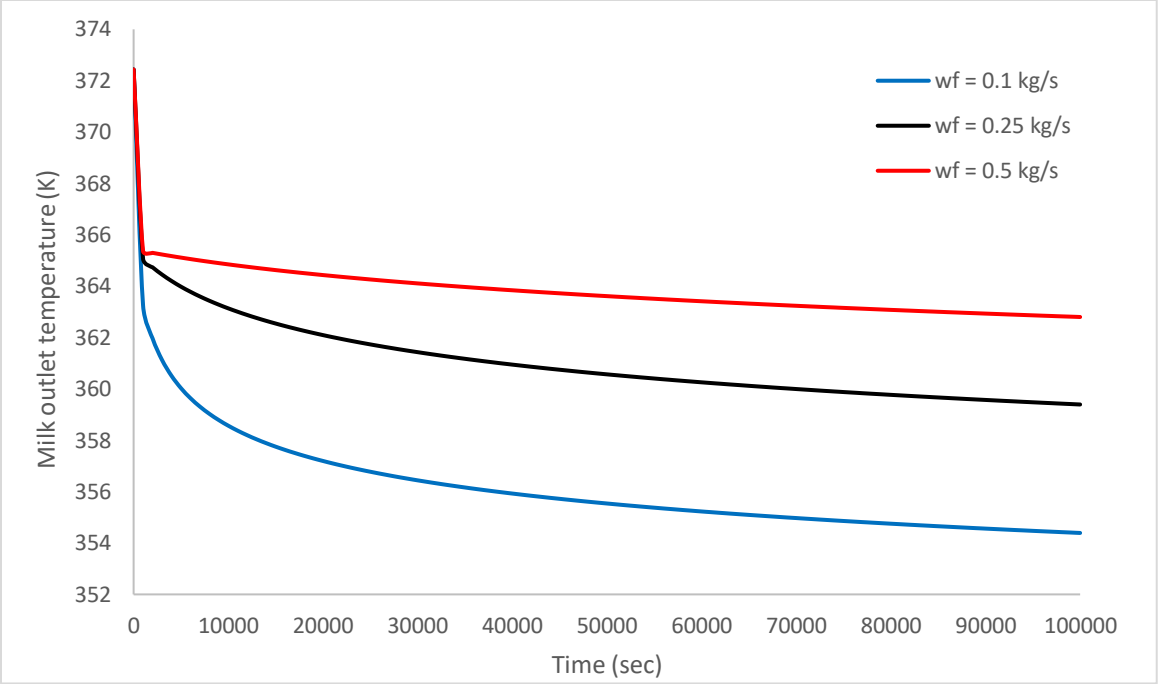

Figure 3.16 Effect of milk flowrate on milk outlet temperature

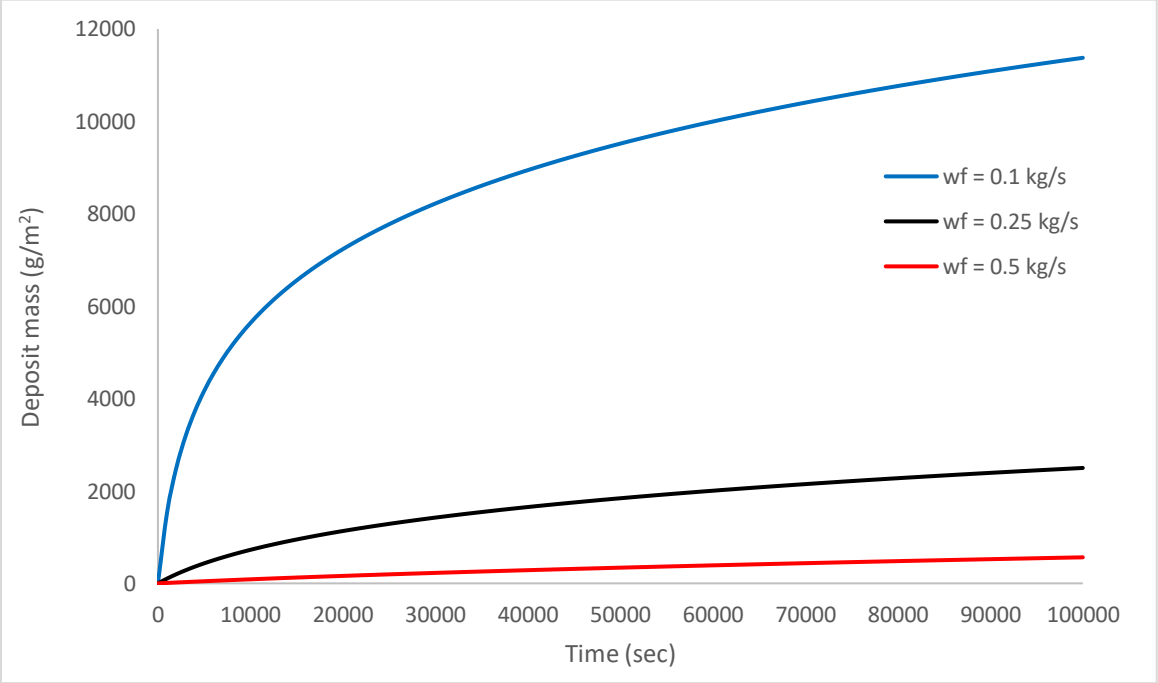

Figure 3.17 Effect of milk flowrate on deposit mass

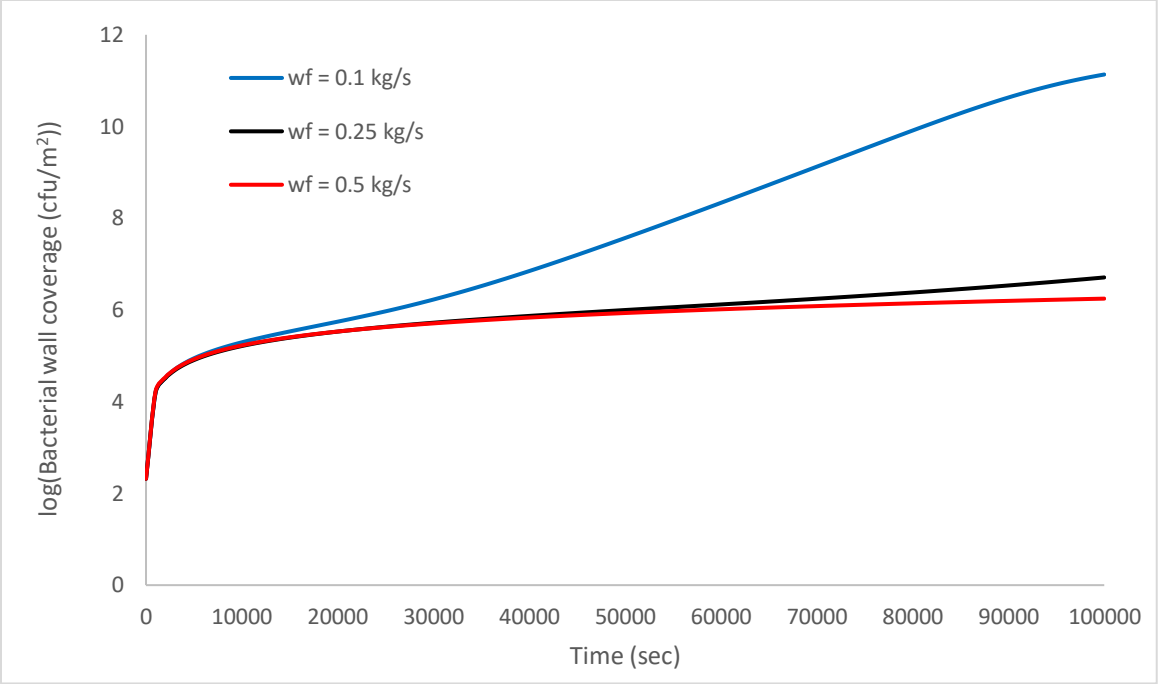

Figure 3.18 Effect of milk flowrate on bacterial wall coverage

Increasing the initial bacterial concentration by 2 orders of magnitude leads to an increase in wall coverage by 2 orders of magnitude as well as it is expected (Figure 3.19).

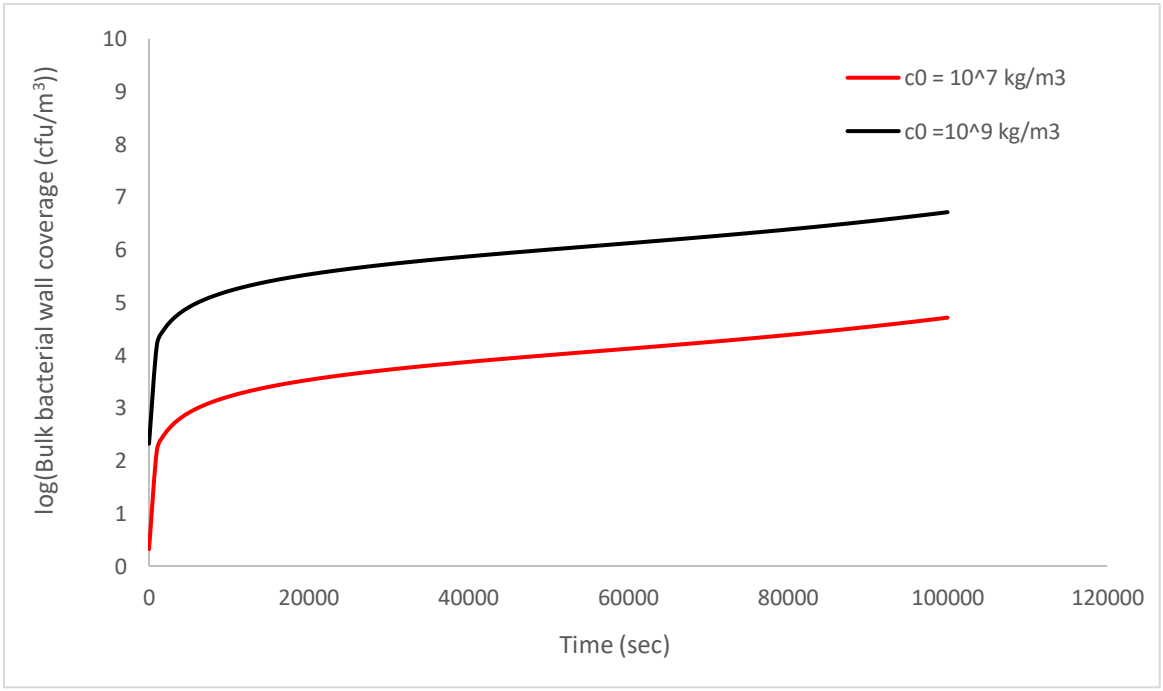

Figure 3.19 Effect of initial bacterial concentration on bacterial wall coverage

Chapter 4

Modeling and Simulation of Plate Heat Exchangers under Fouling

4.1 Mathematical Model

4.1.1 Description of Mathematical Model

The reaction scheme used for the fouling model is the same used for the modeling of shell and tube heat exchangers in Chapter 3. There are challenges in the mathematical modeling associated with the presence of both counter-current and co-current flows, the significant energy interactions between fluids in adjacent channels, and variety of complex geometries encountered in industrial applications (Georgiadis & Macchietto, 2000). For an effective study of fouling, it is essential to capture the interrelationship between the chemical reactions that lead to deposition and the fluid mechanics associated with the heat-transfer equipment taking into account the fluid velocity, the milk composition and temperature (Georgiadis et al., 1998a).

4.1.2 Modeling Framework

The mathematical model used concerning protein fouling was based on that of Georgiadis & Macchietto (2000) while the one concerning biofouling was based on that of de Jong (2002). The mathematical model of Georgiadis & Macchietto (2000) has been validated by experimental data from Delplace et al. (1995) and presents a good agreement with these data. The mathematical model of de Jong (2002) has been validated by experimental data for temperature range 27.9-48.4^{o}C, where bacterial growth is observed, for a heating time of 12 hours (de Jong, 2002). However, for the simulation conditions there are not available experimental data for model validation. The model was created based on the following assumptions considering a differential element of the PHE channel *j* (Figure 4.1) (Georgiadis & Macchietto, 2000):

- Heat diffusion in the axial direction is not taken into account.
- The flowrate and temperature profiles are assumed to be consistent across the channel and plate width.
- Each fluid is evenly distributed among all connected channels. Heat losses to the environment are insignificant.
- The head and follower parts of the PHE are insulated functioning as adiabatic plates.
- The adhesion of bacteria is a heterogeneous adsorption reaction of bacteria to a solid surface.
- The adhesion rate constant, k_a, is constant within the temperature range considered.
- The growth rate at the surface is equal to that of bacteria in the bulk.
- The bacteria release from the wall is related to the wall coverage by Equation (4.1). Equation (4.2) implies that at complete wall coverage all the grown bacteria at the bacteria – liquid interface is released to the bulk.

$$\beta_p = 1 - Ae^{-k_r \cdot mean\_n_{wp}} \tag{4.1}$$

$$A = 1 - \beta \; at \; n_{wp} = 0 \tag{4.2}$$

where k_r is a release constant equal to $6.1 \cdot 10^{-12}$ m^2/cfu and A is equal to 0.82 (de Jong, 2002).

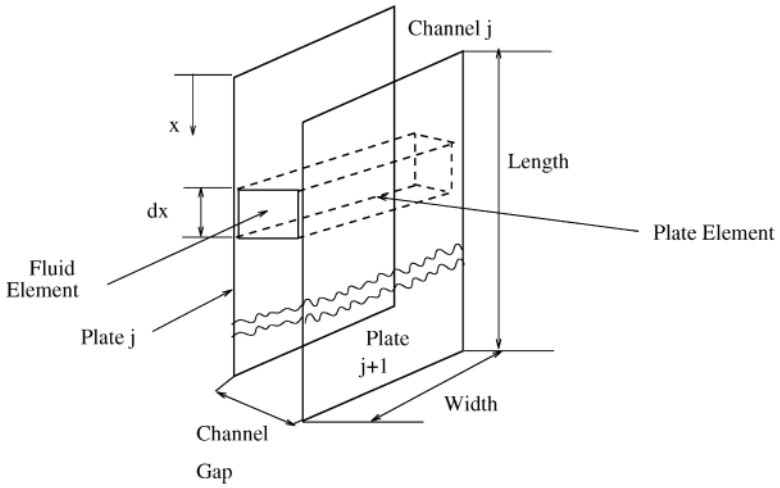

Figure 4.1 Differential element of PHE (Georgiadis & Macchietto, 2000)

4.1.3 Energy Balances

The energy balances for the process fluid or heating medium in channel *j* and its adjacent plates p_j and p_{j+1} are given by Equations (4.3) and (4.4).

Channel *j*

$$A_x \rho_j Cp_j \left(\frac{\partial T_j}{\partial t} + n_j u_z \frac{\partial T_j}{\partial z} \right) = U_j A_j \left(T_{pj-1} - T_j \right) + U_j A_j \left(T_{pj} - T_j \right) \tag{4.3}$$

Plate *j* (pj)

$$\rho_j Cp_p A_{x_p} \frac{\partial T_{pj}}{\partial t} = U_j A_j \left(T_j - T_{pj} \right) + U_{j+1} A_j \left(T_{j+1} - T_{pj} \right) \tag{4.4}$$

For the first and last channel, Equation (4.3) is transformed to Equation (4.5) while for the last channel, *m*, to Equation (4.6).

$$A_x \rho_1 Cp_1 \left(\frac{\partial T_1}{\partial t} + n_1 u_1 \frac{\partial T_1}{\partial z} \right) = U_1 A_1 \left(T_{p1} - T_1 \right) \tag{4.5}$$

$$A_x \rho_m Cp_m \left(\frac{\partial T_m}{\partial t} + n_m u_m \frac{\partial T_m}{\partial z} \right) = U_m A_m \left(T_{pm-1} - T_m \right) \tag{4.6}$$

n_j takes a value of +1 or -1 depending on the direction of the flow in channel *j*. The key advantage of the aforementioned model lies in its capability to simulate the transient behavior of various types of PHEs, encompassing counter-current, co-current, multi-channel, etc.

This model is based on energy balances where the synergistic effects between adjacent channels and plates are formally quantified. The model takes into account temperature profiles with respect to the axial distance. The overall heat transfer coefficient under clean conditions, U_0, is determined based on the Nusselt number (*Nu*), which is a function of the Reynolds (*Re*) and Prandtl (*Pr*) numbers by Equations (4.7) - (4.10).

$$Nu = 0.214(Re^{0.662} - 3.2)Pr^{0.4} \tag{4.7}$$

$$Pr = \frac{C_{pf} \cdot \mu_f}{\lambda_f} \tag{4.8}$$

$$Re = \frac{D_e \cdot u_z \cdot \rho_f}{\mu_f} \tag{4.9}$$

$$Nu = \frac{h \cdot D_e}{\lambda_f} \tag{4.10}$$

The equivalent diameter, D_e, is given by Equation (4.11).

$$D_e = 2e_j \tag{4.11}$$

The overall heat transfer coefficient under clean conditions is estimated by Equation (4.12).

$$\frac{1}{U_0} = \frac{1}{h_{hot}} + \frac{1}{h_{cold}} + \frac{p_j}{\lambda_p} \tag{4.12}$$

The thermophysical properties of milk, water, deposit, and plates are given in Table 4.1

Table 4.1 Thermophysical properties of milk, water, deposit, and water

	Density, ρ (kg/m^3)	**Thermal Conductivity, λ (W/m/K)**	**Heat Capacity, C_p (J/kg/K)**	**Viscosity, μ (kg/m/s)**	**Source**
Milk	1030	0.59	3930	$1.5 \cdot 10^{-3}$	(McKetta, 1984)
Deposit	1030	0.5	1970	-	(Leclerq-Perlat & Lalande, 1991; Sharma & Macchietto, 2021)
Plates	7870	16.3	502	-	(Delplace et al., 1994; Sharma & Macchietto, 2021)

4.1.4 Material Balances

The fouling model described in Chapter 3 is used for fouling estimation. Assuming that bulk reactions take place in each channel (where milk flows) at the channel temperature, T_j, and boundary layer reactions take place at the plate temperature, T_{pj}, the milk deposition rate will vary between the two plates that bound the same channel, due to the different temperature and protein concentration conditions on each of these plates.

The material balances for the native, denaturated and aggregated protein in the bulk are given by Equations (4.13), (4.14) and (4.15) respectively for each channel *j* where milk flows.

Native protein

$$\frac{\partial C_{Nj}}{\partial t} + n_j u_z \frac{\partial C_{Nj}}{\partial z} = -k_{No} \exp\left(-\frac{E_N}{RT_j}\right) C_{Nj} + \frac{\partial}{\partial z}\left(D_N \frac{\partial C_{Nj}}{\partial z}\right) + \frac{k_{mN}}{e_j}\left(C_{Nj} - C^*_{Np}\right) \tag{4.13}$$

Denaturated protein

$$\frac{\partial C_{Dj}}{\partial t} + n_j u_z \frac{\partial C_{Dj}}{\partial z} = k_{No} \exp\left(-\frac{E_N}{RT_j}\right) C_{Nj} - k_{Do} \exp\left(-\frac{E_D}{RT_j}\right) C^2_{Dj} + \frac{\partial}{\partial z}\left(D_D \frac{\partial C_{Dj}}{\partial z}\right) + \frac{k_{mD}}{e_j}\left(C_{Dj} - C^*_{Dp}\right) \tag{4.14}$$

Aggregated protein

$$\frac{\partial C_{Aj}}{\partial t} + n_j u_z \frac{\partial C_{Aj}}{\partial z} = k_{Do} \exp\left(-\frac{E_D}{RT_j}\right) C^2_{Dj} + \frac{\partial}{\partial z}\left(D_A \frac{\partial C_{Aj}}{\partial z}\right) + \frac{k_{mA}}{e_j}\left(C_{Aj} - C^*_{Ap}\right) \tag{4.15}$$

The material balances for the native, denaturated and aggregated protein in the thermal boundary layer are expressed by Equations (4.16), (4.17) and (4.18) respectively for the side of plate *p* delimiting channel *j*.

Native protein

$$\frac{\partial C^*_{Np}}{\partial t} + n_j u_z \frac{\partial C^*_{Np}}{\partial z} = -k_{No} \exp\left(-\frac{E_N}{RT_{pj}}\right) C^*_{Np} + \frac{\partial}{\partial z}\left(D_N \frac{\partial C^*_{Np}}{\partial z}\right) - \frac{k_{mN}}{\delta_T}\left(C^*_{Np} - C_{Nj}\right) \tag{4.16}$$

Denaturated protein

$$\frac{\partial C^*_{Dp}}{\partial t} + n_j u_z \frac{\partial C^*_{Dp}}{\partial z} = k_{No} \exp\left(-\frac{E_N}{RT_{pj}}\right) C^*_{Np} - k_{Do} \exp\left(-\frac{E_D}{RT_{pj}}\right) C^{*2}_{Dp} + \frac{\partial}{\partial z}\left(D_D \frac{\partial C^*_{Dp}}{\partial z}\right) - \frac{k_{mD}}{\delta_T}\left(C^*_{Dp} - C_{Dj}\right) \tag{4.17}$$

Aggregated protein

$$\frac{\partial C^*_{Ap}}{\partial t} + n_j u_z \frac{\partial C^*_{Ap}}{\partial z} = k_{Do} \exp\left(-\frac{E_D}{RT_j}\right) C^{*2}_{Dp} + \frac{\partial}{\partial z}\left(D_A \frac{\partial C^*_{Ap}}{\partial z}\right) - \frac{1}{\delta_T}\left[k_{mA}\left(C^*_{Ap} - C_{Aj}\right) + k_w C^*_{Ap}\right] \tag{4.18}$$

The second term of the right-hand side of the Equations (4.13) – (4.18) describes the diffusion phenomena according to Fick's law. The third term of the right-hand side of the

Equations (4.13) – (4.18) describes mass transfer between bulk and layer according to the reaction scheme (Figure 3.1).

The dimensionless Biot (*Bi*) number is used to express the change of heat transfer due to fouling and it is correlated with the deposition rate via constant β (Toyoda et al., 1996). The correlation between Biot number and deposition rate is given by Equation (4.19).

$$\frac{\partial Bi_p}{\partial t} = \beta k_w C_{Ap}^* \tag{4.19}$$

The value of the mass-transfer coefficient to the deposit k_w, is given by Toyoda et al., (1996) and it is equal to 10^{-7} m/s while the value of constant β, is given by Georgiadis et al. (1998a) in Table 4.2 for the two different arrangements.

Table 4.2 Values of β for the three different arrangements

Arrangement	β (m^2/kg)
1	129
2	0.54

4.1.5 Calculation of Transport Properties

The transport properties are calculated as in Section 3.1.6. The values of the variables of the thickness of the thermal boundary layer and the mass transfer coefficients k_{mN}, k_{mD}, k_{mA} that are included in the fouling model of the shell and tube heat exchanger, δ_T, are calculated.

The thickness of the thermal boundary layer, δ_T, is related to that of the laminar boundary layer, δ, and is estimated by Equation (4.20).

$$\frac{\delta_T}{\delta} = Pr^{1/3} \tag{4.20}$$

The mass-transfer coefficients for the three proteins are related to the diffusion coefficients and given by Equation (4.21).

$$k_{mi} = \frac{D_i}{\delta}, \qquad i = N, D, A \tag{4.21}$$

The diffusion coefficients can be estimated by the Wilke-Chang equation (Perry & Green, 2019) and given by Equation (4.22)

$$D_i = 1.31 \cdot 10^{-17} \cdot \frac{T_j}{\mu V_i^{0.6}}, \qquad i = N, D, A \tag{4.22}$$

where V_F, is the molecular volume of the absorbed particles.

$$V_i = N_{AV} \cdot \frac{1}{6} \cdot \pi \cdot d_i^3, \qquad i = N, D, A \tag{4.23}$$

The particle diameters are shown in Table 4.3

Table 4.3 Values of particle diameters for the three proteins (Georgiadis & Macchietto, 2000)

Native, d_N (m)	**Denaturated, d_D (m)**	**Aggregated, d_A (m)**
$9.92 \cdot 10^{-11}$	$9.12 \cdot 10^{-11}$	$5 \cdot 10^{-10}$

The thickness of the boundary layer, δ, can be calculated from the dimensionless Sherwood number, *Sh*, Equation (4.24) (de Jong, 1997).

$$\delta = \frac{D_e}{Sh} \tag{4.24}$$

For Reynolds number in range $2000 < Re < 10^5$ and $Sc > 0.7$, Sherwood number is expressed by Equations (4.25) and (4.26) (de Jong, 1997).

$$Sh = 0.214(Re^{0.662} - 3.2)Sc^{0.4} \tag{4.25}$$

$$Sc = \frac{\mu_f}{\rho_f . D_e} \tag{4.26}$$

4.1.6 Quantifying Fouling

The deposit mass at along position *z* of each plate of heat exchanger, is defined by Equation (4.27)

$$Mass_p(z) = \frac{\lambda_d \cdot Bi_p(z) \cdot \rho_d}{U_0} \tag{4.27}$$

The overall heat-transfer coefficient U is given by Equation (4.28) (Fryer & Slater, 1985)

$$U = \frac{U_0}{1 + Bi_p} \tag{4.28}$$

4.1.7 Quantifying Pressure Drop

The pressure drop due to fouling is calculated by Equations (4.29) and (4.30).

$$fanning = \frac{144}{Re} \tag{4.29}$$

$$\Delta P = \frac{fanning \cdot \rho_f \cdot u_z \cdot 0.6}{D_{eq}} \tag{4.30}$$

$$u_z = \frac{w_f}{A_x} \tag{4.31}$$

4.1.8 Growth and inactivation of bacteria

The bacterial growth is a function of temperature and is given by the modified expanded model of Ratkowsky, et al. (1983). The bacterial growth for the bulk is calculated by Equation (4.32) while for the plates by Equation (4.33).

$$\mu_{Tj} = [a_0(T_j - T_{min})\left(1 - \exp\left(a_1(T_j - T_{max})\right)\right)]^2 \tag{4.32}$$

$$\mu_{Tp} = [a_0(T_{pj} - T_{min})\left(1 - \exp\left(a_1(T_{pj} - T_{max})\right)\right)]^2 \tag{4.33}$$

For temperatures lower than 13.4ºC and higher than 54.2ºC, Equations (4.32) and (4.33) are equal to zero ($\mu_T = 0$). The values of the parameters of Equations (4.32) and (4.33) are the same as presented in Table 3.4.

The destruction of bacteria is also a function of temperature, and it follows the Arrhenius expression:

$$k_{dej} = k_{de0}\exp\left(-\frac{E_a}{RT_j}\right) \tag{4.34}$$

where k_{de0} is pre-exponential factor equal to $1.42 \cdot 10^{108}$ s^{-1} and E_a is the activation energy equal to 723.5 kJ/mol (de Jong et al., 2002).

4.1.9 Adherence, Growth, and Release in Equipment

Bacteria adhere to the surface and multiply. The model is described from two mass balances: one for the wall on which bacteria adhere and one for the milk which are expressed by Equation (4.35) and Equation (4.36) respectively.

$$Change\ in\ wall\ coverage\ with\ time = Produced\ at\ the\ surface - Released + Adhered$$

$$\frac{dn_{wp}}{dt} = \mu_{Tp} \cdot n_{wp} \cdot \left(1 - \beta_p\right) + k_a \cdot c_j \tag{4.35}$$

$$Change\ in\ bulk\ conc\ with\ position = Released - Adhered + Produced\ in\ the\ bulk - Destroyed$$

$$\frac{dc_j}{dz} = \frac{\pi \cdot diam}{\varphi}\left(\bar{\beta} \cdot \mu_{Tj} \cdot \overline{n_w} - k_a \cdot c_j\right) + \frac{\pi \cdot diam^2}{4\varphi}\left(\mu_{Tj} - k_{dej}\right)c_j \tag{4.36}$$

$$\overline{release\_\beta} = \frac{(\beta_p + \beta_{p+1})}{2} \tag{4.37}$$

$$\overline{n_w} = \frac{(n_{wp} + n_{wp+1})}{2} \tag{4.38}$$

$$mean\_n_{wp} = \frac{1}{L}\int_0^L n_{wp}\, dz \tag{4.39}$$

where k_a is the adhesion constant equal to $4.14 \cdot 10^{-8}$ m/s (de Jong et al., 2002).

4.1.10 Boundary Conditions for Arrangement 1

The boundary conditions depend on the specific geometry and are defined for each arrangement separately.

This arrangement is shown in Figure 4.2 and is one channel per pass with total six passes. The heat exchanger has 13 plates and both counter-current and co-current flow exists.

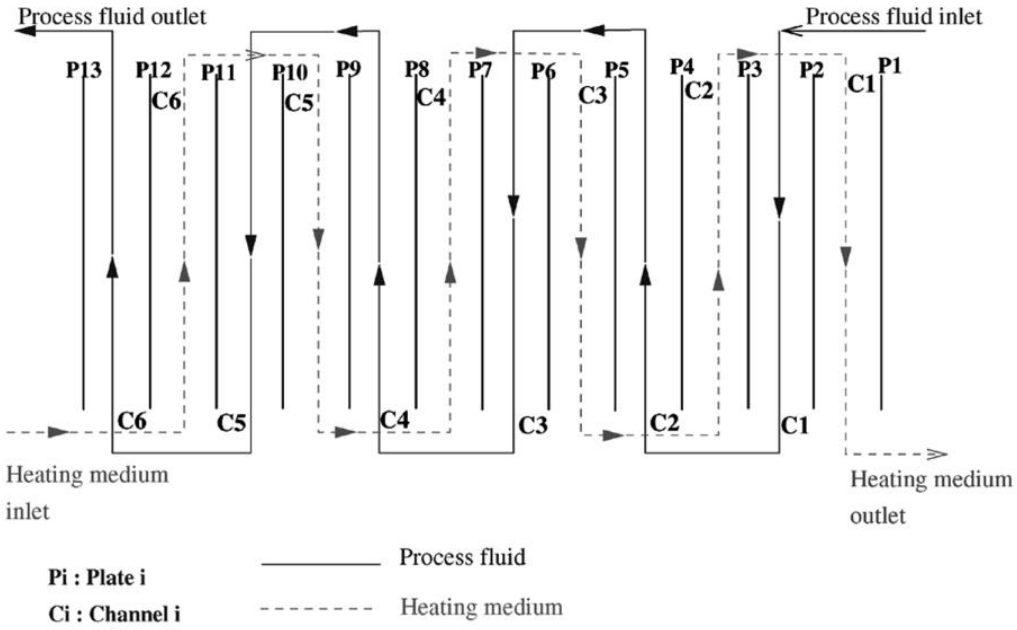

Figure 4.2 PHE Arrangement 1 (Georgiadis & Macchietto, 2000)

For the first arrangement the boundary conditions between channels ensure the continuity of temperature.

$$T_{milk}(1,0) = T_f^{in}$$

$$T_{milk}(j, L) = T_{milk}(j-1, L), \;\; j = 2,4,6$$

$$T_{milk}(j, 0) = T_{milk}(j-1, 0), \;\; j = 3,5$$

$$T_s(6, L) = T_s^{in}$$

$$T_s(j, 0) = T_s(j-1, 0), \;\; j = 2,4,6$$

$$T_s(j, L) = T_s(j-1, L), \;\; j = 3,5$$

T_f and T_s are the milk and the heating medium temperature respectively. The first domain refers to the number of channels and the second to the inlet or outlet point. T_f^{in} and T_s^{in} are the milk and heating medium inlet temperatures respectively.

For the first channel the boundary conditions for the protein concentrations are the following:

$$-D_{N1}\frac{\partial C_{N1}}{\partial z} = u_z\left(C_{N1,in} - C_{N1}\right),\ \ z = 0$$

$$-D_{D1}\frac{\partial C_{D1}}{\partial z} = u_z\left(C_{D1,in} - C_{D1}\right),\ \ z = 0$$

$$-D_{A1}\frac{\partial C_{A1}}{\partial z} = u_z\left(C_{A1,in} - C_{A1}\right),\ \ z = 0$$

$$\frac{\partial C_{N1}}{\partial z} = 0.0,\ \ z = L$$

$$\frac{\partial C_{D1}}{\partial z} = 0.0,\ \ z = L$$

$$\frac{\partial C_{A1}}{\partial z} = 0.0,\ \ z = L$$

The values of the inlet protein concentrations are the following (Delplace et al., 1994):

$$C_{N1,in} = 5.0\ kg/m^3$$

$$C_{D1,in} = 0.0\ kg/m^3$$

$$C_{A1,in} = 0.0\ kg/m^3$$

For the second channel the boundary conditions for the protein concentrations to ensure continuity of concentration are the following:

$$-D_{N2}\frac{\partial C_{N2}}{\partial z} = u_z\left(C_{N1|z=L} - C_{N2}\right),\ \ z = L$$

$$-D_{D2}\frac{\partial C_{D2}}{\partial z} = u_z\left(C_{D1|z=L} - C_{D2}\right),\ \ z = L$$

$$-D_{A2}\frac{\partial C_{A2}}{\partial z} = u_z\left(C_{A1|z=L} - C_{A2}\right),\ \ z = L$$

$$\frac{\partial C_{N2}}{\partial z} = 0.0,\qquad z = 0$$

$$\frac{\partial C_{D2}}{\partial z} = 0.0,\qquad z = 0$$

$$\frac{\partial C_{A2}}{\partial z} = 0.0, \qquad z = 0$$

Similar boundary conditions are imposed for all the other channels and for the layer proteins.

4.1.11 Boundary Conditions for Arrangement 2

This arrangement is shown in Figure 4.3 and is six channels per pass with total one pass. The heat exchanger has 13 plates and both counter-current and co-current flow exists.

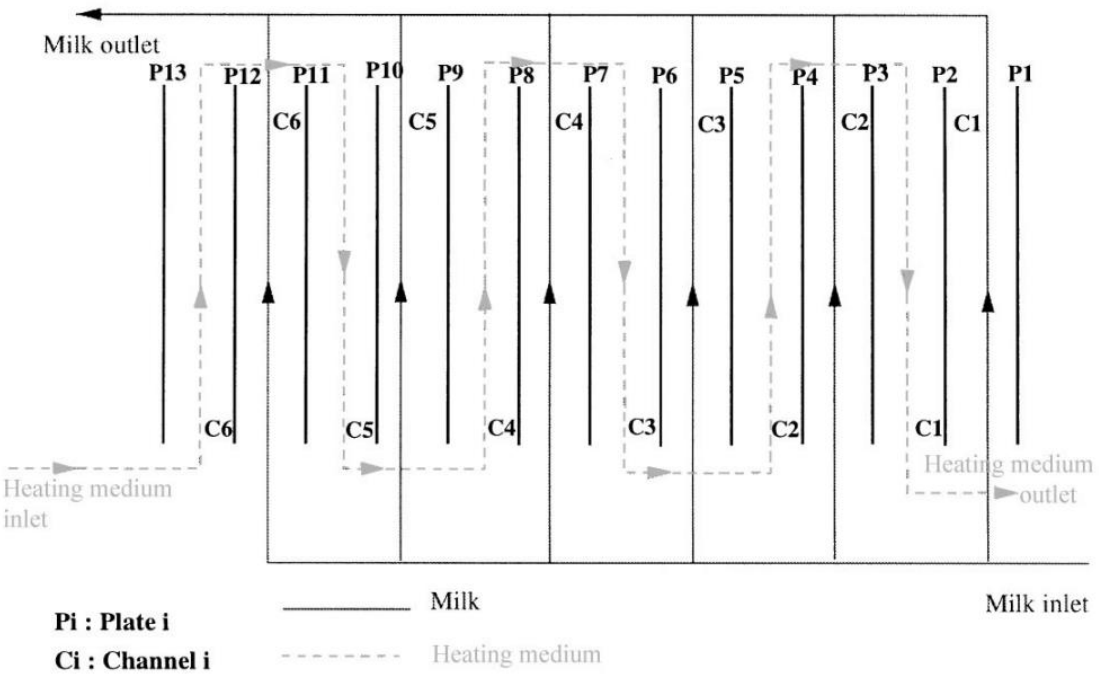

Figure 4.3 PHE Arrangement 2 (Georgiadis & Macchietto, 2000)

For the milk channels special boundary conditions are not required since there are no connected channels. The milk outlet temperature is equal to the mean value of the channel's outlet temperature. For the heating medium, the boundary conditions are the same as those in arrangement 1. For the concentrations the boundary conditions are similar to the other arrangements.

$$T_s(6, L) = T_s^{in}$$

$$T_s(j,0) = T_s(j-1,0), \quad j = 2,4,6$$

$$T_s(j,L) = T_s(j-1,L), \quad j = 3,5$$

4.1.12 Initial Conditions

Similarly with Chapter 3 it is assumed that before milk circulation, and thus prior to the onset fouling, the heat exchanger was running under steady state conditions with a non-fouling fluid on tube side.

$$\frac{\partial T_j}{\partial t} = 0.0, \qquad t = 0 \quad \forall j \quad \forall z \in (0,L)$$

$$\frac{\partial T_{pj}}{\partial t} = 0.0, \qquad t = 0 \quad \forall j \quad \forall z \in (0,L)$$

$$C_{Nj}(z,t) = C_{Dj}(z,t) = C_{Aj}(z,t) = 0.0, \quad t = 0 \quad \forall j \quad \forall z \in (0,L)$$

$$C^*_{Np}(z,t) = C^*_{Dp}(z,t) = C^*_{Ap}(z,t) = 0.0, \qquad t = 0 \quad \forall p,j \quad \forall z \in (0,L)$$

4.1.13 Heat Exchanger Details

The technical details of this exchanger are given in Table 4.4 while in Table 4.5 are given the data used in simulation of PHEs. All the plates have the same geometric characteristics.

Table 4.4 Technical details of heat plate heat exchangers used in simulation (Delplace et al., 1994)

Length of plates (m)	**Width of plates (m)**	**Thickness of plates, p_j (m)**	**Space between plates, e_j (m)**	**A_j heat transfer area, (m^2)**	**A_x, cross-sectional area, (m^2)**
0.75	0.20	$7.45 \cdot 10^{-4}$	$4.0 \cdot 10^{-3}$	0.1875	$1 \cdot 10^{-3}$

Table 4.5 Heat exchanger data used in simulation

Arrangement	T_f^{in} **(K)**	T_f^{out} **(K)**	φ_{milk}**, (m^3/s)**	T_s^{in} **(K)**	φ_{water} **(m^3/s)**
1	333	370	$0.833 \cdot 10^{-4}$	370	$2.4 \cdot 10^{-4}$
2	333	370	$0.833 \cdot 10^{-4}$	383	$0.92 \cdot 10^{-4}$

For arrangement 2 since there are six channels per pass and the milk is homogenously distributed in the channels the flowrate in each channel is $0.1533 \cdot 10^{-4}$ m^3/s.

4.2 Simulation Results

The mathematical model for all plate heat exchangers was solved in gPROMS™ from Siemens Process System Enterprise. In all simulations the solver used for the solution of linear algebraic equations is MA48, for the solution of non-linear algebraic equations is BDNLSOL while for the solution of differential equations is DASOLV (Process Systems Enterprise Ltd, 2023).

The fouling behavior of two different arrangements was investigated as described in Section 4.1. Simulation results are reported via the illustration of the main variables response.

4.2.1 Arrangement 1

In Figure 4.4 is presented the temperature profile for clean conditions. In channels 1 and 2 the milk temperature reaches its maximum value, while in the other channels the temperature difference along the tube is small.

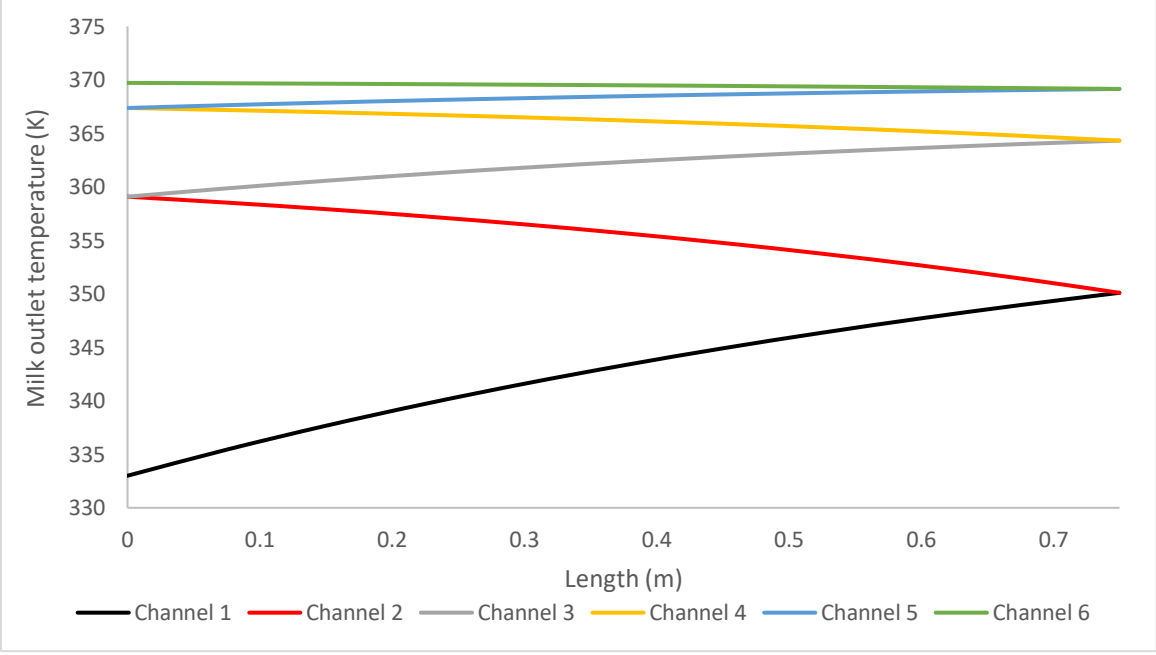

Figure 4.4 Temperature profile for clean conditions for all channels

In Figure 4.5 and in Figure 4.6 is presented the profile of deposit mass in plates 1-6 and in plates 7-12 respectively over a time period of 8.3 hours. The deposit mass in all plates increases linear with time and is observed that in plates 5 and 6 is maximum and decreases in plate 7. Moreover, fouling differs even among plates that define the same channel, such as plates 1 and 2 due to the temperature profile as it is shown in Figure 4.7. As expected, milk outlet temperature decreases with time. Comparing the temperature drop of PHE and shell and tube heat exchangers is evident that in latter is more severe. This phenomenon can be clarified by considering PHE as a sequence of co-current and counter-current shell and tube heat exchangers with significant thermal interconnections between channels. Fouling leads to a decrease in milk temperature in one channel and the heat losses are compensated by the heating medium in the adjacent channels.

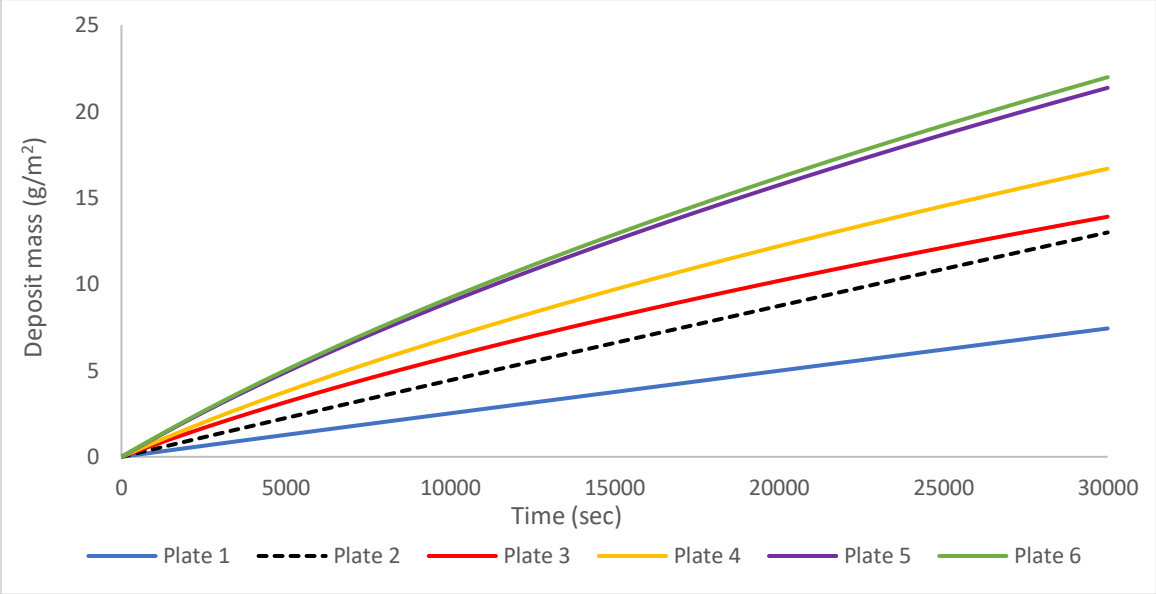

Figure 4.5 Deposit mass for plates 1-6 – Arrangement 1

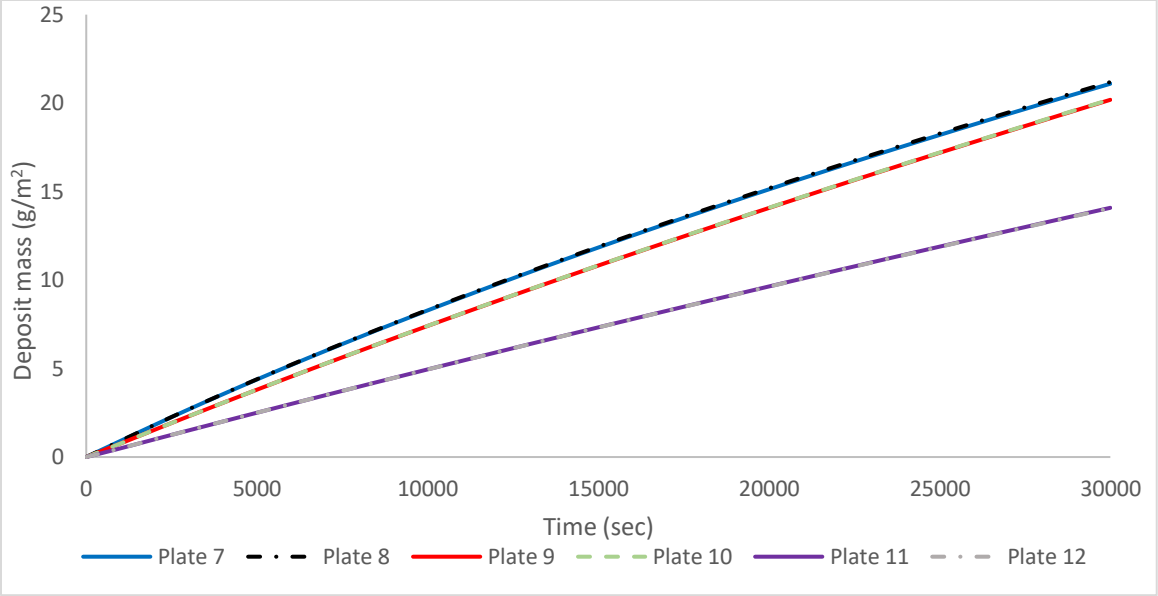

Figure 4.6 Deposit mass for plates 7-12 – Arrangement 1

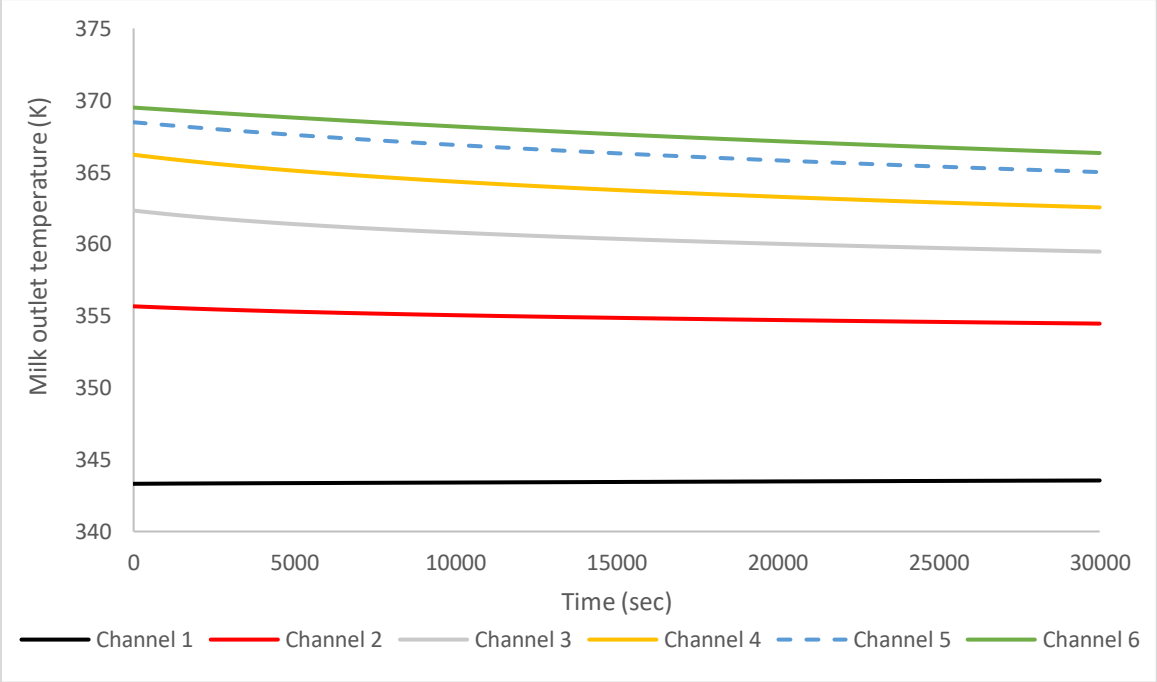

Figure 4.7 Milk outlet temperature for channels 1-6 and channel length 0.375 m. – Arrangement 1

4.2.2 Arrangement 2

This arrangement results in lower fouling than the other as it is shown in Figure 4.8. The maximum value of deposit mass for this arrangement is about 8 g/m^2 while in the other geometry exceeds 15

g/m^2. This is expected due to the lower heating load in this arrangement. The bacterial wall coverage has a similar behavior to deposit mass as it is depicted in Figure 4.9.

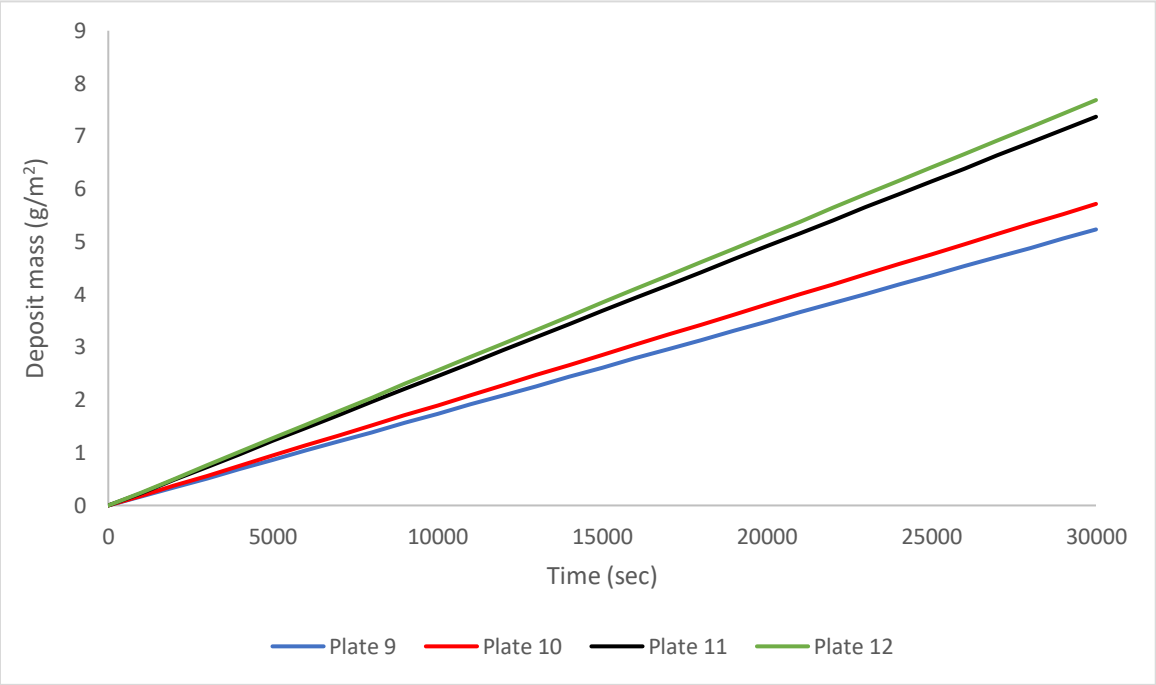

Figure 4.8 Deposit mass for plates 9-12 – Arrangement 2

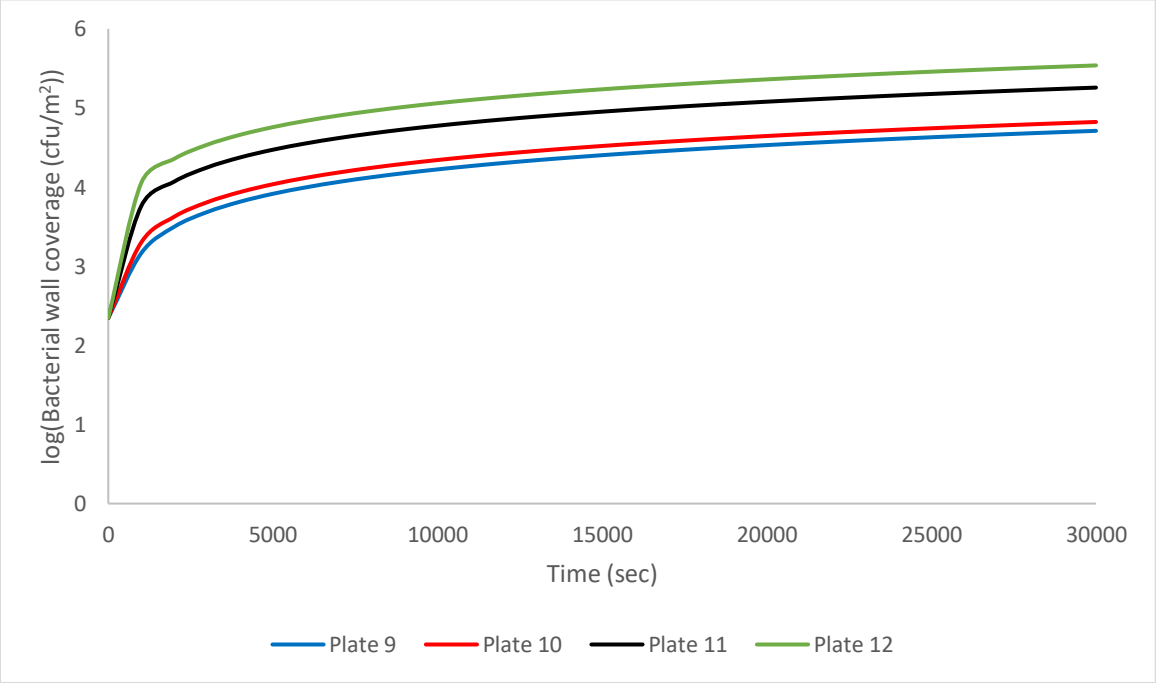

Figure 4.9 Bacterial wall coverage for plates 9-12 – Arrangement 2

4.3 Sensitivity Analysis

As described in Section 3.3, there are parameters with uncertainty. Hence, in this section is investigated the effect fouling in milk outlet temperature for different values of inlet protein concentration and different Reynolds number. For simplicity all the results presented in this section are from the simulation of Arrangement 1, but similar are the results from the other two cases.

The effect of inlet native protein concentration on fouling is depicted in Figure 4.10 for two values of 2.5 and 5 kg/m^3. Lower inlet protein concentration results in lower temperature drop and hence less fouling.

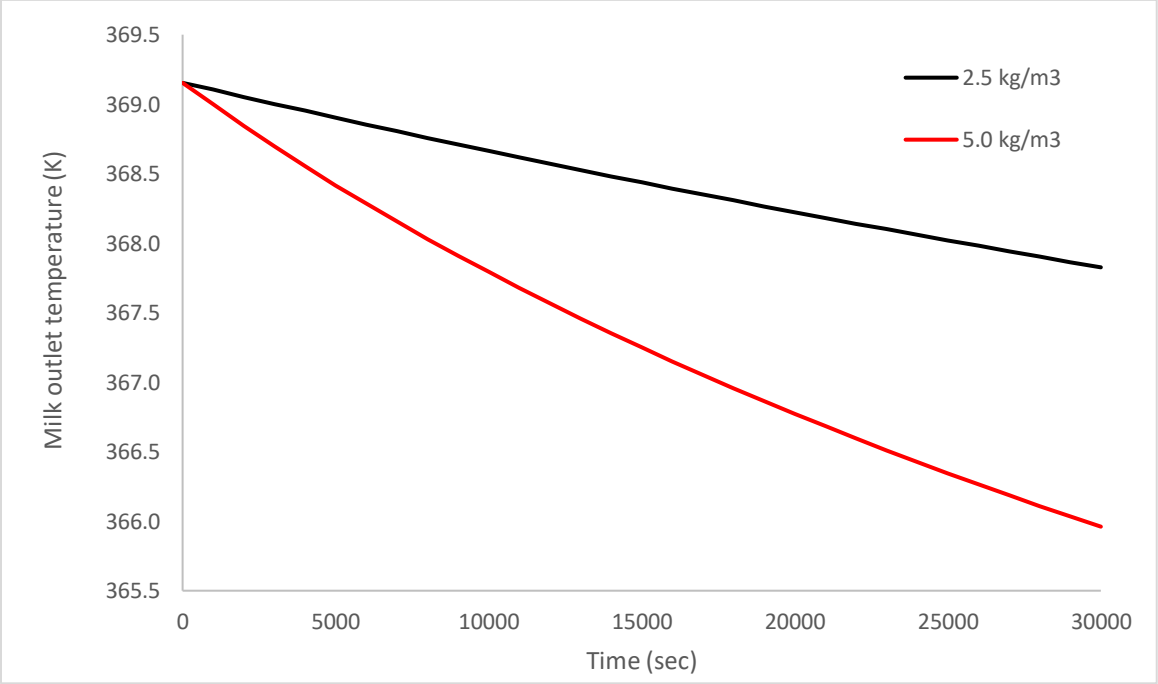

Figure 4.10 Effect of initial native protein concentration on milk outlet temperature

The effect of Reynolds number is illustrated in Figure 4.11. By doubling the milk flowrate and hence Reynolds number, it is observed a significant mitigation of fouling. The same trend also holds for the shell and tube heat exchanger as described in Section 3.3. The Reynolds number on bacterial wall coverage has a minor impact on bacterial wall coverage as it is shown in Figure 4.12.

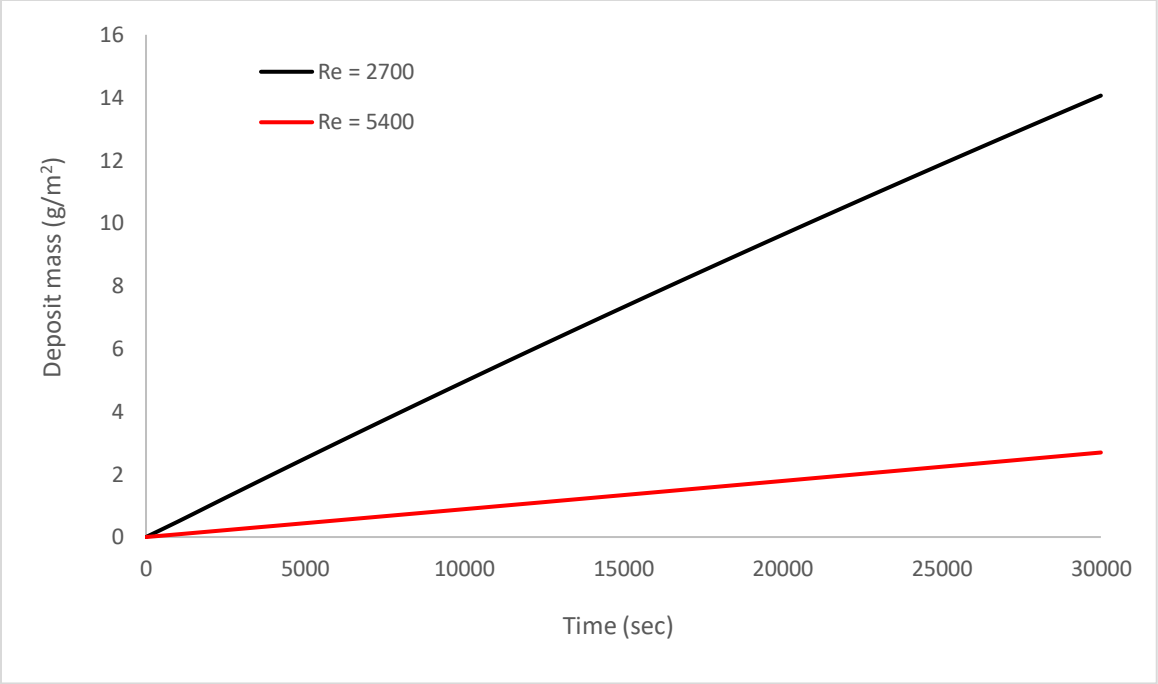

Figure 4.11 Effect of Reynolds on deposit mass

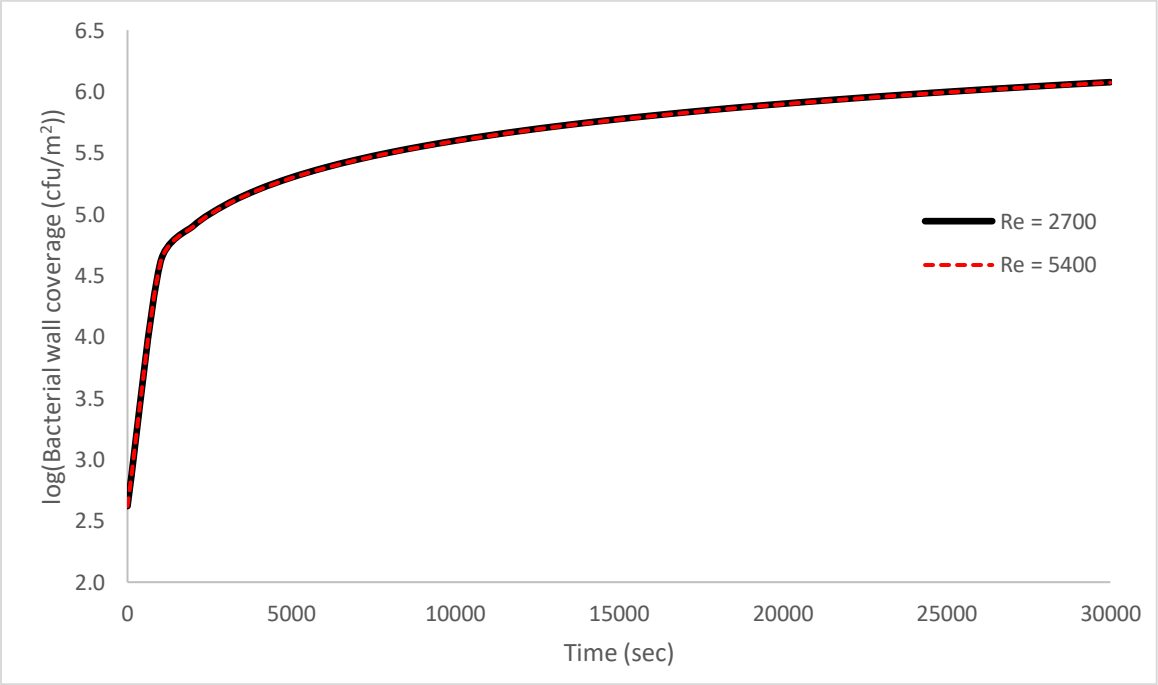

Figure 4.12 Effect of Reynolds number on bacterial wall coverage

Chapter 5

Dynamic Optimization of Shell and Tube Heat Exchangers under Fouling

5.1 Mathematical Model

The mathematical model used for the optimization is the mathematical model of shell and tube heat exchangers as described in Chapter 3. The cost objective function has to be minimized and takes into account the cleaning cost due to fouling, the cost due to interruption of production, which represents the direct economic impact of fouling, the annualized capital cost and energy costs.

5.1.1 Cost of Cleaning

The cost of cleaning includes the water cost, the NaOH cost, the cost of effluent disposal and the cost of steam used for cleaning. The cost coefficients are given in Table 5.1 assuming the cleaning solution velocity is equal to 0.174 m/s for the necessary unit transformations.

- Water cost: The overall water consumption during the cleaning process depends on both the tube's cross-sectional area and the duration of the cleaning operation. The total cost of water during the heating-cleaning cycle is estimated by Equation (5.1).

$$CO_{water}\left(\frac{\$}{cycle}\right) = \frac{0.087 \cdot \pi \cdot diam^2}{4} \cdot t_{clean} \tag{5.1}$$

- NaOH cost: For the cleaning process a 1% wt. NaOH solution is used. Analogically to water cost, the total cost of NaOH during the heating-cleaning cycle is calculated by Equation (5.2).

$$CO_{NaOH}\left(\frac{\$}{cycle}\right) = \frac{69.19 \cdot \pi \cdot diam^2}{4} \cdot t_{clean} \tag{5.2}$$

- Cost of effluent disposal: The total cost of effluent disposal during the heating-cleaning cycle is given by Equation (5.3).

$$CO_{ef}\left(\frac{\$}{cycle}\right) = \frac{0.174 \cdot \pi \cdot diam^2}{4} \cdot t_{clean} \quad (5.3)$$

- Steam cost: The steam is used for heating the cleaning solution to the desired temperature, 60°C. The total cost of steam is estimated by Equation (5.4).

$$CO_{steam}\left(\frac{\$}{cycle}\right) = \frac{0.424 \cdot \pi \cdot diam^2}{4} \cdot t_{clean} \quad (5.4)$$

Hence, the total cleaning cost is given by Equation (5.5).

$$C_{cleaning}\left(\frac{\$}{cycle}\right) = CO_{water} + CO_{NaOH} + CO_{ef} + CO_{steam} \quad (5.5)$$

Table 5.1 Cost coefficients (Khalid et al., 2016)

	Cost coefficient	Units
Water	0.50	$/m^3
NaOH	397.64	$/m^3
Effluent Disposal	1.00	$/m^3
Steam	0.32	$/kg

5.1.2 Cost of Heating Medium

As in Chapter 3 three heating configurations are considered and they are optimized:

1. Constant wall temperature with steam as heating medium
2. Co-current operation with water as heating medium
3. Counter-current operation with water as heating medium

The steam needed is given by Equation (5.6).

$$m_{steam}(\frac{kg}{s}) = \frac{w_f \cdot Cp_f \cdot (T_f^{out} - T_f^{in})}{\lambda_{steam}} \quad (5.6)$$

where λ_{steam} is the enthalpy of vaporization and is given by Equation (5.7).

$$\lambda_{steam}\,(\frac{J}{kg}) = 2537 - 2.8013 \cdot T_w \quad (5.7)$$

The total steam cost over the heating operations is given by Equation (5.8).

$$C_{steam2}\left(\frac{\$}{cycle}\right) = \int_0^{t_{heat}} 0.062 \cdot m_{steam} dt \tag{5.8}$$

For the co-current and counter-current operation, the needed steam is calculated by a similar energy balance as in case of constant wall temperature by Equation (5.9). As the inlet temperature is a control variable, it is presumed that this temperature is set by using steam from the utility system through an auxiliary exchanger.

$$m_{steam}\,(\frac{kg}{s}) = \frac{w_s \cdot Cp_s \cdot (T_s^{in} - T_s^{out})}{\lambda_{steam}} \tag{5.9}$$

The total steam cost over the heating operations is given again by Equation (5.8).

5.1.3 Cost of Heat Exchanger

The capital cost of the heat exchanger is determined based on its material and heat-transfer area, assuming stainless steel as the construction material for both the shell and the tube. It is expressed over a one-year period using an appropriate charge factor (Peters S. M. et al., 2006).

$$C_{HE}(\frac{\$}{year}) = 1000 \cdot Area2^{0.65} \tag{5.10}$$

$$Area2 = \pi \cdot d \cdot L \tag{5.11}$$

5.1.4 Cost due to Production Interruption

During the cleaning of the heat exchanger production is interrupted. Hence, this results in considerable loss of production. The cost due to production losses is estimated by Equation (5.12).

$$C_{losses}\left(\frac{\$}{cycle}\right) = w_f \cdot S_{net} \cdot t_{clean} \tag{5.12}$$

where S_{net} is a sales values representing the net profit per unit of product. The value for milk is 0.1$/kg.

5.1.5 Objective Function

The objective function that depicts the total cost during in one year horizon is given by Equation (5.13).

$$CC\ (\frac{\$}{year}) = NCL \int_0^{t_{heat}} (C_{cleaning}\ +\ C_{losses})dt + C_{steam2} + C_{HE} \tag{5.13}$$

NCL are calculated by Equation (5.14).

$$NCL = \frac{365\left(\frac{days}{year}\right) \cdot 0.85 \cdot 24\left(\frac{hours}{day}\right)}{(t_{heat} + t_{clean})\left(\frac{hours}{cycle}\right)} \tag{5.14}$$

where according to Georgiadis et al. (1998b) t_{clean} is given by Equation (5.15).

$$t_{clean} = 0.353 + 0.01237 \cdot t_{heat} - 2.55 \cdot 10^{-4} \cdot t_{heat}^2 + 1.87 \cdot 10^{-6} \cdot t_{heat}^3 \tag{5.15}$$

Hence, *NCL* is expressed finally by Equation (5.16).

$$NCL(\frac{cycles}{year}) = \frac{7446}{0.353 + 1.01237 \cdot t_{heat} - 2.55 \cdot 10^{-4} \cdot t_{heat}^2 + 1.87 \cdot 10^{-6} \cdot t_{heat}^3} \tag{5.16}$$

5.1.6 Constraints

The constraints must be satisfied in the optimization process are the following:

- The average pressure drop at the milk side must be less than an upper bound, which is according to Kern (1965) equals to 7 psi.

$$\overline{\Delta P} \leq 7\ psi\ \forall t \in [0, t_{heat}]$$

- The outlet temperature of milk must be very close to target value. A lower bound of 364.9K is assumed.

$$364.9 \leq T_f^{out}\ K\ \forall t \in [0, t_{heat}]$$

- The outlet average bacterial concentration must be less than an upper bound, which is according to U.S. Department of Health and Human Services, Public Health Service and

Food and Drug Administration (U.S. Department of Health and Human Services, 2017) equals to $5 \cdot 10^8$ cfu/m^3.

$$\bar{c} \leq 5 \cdot 10^8 \, cfu/m^3$$

- The lower bound of the tube diameter is 0.018 m and the upper bound is 0.030 m.

$$0.018 \leq diam \leq 0.030 \, m$$

- The lower and the upper bound of tube length are determined by manufacturing data of heat exchangers.

$$1 \leq L \leq 20 \, m$$

- The upper bound for time horizon is defined by microbiological constraints. The bounds for the time horizon are the following:

$$3 \leq t_{heat} \leq 70 \, h$$

The first two constraints must always be satisfied during the heating process ("path constraints"), the third constraint must be satisfied at the end of time horizon (inequality end point constraint) while the other two constraints are time invariant concerning the exchanger design.

5.1.7 Control Variables

For the case of constant wall temperature where steam is used as heating medium the only decision variable is the wall temperature. The bounds of wall temperature are the following:

$$370 \leq T_w \leq 390 \, K$$

For the case of co-current and counter-current where water is used as heating medium the decision variables are the inlet temperature of water and its flowrate. For the case of counter-current operation it is not possible to find a feasible solution with these two variables, so the milk flowrate is considered as an additional control variable. The bounds of these three variables are the following respectively:

$$365 \leq T_s^{in} \leq 400 \, K$$

$$0.1 \leq w_s \leq 10\ kg/s$$

$$0.14 \leq w_f \leq 0.57\ kg/s\ \ (counter - current\ case\ only)$$

5.2 Optimization Results

For the optimization of the system of differential – algebraic equations the optimization tool gOPT that is incorporated in gPROMS™ from Siemens Process System Enterprise is used. The solver used for the optimization problem is CVP_SS which is the default solver in gPROMS™ and is based on a control vector parametrization (CVP) approach. This approach assumes that the time - varying control variables are piecewise constant functions of time over a specified number of control intervals (Process Systems Enterprise Ltd, 2023).

5.2.1 Constant Wall Temperature

For the constant wall temperature case, where steam is used as heating medium, only wall temperature, T_w, is used as control variable. The optimization results for different number of intervals of the constant wall temperature case are shown in Table 5.2.

Table 5.2 Optimization results for constant wall temperature

Number of intervals	Heating time (h)	Objective Function ($/year)	Diameter (m)	Length (m)
6	28.98	57,620	0.018	8
8	37.38	53,426	0.018	8
12	50.00	49,772	0.018	8

It is observed that the number of control intervals affects the objective function. The increase in the number of control intervals improves the objective function. Using 12 intervals the objective function presents about 14% improvement compared with 6 intervals. In addition, it is observed that the objective function is inversely proportional to the heating time as is shown in Figure 5.1 for the case of constant wall temperature. This behavior is also observed in the other two cases.

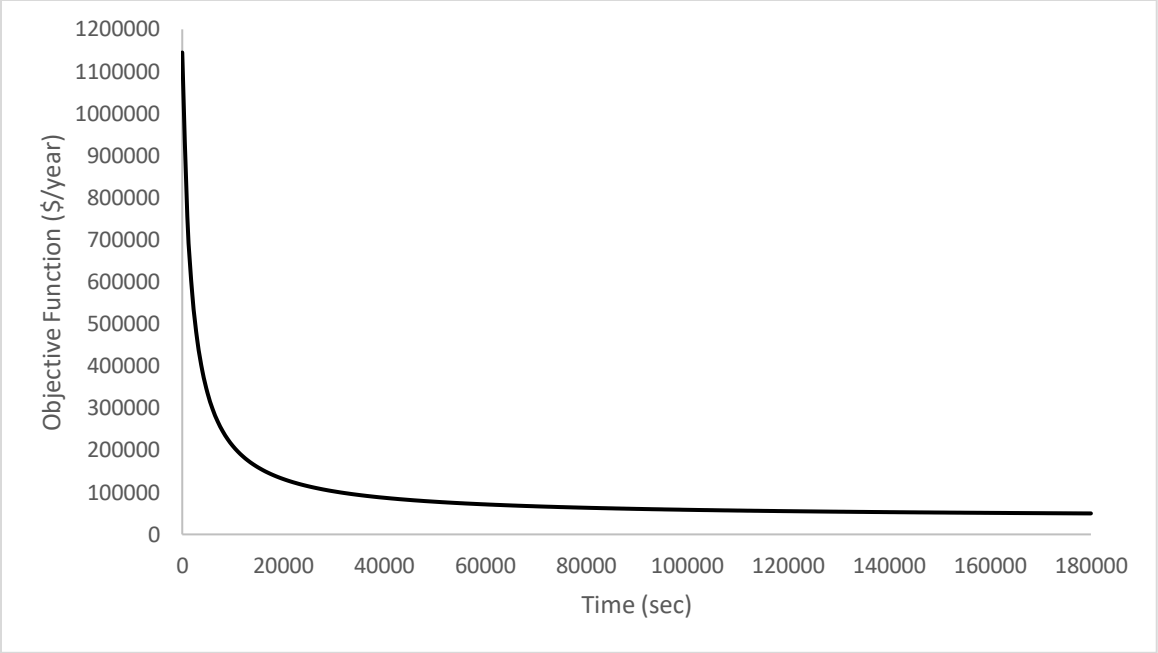

Figure 5.1 Objective function profile – Constant wall temperature

Since 12 control intervals present the most improved behavior concerning the value of objective function, this case is used for simulation and comparison with the base case. The control profile of wall temperature is shown in Figure 5.2 while the milk outlet temperature is shown in Figure 5.3. The milk outlet temperature is kept above the lower limit and the constraint is satisfied.

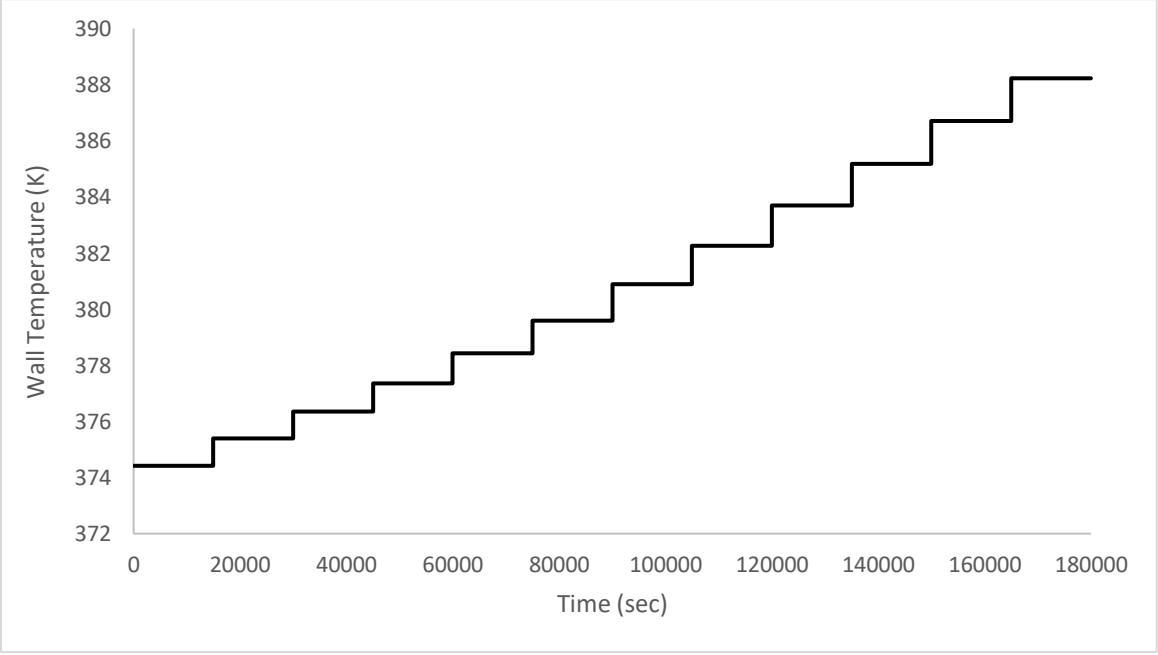

Figure 5.2 Control profile for wall temperature – Constant wall temperature case

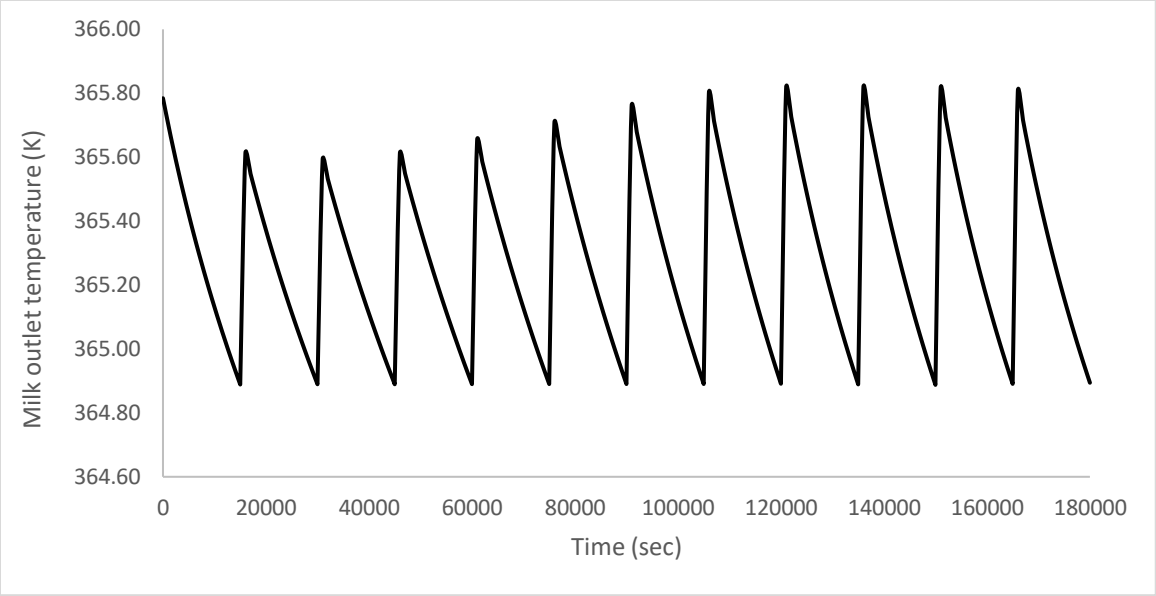

Figure 5.3 Milk outlet temperature under control – Constant wall temperature case

In Figure 5.4 is compared the deposit thickness of the optimized case with the base case (case before optimization). It is observed that in the optimized case the deposit thickness is smaller throughout the time horizon compared with the base case and it presents almost linear behavior. The bacterial wall coverage of the base and optimized case is shown in Figure 5.5. The bacterial wall coverage is the same until 11 hours for both cases but then although in the optimized case seems to be almost constant in the base case increases significantly.

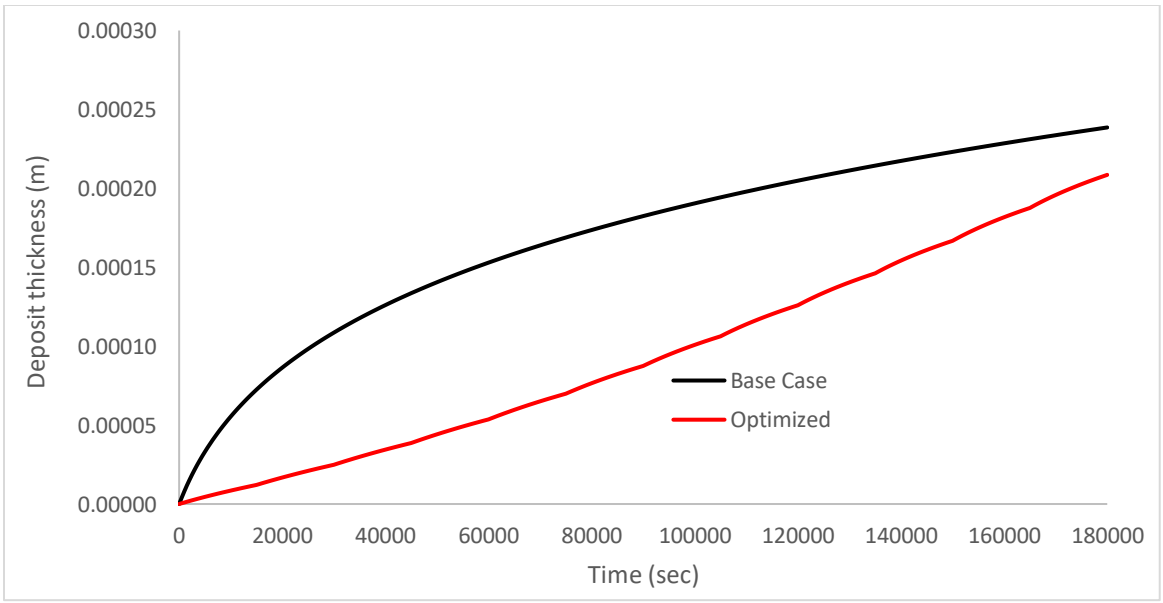

Figure 5.4 Deposit thickness for base and optimized case – Constant wall temperature case

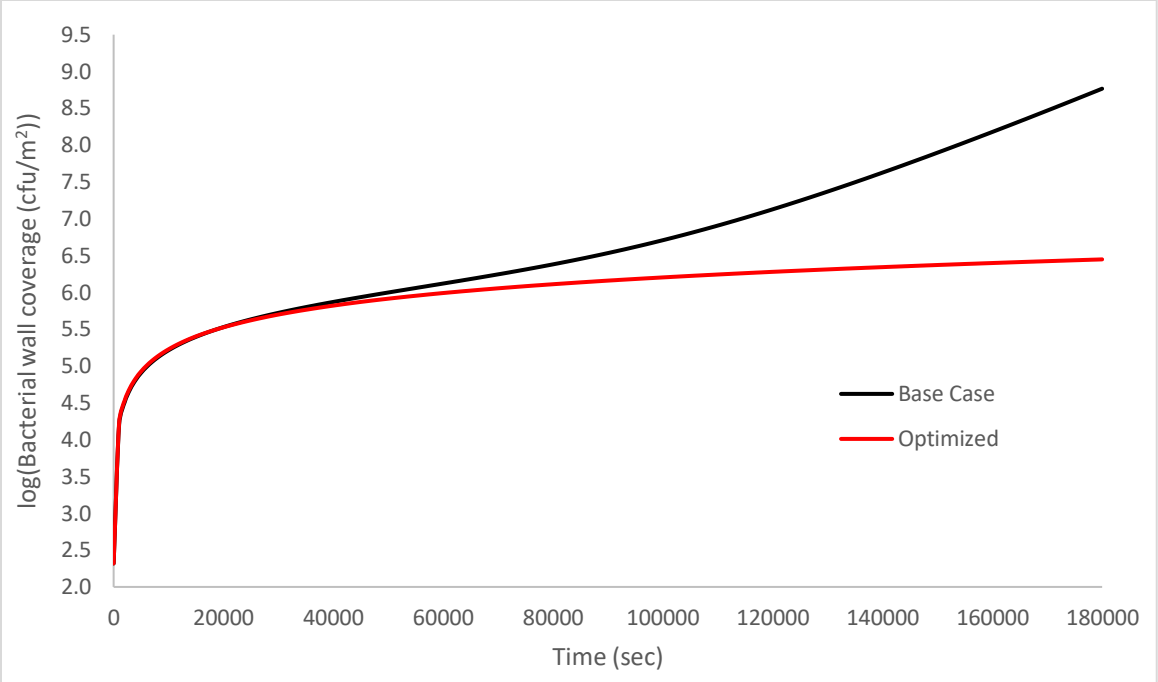

Figure 5.5 Bacterial wall coverage for base and optimized case - Constant wall temperature case

5.2.2 Co-current Operation

For the case of co-current operation, where water is used as heating medium, the heating medium inlet temperature, T_s^{in}, and the heating medium flowrate, w_s, are used as control variables. Again, it was investigated the case of having only the flowrate of heating medium as control variable since in the dairy industry is a common practice to have only the heating medium flowrate as control variable, but it was proved to be infeasible. Optimization results for the different number of control intervals are presented in Table 5.3. Heating medium flowrate, w_s, although it is piecewise constant variable is chosen to have constant value throughout the time horizon by optimization. Hence, heating medium flowrate value is 1 kg/s.

Table 5.3 Optimization results for co-current operation

Number of intervals	Heating time (h)	Objective Function ($/year)	Diameter (m)	Length (m)	w_s (kg/s)
6	24.17	60,147	0.0192	8	1
8	24.44	59,808	0.0195	8	1
12	26.67	57,757	0.0198	8	1

The control profile of heating medium inlet temperature is shown in Figure 5.6 while the milk outlet temperature is shown in Figure 5.7. The milk outlet temperature is kept above the lower limit over the entire time horizon and the constraint is satisfied.

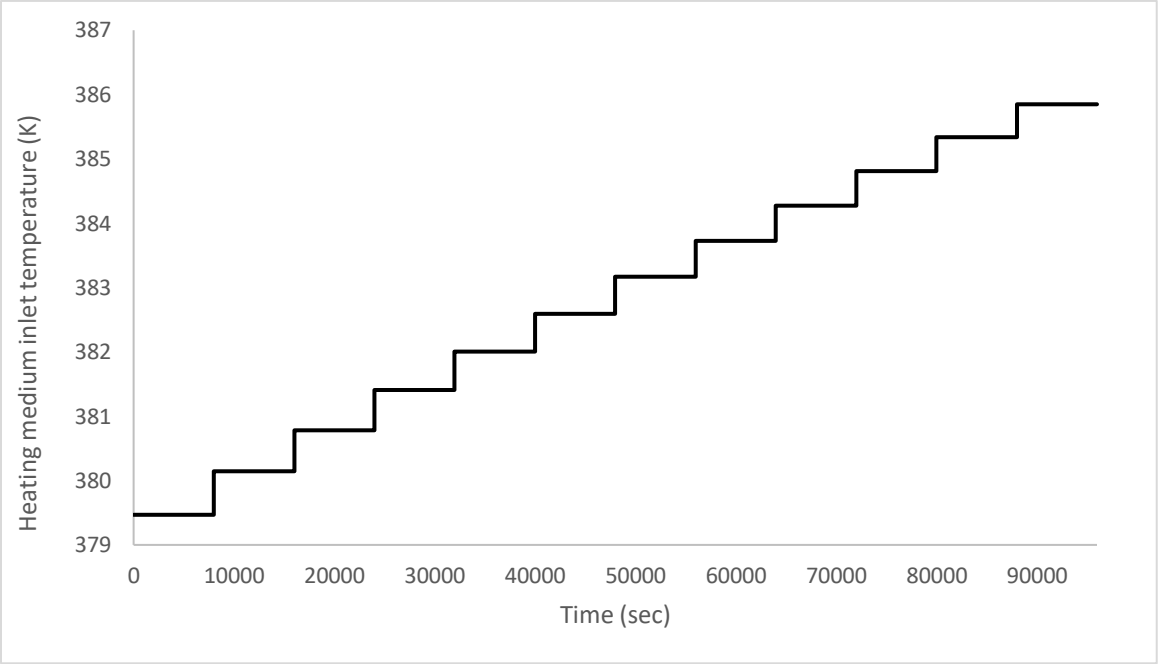

Figure 5.6 Control profile for wall temperature – Co-current operation case

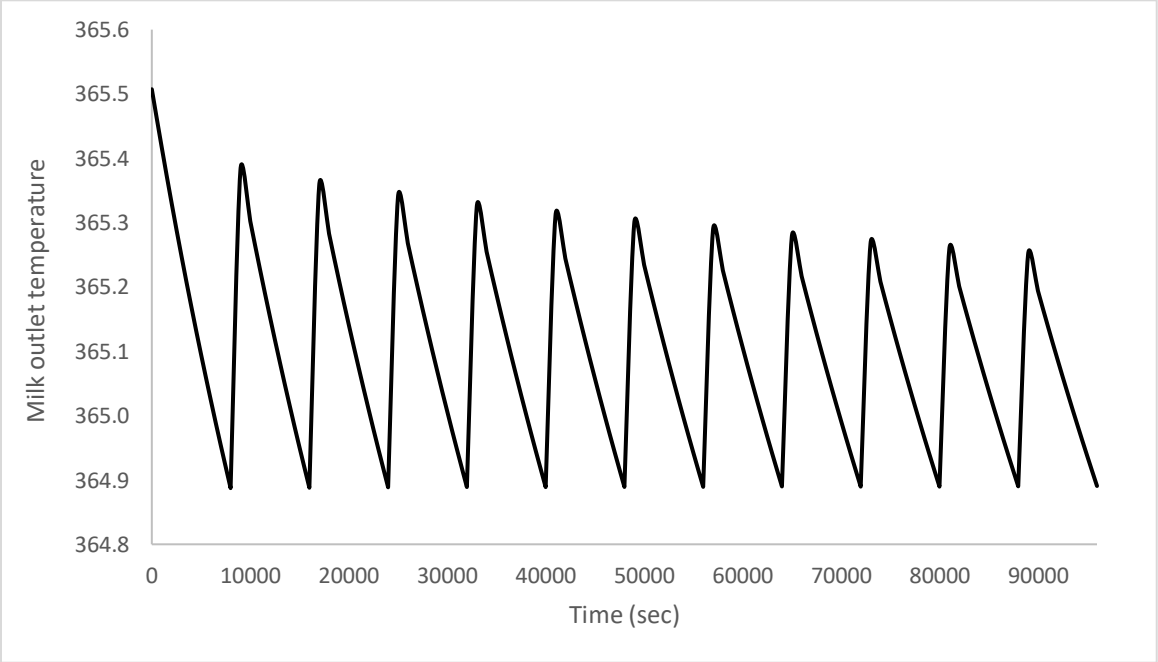

Figure 5.7 Milk outlet temperature under control – Co-current operation case

In Figure 5.8 is compared the deposit thickness of the optimized case with the base case (case before optimization). It is observed that in the optimized case the deposit thickness is significantly smaller throughout the time horizon compared with the base case and it presents almost linear behavior while in the base case exponential behavior. The bacterial wall coverage of the base and optimized case is shown in Figure 5.9. The bacterial wall coverage is almost the same for both cases. Therefore, the optimization procedure does not manipulate the bacterial wall coverage since during the time horizon the bacterial bulk concentration is smaller than the posed upper bound.

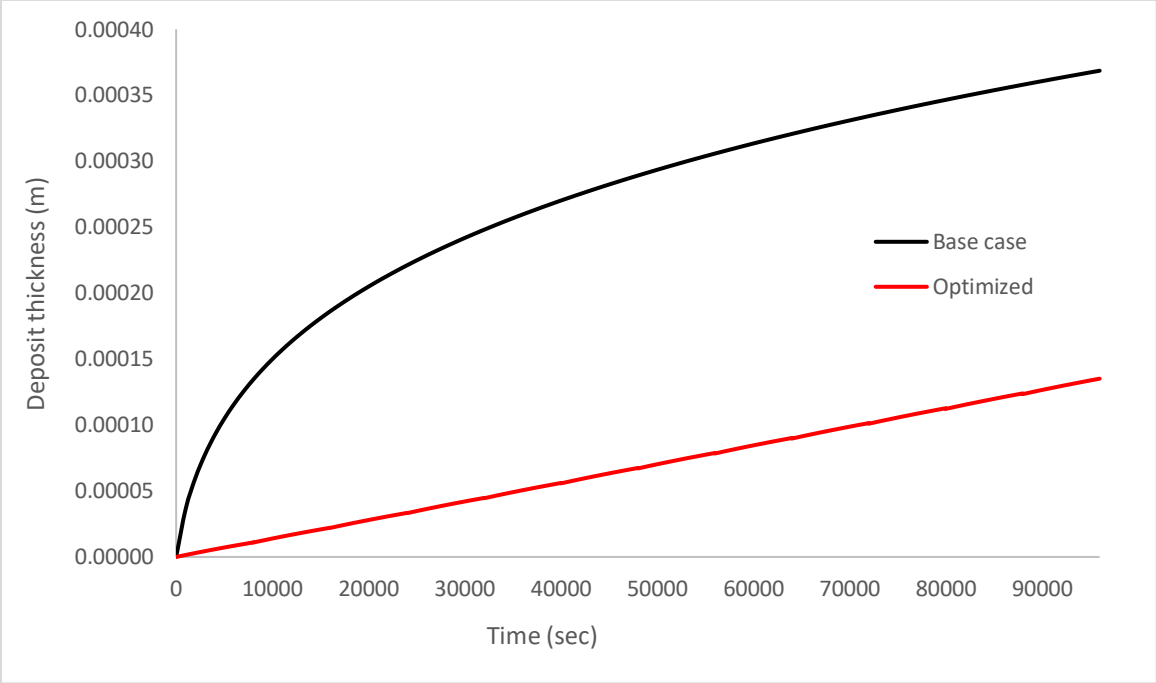

Figure 5.8 Deposit thickness for base and optimized case – Co-current operation case

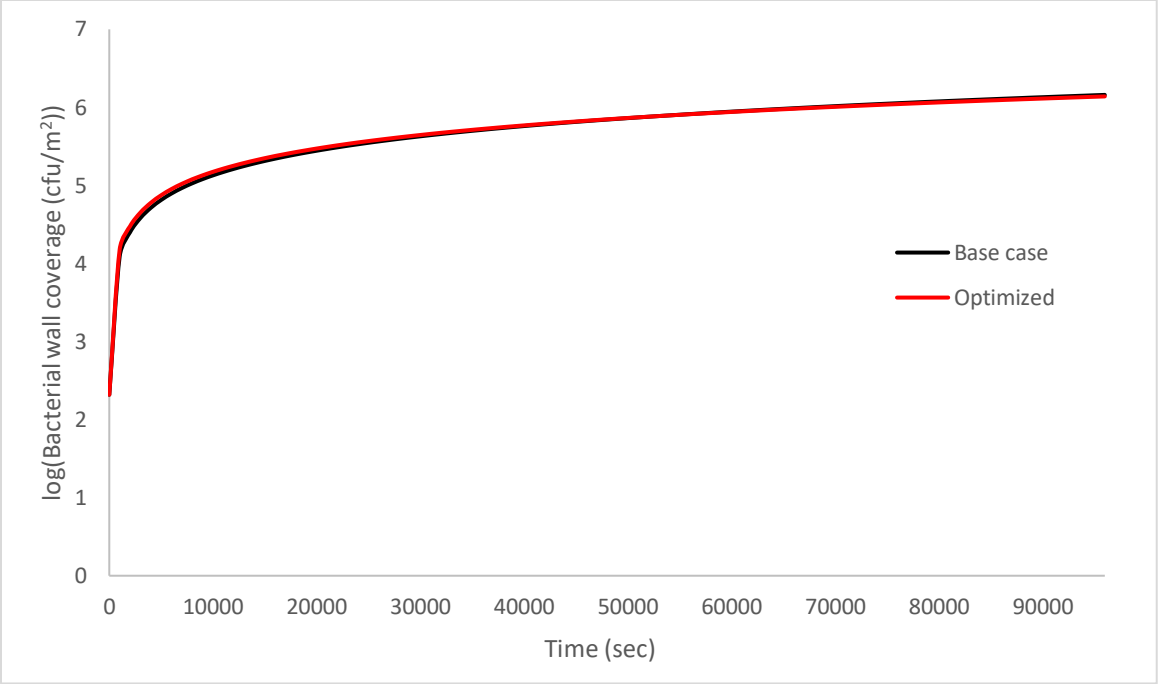

Figure 5.9 Bacterial wall coverage for base and optimized case - Co-current operation case

5.2.3 Counter-current Operation

For the case of counter-current operation, where water is used as heating medium, the heating medium inlet temperature, T_s^{in}, and the heating medium flowrate, w_s, are used as control variables. However, using only these two variables as control variables, finding a feasible optimal solution is not possible. Hence, the milk flowrate is used as an extra control variable, w_f. Again, it was investigated the case of having only the flowrate of heating medium as control variable and was proved to be infeasible. Optimization results for the different number of control intervals are summarized in Table 5.4. Heating medium flowrate, w_s, and milk flowrate, w_f, although they are piecewise constant variables are chosen to have constant value throughout the time horizon by optimization. Hence, heating medium flowrate value is 0.1 kg/s and milk flowrate value is 0.14 kg/s.

Table 5.4 Optimization results for counter-current operation

Number of intervals	Heating time (h)	Objective Function ($/year)	Diameter (m)	Length (m)	w_s (kg/s)	w_f (kg/s)
6	8.0	62,810	0.018	8	0.1	0.14
8	8.9	58,052	0.018	8	0.1	0.14
12	9.0	57,520	0.018	8	0.1	0.14

The control profile of heating medium inlet temperature and the milk outlet temperature are shown in Figure 5.10 and in Figure 5.11 respectively. Again, the milk outlet temperature is kept above the lower limit. The control profile of heating medium inlet temperature in this configuration is quite different from the co-current operation case as this temperature slightly increases (total temperature difference 0.1^{o}C after about 5.5 hours) and then it fluctuates. On the other hand, in the co-current operation the water inlet temperature increases about 1^{o}C in each time interval, so the total temperature difference is 6.5^{o}C after 25 operating hours.

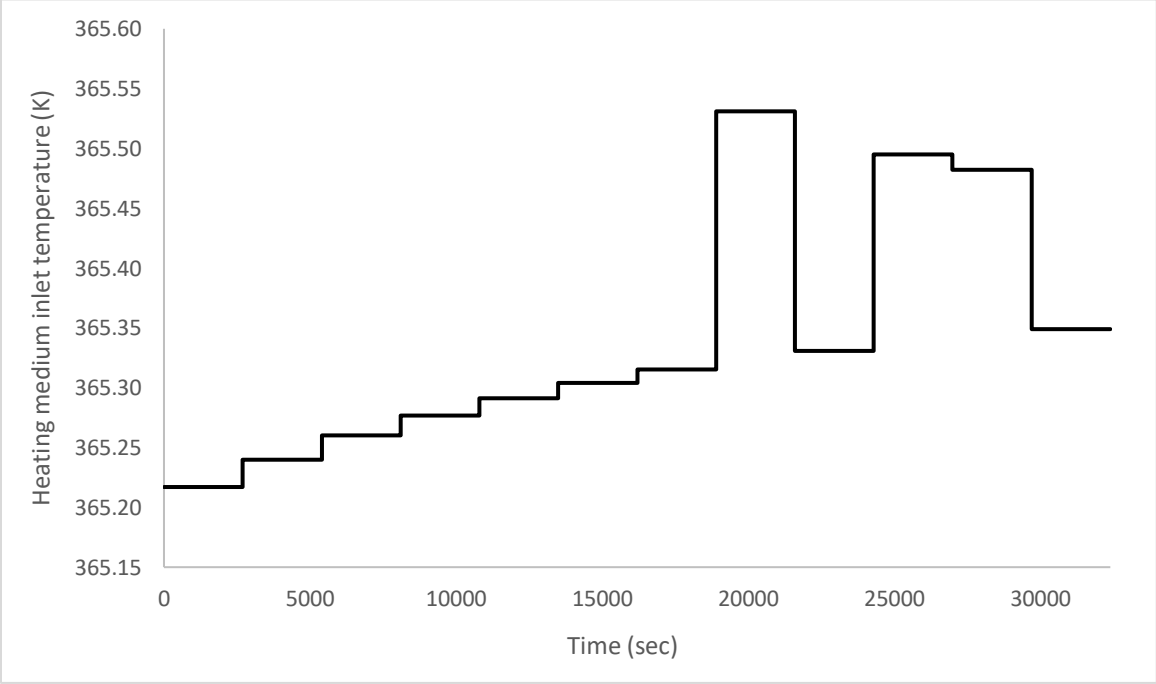

Figure 5.10 Control profile for heating medium inlet temperature – Counter-current operation case

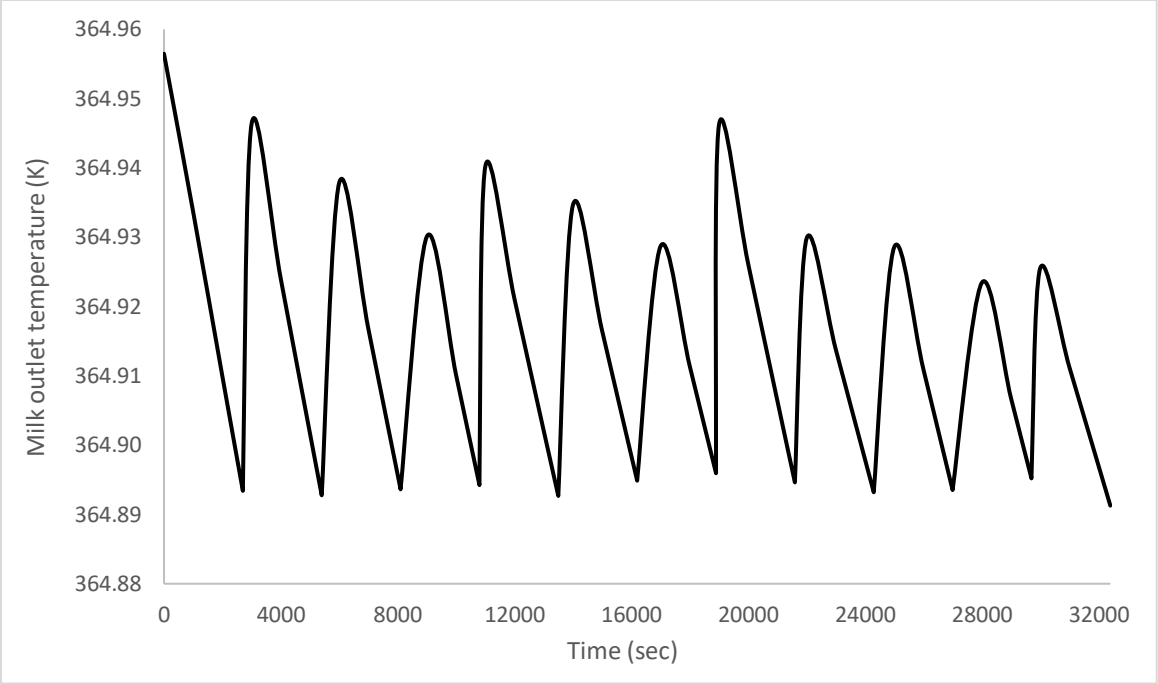

Figure 5.11 Milk outlet temperature under control – Counter-current operation case

In Figure 5.12 is compared the deposit thickness of the optimized case with the base case (case before optimization). It is observed that in the optimized case the deposit thickness is significantly smaller throughout the time horizon compared with the base case and it presents almost linear behavior while in the base case exponential behavior. The “spikes” that are present in the optimized case are due to the heating medium inlet temperature fluctuations. The bacterial wall coverage of the base and the optimized case is shown in Figure 5.13. The bacterial wall coverage for the base case is higher compared to that of optimized during the heating horizon.

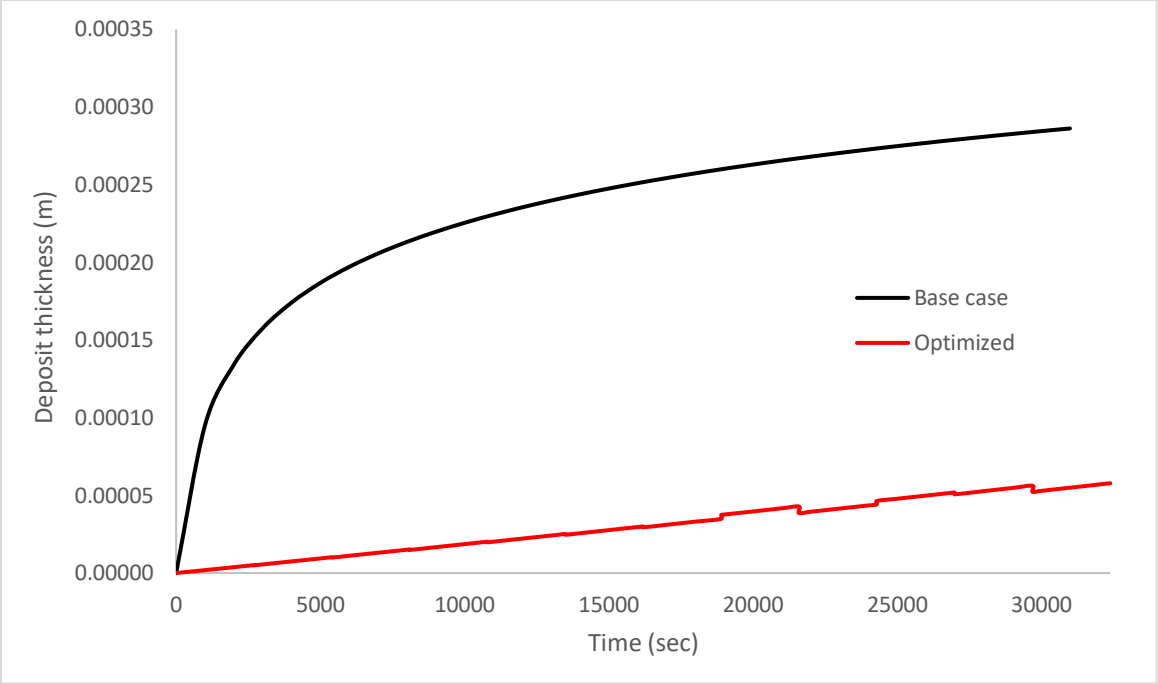

Figure 5.12 Deposit thickness for base and optimized case – Counter-current operation case

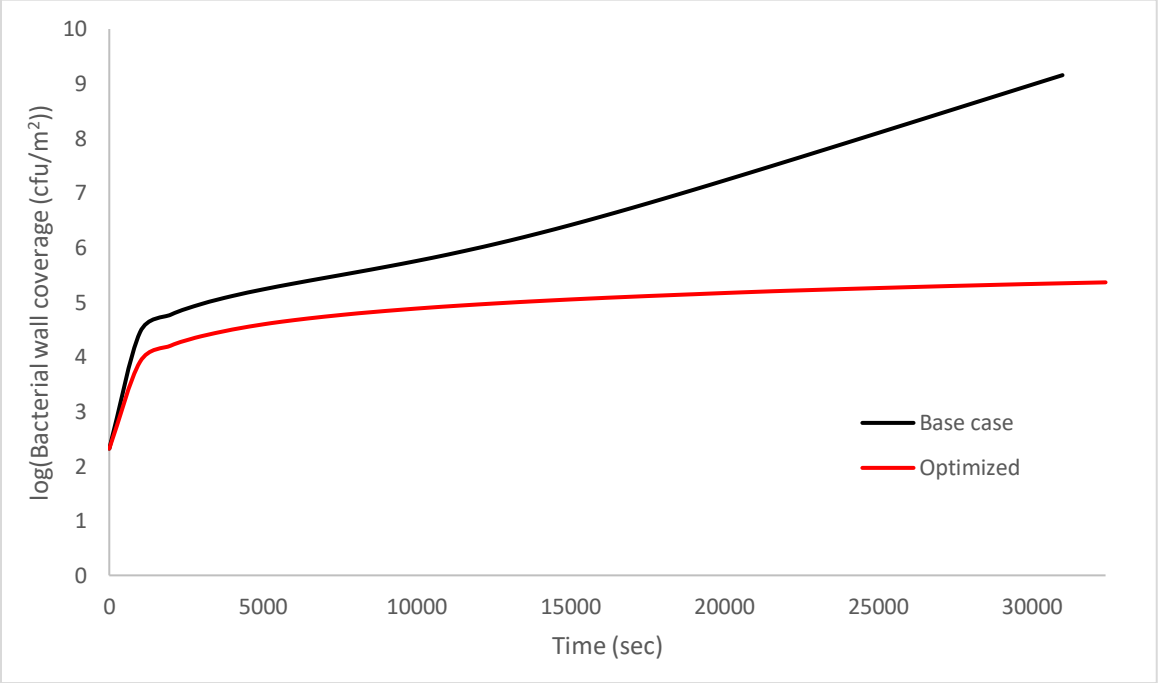

Figure 5.13 Bacterial wall coverage for base and optimized case – Counter-current operation case

5.2.4 Comparison of the Optimization Results of the Three Configurations

For all the cases the optimal diameter is relatively small. For the cases of the constant wall temperature and the counter-current operation the optimal diameter is fixed at its lower bound. For the co-current operation, the optimal diameter is very close to the lower bound. Tube length is between the bounds and the same for all the cases. It is relatively large to allow gradual heat of milk, which is in agreement with dairy industry practice where heat exchangers are oversized to mitigate the undesirable fouling. However, an oversized heat exchanger with length fixed at its upper bound would result in extra capital cost and the profit from the extra fouling mitigation would be counterbalanced.

The configuration of constant wall temperature runs for longer heating time comparing with the other two configurations because milk's heating is gradual and fouling is minimized, while the configuration of counter-current operation runs for shorter heating time because this configuration enables maximum heat recovery that favors fouling.

In the constant wall temperature case, the steam temperature gradually increases 14^{o}C, in the co-current operation the water temperature gradually increases 6.5^{o}C while in the counter-current operation the water temperature increases only 0.1^{o}C. This can be explained since the counter-current operation enables maximum heat recovery.

The optimized counter-current operation case presents lower deposit thickness and lower bacterial wall coverage compared to the other two configurations while the case of constant wall temperature presents the highest.

Comparing the value of the objective function for the base and the optimized case of the three different configurations it is highlighted that counter-current operation presents the most significant improvement since the nominal inlet water temperature (385K) is significantly greater than the temperature range chosen from optimization as it is illustrated in Table 5.5.

Table 5.5 Objective function value before and after optimization for all configurations

	Objective Function ($/year)		Difference
	Base case	**Optimized case**	
Constant Wall Temperature	59,684	49,772	-16.6%
Co-current	66,774	57,757	-13.5%
Counter-current	121,554	57,520	-52.8%

Chapter 6

Conclusions and Future Work

6.1 Conclusions

In this thesis, a mathematical model that describes both milk protein fouling, and bacterial contamination has been developed for plate and shell and tube heat exchangers. Three different configurations of shell and tube heat exchangers and two different arrangements for plate heat exchangers have been investigated for better understanding of the fouling behavior and its effect on the process operation. Plate heat exchangers are less prone to fouling compared with shell and tube heat exchangers due to their lower surface temperature and to their higher turbulence. The second arrangement of plate heat exchanger results in lower fouling than the other due to the lower heating load. The increased initial native protein concentration as well as the decreased Reynolds number results in higher deposits. Hence, higher Reynolds number is preferred for fouling mitigations.

Furthermore, the three cases of shell and tube heat exchangers have been optimized, considering all the cost factors related to the milk heat treatment. For all configurations the optimal heat exchanger size (diameter and length) is determined by exploiting the trade-off between operating and capital costs. Generally, fouling decreased with the size of the heat exchanger, as it allows a gradual heat of milk but with an increased capital cost. The optimized configuration of counter-current operation leads to shorter heating time as it enables maximum heat recovery that favors fouling and presents lower deposit thickness and lower bacterial wall coverage, compared to the other two configurations.

6.2 Future work

An aspect for further investigation is the possible interaction between microbial and protein fouling and the development of relevant correlations in the mathematical model. Moreover, for a better understanding of the phenomena of bacterial fouling, it would be useful to extend the mathematical

model of de Jong (2002) in two dimensions (radial and axial) and to validate it with experimental data since the radial profile of velocity may affect both the heat and the mass transfer operation.

In order for the models that have been presented in this work to be more realistic, experiments in different operating conditions (e.g., temperature, inlet concentration, milk flowrate) could be conducted which providing an opportunity for model parameter estimation. However, experimental data are not easily available and collaborations between industry, research institutions and academia are required.

Finally, the presented mathematical model for microbial and protein fouling could be incorporated into a complete dairy plant model so as to simulate the overall plant operation. The complete dairy plant model could be used for the optimization of the equipment design and the derivation of optimal operating policies.

References

al-Makhlafi, H., McGuire, J., & Daeschel, M. (1994). Influence of preadsorbed milk proteins on adhesion of Listeria monocytogenes to hydrophobic and hydrophilic silica surfaces. *Applied and Environmental Microbiology*, *60*(10), 3560–3565. https://doi.org/10.1128/aem.60.10.3560-3565.1994

Austin, J. W., & Bergeron, G. (1995). Development of bacterial biofilms in dairy processing lines. *Journal of Dairy Research*, *62*(3), 509–519. https://doi.org/10.1017/S0022029900031204

Bansal, B., & Chen, X. D. (2006). A Critical Review of Milk Fouling in Heat Exchangers. *Comprehensive Reviews in Food Science and Food Safety*, *5*(2), 27–33. https://doi.org/10.1111/j.1541-4337.2006.tb00080.x

Barnes, L., Adams, M. R., Watts, J. F., Zhdan, P. A., & Chamberlain, A. H. L. (2001). Correlated XPS, AFM and bacterial adhesion studies on milk and milk proteins adherent to stainless steel. *Biofouling*, *17*(1), 1–22. https://doi.org/10.1080/08927010109378460

Barnes, L.-M., Lo, M. F., Adams, M. R., & Chamberlain, A. H. L. (1999). Effect of Milk Proteins on Adhesion of Bacteria to Stainless Steel Surfaces. *Applied and Environmental Microbiology*, *65*(10), 4543–4548. https://doi.org/10.1128/AEM.65.10.4543-4548.1999

Belmar-Beiny, M. T., Gotham, S. M., Paterson, W. R., Fryer, P. J., & Pritchard, A. M. (1993). The effect of Reynolds number and fluid temperature in whey protein fouling. *Journal of Food Engineering*, *19*(2), 119–139. https://doi.org/10.1016/0260-8774(93)90038-L

Bott, T. R. (1993). Aspects of Biofilm Formation and Destruction. *Corrosion Reviews*, *11*(1–2), 1–24. https://doi.org/10.1515/CORRREV.1993.11.1-2.1

Boulangé-Petermann, L., Rault, J., & Bellon-Fontaine, M. (1997). Adhesion of *streptococcus thermophilus to* stainless steel with different surface topography and roughness. *Biofouling*, *11*(3), 201–216. https://doi.org/10.1080/08927019709378331

Bouman, S., Lund, D. B., Driessen, F. M., & Schmidt, D. G. (1982). Growth of Thermoresistant Streptococci and Deposition of Milk Constituents on Plates of Heat Exchangers During Long Operating Times. *Journal of Food Protection*, *45*(9), 806–813. https://doi.org/10.4315/0362-028X-45.9.806

Bremer, P. J., Monk, I., & Osborne, C. M. (2001). Survival of Listeria monocytogenes Attached to Stainless Steel Surfaces in the Presence or Absence of Flavobacterium spp. *Journal of Food Protection*, *64*(9), 1369–1376. https://doi.org/10.4315/0362-028X-64.9.1369

Briandet, R., Herry, J.-M., & Bellon-Fontaine, M.-N. (2001). Determination of the van der Waals, electron donor and electron acceptor surface tension components of static Gram-positive microbial biofilms. *Colloids and Surfaces B: Biointerfaces*, *21*(4), 299–310. https://doi.org/10.1016/S0927-7765(00)00213-7

Brodkey R. S., & Hershey H. C. (2003). *Transport Phenomena: A Unified Approach*. McGraw-Hill.

Burgess, S. A., Flint, S. H., Lindsay, D., Cox, M. P., & Biggs, P. J. (2017). Insights into the Geobacillus stearothermophilus species based on phylogenomic principles. *BMC Microbiology*, *17*(1), 140. https://doi.org/10.1186/s12866-017-1047-x

Burton, H. (1968). Deposits from whole milk in heat treatment plant—a review and discussion. *Journal of Dairy Research*, *35*(2), 317–330. https://doi.org/10.1017/S0022029900019038

Bylund Gosta. (1995). *Dairy Processing Handbook*. Tetra Pak Processing Systems AB.

Changani, S. D., Belmar-Beiny, M. T., & Fryer, P. J. (1997). Engineering and chemical factors associated with fouling and cleaning in milk processing. *Experimental Thermal and Fluid Science*, *14*(4), 392–406. https://doi.org/10.1016/S0894-1777(96)00141-0

Corredig, M., & Dalgleish, D. G. (1996). Effect of temperature and pH on the interactions of whey proteins with casein micelles in skim milk. *Food Research International*, *29*(1), 49–55. https://doi.org/10.1016/0963-9969(95)00058-5

Dalgleish, D. G. (1990). Denaturation and aggregation of serum proteins and caseins in heated milk. *Journal of Agricultural and Food Chemistry*, *38*(11), 1995–1999. https://doi.org/10.1021/jf00101a001

de Jong, P. (1997). Impact and control of fouling in milk processing. *Trends in Food Science & Technology*, *8*(12), 401–405. https://doi.org/10.1016/S0924-2244(97)01089-3

de Jong, P. (2002). Prediction of the adherence, growth and release of microorganisms in production chains. *International Journal of Food Microbiology*, *74*(1–2), 13–25. https://doi.org/10.1016/S0168-1605(01)00713-9

de Jong, P., Bouman, S., & van der Linden, H. J. L. J. (1992). *Fouling of heat treatment equipment in relation to the denaturation of β-lactoglobulin.* https://api.semanticscholar.org/CorpusID:100480033

de Jong, P., te Giffel, M. C., Straatsma, H., & Vissers, M. M. M. (2002). Reduction of fouling and contamination by predictive kinetic models. *International Dairy Journal*, *12*(2–3), 285–292. https://doi.org/10.1016/S0958-6946(01)00165-0

De Jong, P., & Van Der Linden, H. J. L. J. (1992). Design and operation of reactors in the dairy industry. *Chemical Engineering Science*, *47*(13–14), 3761–3768. https://doi.org/10.1016/0009-2509(92)85095-S

Delplace, F., Leuliet, J. C., & Bott, T. R. (1995). Influence of plates geometry on fouling of plate heat exchangers by why proteins. *Fouling Mitigation of Industrial Heat Exchangers*.

Delplace, F., Leuliet, J. C., & Tissier, J. P. (1994). Fouling experiments of a plate heat exchanger by whey proteins solutions. *Food and Bioproducts Processing: Transactions of the Institution of Chemical Engineers, Part C*, *72*(C3), 163 – 169. https://www.scopus.com/inward/record.uri?eid=2-s2.0-0028515231&partnerID=40&md5=846fd48078ad3f4eaeb453344a00e798

Elofsson, U. M., Paulsson, M. A., Sellers, P., & Arnebrant, T. (1996). Adsorption during Heat Treatment Related to the Thermal Unfolding/Aggregation of β-Lactoglobulins A and B. *Journal of Colloid and Interface Science*, *183*(2), 408–415. https://doi.org/10.1006/jcis.1996.0563

Flint, S., Bremer, P., Brooks, J., Palmer, J., Sadiq, F. A., Seale, B., Teh, K. H., Wu, S., & Md Zain, S. N. (2020). Bacterial fouling in dairy processing. In *International Dairy Journal* (Vol. 101). Elsevier Ltd. https://doi.org/10.1016/j.idairyj.2019.104593

Flint, S. H., Bremer, P. J., & Brooks, J. D. (1997). Biofilms in dairy manufacturing plant - Description, current concerns and methods of control. *Biofouling*, *11*(1), 81–97. https://doi.org/10.1080/08927019709378321

Flint, S. H., Brooks, J. D., & Bremer, P. J. (1997). The influence of cell surface properties of thermophilic streptococci on attachment to stainless steel. *Journal of Applied Microbiology*, *83*(4), 508–517. https://doi.org/10.1046/j.1365-2672.1997.00264.x

Flint, S. H., Tte Van Den Elzen, H., Brooks, J. D., & Bremer, P. J. (1999). Removal and inactivation of thermo-resistant streptococci colonising stainless steel. In *International Dairy Journal* (Vol. 9).

Flint, S., Palmer, J., Bloemen, K., Brooks, J., & Crawford, R. (2001). The growth of Bacillus stearothermophilus on stainless steel. *Journal of Applied Microbiology*, *90*(2), 151–157. https://doi.org/10.1046/j.1365-2672.2001.01215.x

Fryer, P. J. (1989). The uses of fouling models in the design of food process plant. *International Journal of Dairy Technology*, *42*(1), 23–29. https://doi.org/10.1111/j.1471-0307.1989.tb01703.x

Fryer, P. J., Robbins, P. T., Green, C., Schreier, P. J. R., Pritchard, A. M., Hasting, A. P. M., Royston, D. G., & Richardson, J. F. (1996). A Statistical Model for Fouling of a Plate Heat Exchanger by Whey Protein Solution at UHT Conditions. *Food and Bioproducts Processing*, *74*(4), 189–199. https://doi.org/10.1205/096030896531181

Fryer, P. J., & Slater, N. K. H. (1985). A direct simulation procedure for chemical reaction fouling in heat exchangers. *The Chemical Engineering Journal*, *31*(2), 97–107. https://doi.org/10.1016/0300-9467(85)80048-4

Georgiadis, M. C., & Macchietto, S. (2000). Dynamic modelling and simulation of plate heat exchangers under milk fouling. *Chemical Engineering Science*, *55*(9), 1605–1619. https://doi.org/10.1016/S0009-2509(99)00429-7

Georgiadis, M. C., Rotstein, G. E., & Macchietto, S. (1998a). Modeling and simulation of shell and tube heat exchangers under milk fouling. *AIChE Journal*, *44*(4), 959–971. https://doi.org/10.1002/aic.690440422

Georgiadis, M. C., Rotstein, G. E., & Macchietto, S. (1998b). Optimal design and operation of heat exchangers under milk fouling. *AIChE Journal*, *44*(9), 2099–2111. https://doi.org/10.1002/aic.690440917

Giffel, M. C. te, Wagendorp, A., Herrewegh, A., & Driehuis, F. (2002). Bacterial spores in silage and raw milk. *Antonie van Leeuwenhoek*, *81*(1/4), 625–630. https://doi.org/10.1023/A:1020578110353

Gotham, S. M., Fryer, P. J., & Pritchard, A. M. (2007). β-lactoglobulin denaturation and aggregation reactions and fouling deposit formation: a DSC study. *International Journal of Food Science & Technology*, *27*(3), 313–327. https://doi.org/10.1111/j.1365-2621.1992.tb02033.x

Hinton, A. R. (2003). *Thermophiles and Fouling Deposits in Milk Powder Plants*. Massey University.

Jeurnink, T., Verheul, M., Stuart, M. C., & de Kruif, C. G. (1996). Deposition of heated whey proteins on a chromium oxide surface. *Colloids and Surfaces B: Biointerfaces*, *6*(4–5), 291–307. https://doi.org/10.1016/0927-7765(95)01262-1

Jun, S., & Puri, V. M. (2005). Fouling Models for Heat Exchangers in Dairy Processing: A Review. *Journal of Food Process Engineering*, *28*(1), 1–34. https://doi.org/10.1111/j.1745-4530.2005.00473.x

Kern, D. Q. (1965). *Process Heat Transfer* (1st ed.). McGraw-Hill.

Khalid, N. I., Nordin, N., Chia, Z. Y., Ab Aziz, N., Nuraini, A. A., Taip, F. S., & Ahmedov, A. (2016). A removal kinetics approach for evaluation of economic cleaning protocols for pink guava puree fouling deposit. *Journal of Cleaner Production*, *135*, 1317–1326. https://doi.org/10.1016/j.jclepro.2016.06.095

Lalande, M., Rene, F., & Tissier, J. P. (1989). Fouling and its control in heat exchangers in the dairy industry. *Biofouling*, *1*(3), 233–250. https://doi.org/10.1080/08927018909378111

Lalande, M., & Tissier, J. (1985). Fouling of Heat Transfer Surfaces Related to β-Lactoglobulin Denaturation During Heat Processing of Milk. *Biotechnology Progress*, *1*(2), 131–139. https://doi.org/10.1002/btpr.5420010210

Leclerq-Perlat, M. N., & Lalande, M. (1991). A review on the modelling of the removal of porous contaminants deposited on heat transfer surfaces. *International Journal of Chemical Engineering*, *31*(1), 74–93.

Lindsay, D., Brözel, V. S., Mostert, J. F., & von Holy, A. (2000). Physiology of dairy-associated Bacillus spp. over a wide pH range. *International Journal of Food Microbiology*, *54*(1–2), 49–62. https://doi.org/10.1016/S0168-1605(99)00178-6

Lindsay, D., & Flint, S. (2009). Biofilm formation by spore-forming bacteria in food processing environments. In *Biofilms in the Food and Beverage Industries* (pp. 270–299). Elsevier. https://doi.org/10.1533/9781845697167.2.270

Lyster, R. L. J. (1970). The denaturation of α-lactalbumin and β-lactoglobulin in heated milk. *Journal of Dairy Research*, *37*(2), 233–243. https://doi.org/10.1017/S0022029900013297

McKetta, J. J. (1984). *Chemical Engineering Design Encyclopedia*. Marcel Dekker.

Morr, C. V. (1985). Functionality of Heated Milk Proteins in Dairy and Related Foods. *Journal of Dairy Science*, *68*(10), 2773–2781. https://doi.org/10.3168/jds.S0022-0302(85)81165-6

Mozes, N., Marchal, F., Hermesse, M. P., Van Haecht, J. L., Reuliaux, L., Leonard, A. J., & Rouxhet, P. G. (1987). Immobilization of microorganisms by adhesion: Interplay of electrostatic and nonelectrostatic interactions. *Biotechnology and Bioengineering*, *30*(3), 439–450. https://doi.org/10.1002/bit.260300315

Müller-Steinhagen, H. (1993). Methoden zur Verminderung der Ablagerungsbildung in Wärmeübertragern. *Chemie Ingenieur Technik*, *65*(5), 523–532. https://doi.org/10.1002/cite.330650504

Murphy, P. M., Lynch, D., & Kelly, P. M. (1999). Growth of thermophilic spore forming bacilli in milk during the manufacture of low heat powders. *International Journal of Dairy Technology*, *52*(2), 45–50. https://doi.org/10.1111/j.1471-0307.1999.tb02069.x

Paterson, W. R., & Fryer, P. J. (1988). A reaction engineering approach to the analysis of fouling. *Chemical Engineering Science*, *43*(7), 1714–1717. https://doi.org/10.1016/0009-2509(88)85166-2

Peters S. M., Timmerhaus D. K., & West E. R. (2006). *Plant Design and Economics for Chemical Engineers* (5th ed.). Tziolas Publications.

Process Systems Enterprise Ltd. (2023). *gPROMS Introductory User Guide*.

Ratkowsky, D. A., Lowry, R. K., Mcmeekin, T. A., Stokes, A.. N., & Chandler, R. E. (1983). Model for Bacterial Culture Growth Rate Throughout the Entire Biokinetic Temperature Range. *Journal of Bacteriology*, *154*(3), 1222–1226. https://doi.org/10.1128/jb.154.3.1222-1226.1983

Robert H. Perry, & Don W. Green. (2019). *Perry's Chemical Engineers' Handbook* (9th ed.). McGraw-Hill Education.

Sandu, C. (1989). *Physicomathematical Model for Milk Fouling in Plate Heat Exchanger*. University of Wisconsin-Madison.

Sandu C., & Lund D. (1985). Minimizing Fouling in Heat Exchanger Design. *Biotechnology Progress*, *10*(1).

Sandu C., & Singh R. K. (1991). Energy Increase in Operation and Cleaning Due to Heat-Exchanger Fouling in Milk Pasteurization. *Food Technology*, *84*(32).

Santos, O., Nylander, T., Rizzo, G., Müller-Steinhagen, H., Trägårdh, C., & Paulsson, M. (2003). *Study of Whey Protein Adsorption under Turbulent Flow*. http://dc.engconfintl.org/heatexchanger/24

Scott, S. A., Brooks, J. D., Rakonjac, J., Walker, K. M. R., & Flint, S. H. (2007). The formation of thermophilic spores during the manufacture of whole milk powder. *International Journal of Dairy Technology*, *60*(2), 109–117. https://doi.org/10.1111/j.1471-0307.2007.00309.x

Sharma, A., & Macchietto, S. (2021). Fouling and cleaning of plate heat exchangers: Dairy application. *Food and Bioproducts Processing*, *126*, 32–41. https://doi.org/10.1016/j.fbp.2020.12.005

Skudder, P. J., Thomas, E. L., Pavey, J. A., & Perkin, A. G. (1981). Effects of adding potassium iodate to milk before UHT treatment: I. Reduction in the amount of deposit on the heated

surfaces. *Journal of Dairy Research*, *48*(1), 99–113. https://doi.org/10.1017/S0022029900021518

Te Giffel, M. (1997). Isolation and characterisation of Bacillus cereus from pasteurised milk in household refrigerators in the Netherlands. *International Journal of Food Microbiology*, *34*(3), 307–318. https://doi.org/10.1016/S0168-1605(96)01204-4

Toyoda, I., Schreier, P. J. R., & Fryer, P. J. (1994). A computational model for reaction fouling from whey protein solutions. *Europace*, 222–229. https://api.semanticscholar.org/CorpusID:78270082

U.S. Department of Health and Human Services. (2017). *Grade "A" Pasteurized Milk Ordinance. 2017 Revision*.

Van Asselt, A. J., Vissers, M. M., Smit, F., & De Jong, P. (2005). In-line control of fouling. In Kloster Irsee (Ed.), *Proceedings of Heat Exchanger Fouling and Cleaning - Challenges and Opportunities*.

Visser, J., & Jeurnink, Th. J. M. (1997). Fouling of heat exchangers in the dairy industry. *Experimental Thermal and Fluid Science*, *14*(4), 407–424. https://doi.org/10.1016/S0894-1777(96)00142-2

Yoo, J. A., Hardin, M. T., & Chen, X. D. (2006). The influence of milk composition on the growth of Bacillus stearothermophilus. *Journal of Food Engineering*, *77*(1), 96–102. https://doi.org/10.1016/j.jfoodeng.2005.06.053

Yoo, J.-A., Hardin, M. T., & Chen, X. D. (2006). The influence of milk composition on the growth of Bacillus stearothermophilus. *Journal of Food Engineering*, *77*(1), 96–102. https://doi.org/10.1016/j.jfoodeng.2005.06.053

Yoon, J., & Lund, D. B. (1994). Comparison of Two Operating Methods of a Plate Heat Exchanger Under Constant Heat Flux Condition and their Effect on the Temperature Profile During Milk Fouling. *Journal of Food Process Engineering*, *17*(3), 243–262. https://doi.org/10.1111/j.1745-4530.1994.tb00338.x

Zhao, Y., Caspers, M. P. M., Metselaar, K. I., de Boer, P., Roeselers, G., Moezelaar, R., Nierop Groot, M., Montijn, R. C., Abee, T., & Kort, R. (2013). Abiotic and Microbiotic Factors

Controlling Biofilm Formation by Thermophilic Sporeformers. *Applied and Environmental Microbiology*, *79*(18), 5652–5660. https://doi.org/10.1128/AEM.00949-13

Zottola, E. A., & Sasahara, K. C. (1994). Microbial biofilms in the food processing industry—Should they be a concern? *International Journal of Food Microbiology*, *23*(2), 125–148. https://doi.org/10.1016/0168-1605(94)90047-7